



**CLIMATE CHANGE IMPACT ASSESSMENT ON SOIL WATER  
AVAILABILITY AND CROP YIELD IN ANJENI WATERSHED  
BLUE NILE BASIN**

A Thesis Submitted to School of Graduate Studies Arba Minch University  
in Partial Fulfillment of the Requirement for the  
Degree of Master of Science in Meteorology

BY  
Yakob Mohammed

Arba Minch, Ethiopia  
August, 2009

**CLIMATE CHANGE IMPACT ASSESSMENT ON SOIL WATER  
AVAILABILITY AND CROP PRODUCTION IN ANJENI  
WATERSHED BLUE NILE BASIN**

BY  
Yakob Mohammed

Supervised by : Solomon Seyoum (PhD)  
Co-supervised by: Kassa Tadele (PhD, Candidate)  
Co-supervised by: Wondmagagn Yazea (MSc)

Arba Minch University, Ethiopia

August, 2009

## CERTIFICATION

I, The undersigned certify that i read and here by recommended to the School of Graduate Studies for acceptance of a thesis entitled: Climate Change Impact Assessment on soil Water Availability and Crop Production in Anjeni Water shade Blue Nile Basin in partial fulfilment of the requirement for the degree of Master of Science in meteorology

---

Solomon Seyoum (PhD)

(Advisor)

---

Kassa Tadele (PhD, Candidate)

(Co-advisor)

---

Wondmagagn Yazea (MSc)

(Co-advisor)

## **DECLARATION AND COPYRIGHT**

I, Yakob Mohammed, declare that this thesis is my own original work and that it has not been presented and will not be presented by me to any other university for similar or any other degree award.

Signature: \_\_\_\_\_

Date: \_\_\_\_\_

**CLIMATE CHANGE IMPACT ASSESSMENT ON SOIL WATER  
AVAILABILITY AND CROP PRODUCTION IN ANJENI  
WATERSHED BLUE NILE BASIN**

A Thesis Submitted to School of Graduate Studies Arba Minch University in Partial  
Fulfillment of the Requirement for the Degree of Master Science in Meteorology

Date defended -----

Thesis Assessment Board

1. Chairman----- Signature ----- Date -----
2. External examiner-----Signature ----- Date -----
3. Internal examiner-----Signature ----- Date -----
4. Dean SGS-----Signature ----- Date -----

## ABSTRACT

Through out the world, climate change impact is the main concern for sustainability of water management and water use activities like agricultural production. General Circulation Models (GCMs) which are considered as the most advance tools for estimating future climate change scenarios operate on coarse resolutions. Downscaling of GCM out put is used to assess the impact of climate change on local water management activities. This study was conducted at Anjeni gauged watershed, which is situated in 37°31'E / 10°40'N, in the Northern part of Ethiopia. The watershed is characterized by in-situ storage by soil and water conservation practices. The study assesses quantitatively the variations of water availability and crop production under changing global climate change scenarios in the watershed.

In order to estimate the level of climate change impact on the water availability and crop production of the watershed, climate change scenarios of precipitation and temperature were developed for South Gojam sub basin, in which the watershed is situated for two future climate periods of 30 years from 2011 until 2070. The outputs of HadCM3 coupled atmosphere-ocean GCM model for the SRES A2 and B2 SRES emission scenarios were used to produce the future scenarios. These outputs were downscaled to the watershed scale through the application of the SDSM model. The study found that there is an over all increasing trend in annual temperature and significant variation of monthly and seasonal precipitation from the base period level. These changes of the climate variables were applied to SWAT hydrological model to simulate future water availability and crop production. SWAT was calibrated with five years of data (1986-1990) to assess the possible impact of climate change in the watershed. The results indicate that the annual potential evapotranspiration will show increasing trend for both future climate periods. Results also revealed that there is reduction in soil water content in the watershed. The study investigate that due to combined effect of projected variation in seasonal rainfall and increase in temperature and then reduction in soil water content there will be over all variation in crop production in the watershed.

## **ACKNOWLEDGEMENT**

First and foremost, thanks to almighty Allah for granting me His limitless care, love and blessings all along the way. I thank Arba Minch University for awarding me a scholarship to attend my education and International Water management Institute for awarding me a fund to follow my MSc thesis.

I am deeply indebted to my main supervisor Dr. Solomon Seyoum for his passionate and unreserved support, guidance, encouragement and patience which contributed to the success of this study.

I am also so much thankful to my co-supervisor Dr. Kassa Tadele, who thought me the SWAT model from the grass root level and guided me throughout the progress of the work. Without his encouragement, guidance, and help; this work would have not taken this shape. I feel fortunate to have got this opportunity to work with him.

I would like to thank Amhara Region Agricultural research Institute (ARARI) and National meteorological Agency (NMA) for providing me Hydrological, and Meteorological data for my study area.

I would like to acknowledge the invaluable input of all individuals and organizations, in particular those who provided materials and information and who helped me a lot during the data collection period: Dr. Gete Zeleke, Ato deresse, and Ato Biniam Bruk.

I am highly indebted to all my class Mats and staff members of Meteorology department for their ideal and technical supports. Thanks are also to all my university friends who give me their comments, ideas, shared love and happiness.

DEDICATED

*To*

*My family*

## **ABBREVIATIONS AND ACRONYMS**

AGCM – Atmospheric General Circulation Model

AOGCM – Coupled Atmosphere-Ocean General Circulation Models

Arc SWAT – The Arc GIS Integrated SWAT Hydrological Model

CGCM1 – The Canadian Global Coupled Model

CICS – Canadian Institute for Climate Studies

CN – Curve Number

DDC – Data Distribution Centre of IPCC

DEM – Digital Elevation Model

DEW02 – Dew Point Temperature Calculator

ESCO – Soil Evaporation Compensation Factor

FAO – Food and Agricultural Organization of the United Nations

GCM – General Circulation Model

GIS – Geographic Information System

GUI – Graphical User Interface

GW\_DELAY – Groundwater Delay time

GW\_REVAP – The groundwater Revap coefficient

GWQMN – Threshold Water Depth in the shallow aquifer for flow

HadCM3 – Hadley Centre Coupled Model, version 3

HadCM3A2a – Hadley Centre Coupled Model, version 3, for the A2a emission scenario

HadCM3B2a – Hadley Centre Coupled Model, version 3, for the B2a emission scenario

HRU – Hydrological Response Units

IPCC – International Panel on Climate Change

ITCZ – Inter Tropical Convergence Zone

m.a.s.l – meters above sea level

MRS – Mean Relative Sensitivity

NCEP – National Centre for Environmental Prediction

NMSA – National Meteorological Services Agency, Ethiopia

NRCS – US Natural Resource Conservation Service

OGCM – Ocean General Circulation Models

PET – Potential Evapotranspiration

RCM – Regional Climate Model

SCS – Soil Conservation System

SDSM – Statistical Downscaling Model

SRES – Special Report on Emission Scenarios

SWAT – The Soil and Water Assessment Tool

TAR – Third Assessment Report

TGCI – Task Group on Scenarios for Climate and Impact Assessment

UNEP – United Nations Environment Program

UNFCCC – United Nations Framework Convention on Climate Change

WGEN – Weather Generator

WUE – Water Use Efficiency

WXPARM – Weather Parameter Calculator

# TABLE OF CONTENTS

CERTIFICATION.....	i
DECLARATION AND COPYRIGHT .....	ii
ABSTRACT.....	iv
ACKNOWLEDGEMENT .....	v
ABBREVIATIONS AND ACRONYMS .....	vii
TABLE OF CONTENTS .....	ix
LIST OF FIGURES.....	xii
LIST OF TABLES.....	xiv
CHAPTER ONE .....	1
INTRODUCTION.....	1
1.1 Back ground .....	1
1.2 Problem Statement.....	4
1.3 Hypothesis.....	5
1.4 Research Questions.....	5
1.5 Objective of the study .....	6
1.6 Scope of the study.....	6
CHAPTER TWO.....	7
LITERATURE REVIEW .....	7
2.1 General.....	7
2.2 Pervious Work on related Topic.....	11
CHAPTER THREE .....	15
METHODOLOGY .....	15
3.1 Location of Anjeni Watershed.....	15
3.2 Topography .....	17
3.3 Climate .....	17
3.4 Soils .....	19
3.5 Land Use.....	21
3.6 Hydrology.....	21
3.7 Soil and Water Conservation practice in the watershed .....	22
3.8 Data used.....	24
3.9 Climate Change Scenarios .....	25
3.10 Statistical Downscaling Model (SDSM) .....	27

3.10.1 SDSM Model Inputs.....	28
3.10.2 SDSM Model Approach.....	32
3.11 Hydrological Modeling with SWAT .....	37
3.11.1 Arc SWAT Model Approach .....	38
3.11.2 Weather Generator .....	39
3.11.3 Hydrological Component of SWAT .....	40
3.11.3 Sediment Component.....	44
3.11.4 Routing phase of the hydrological cycle.....	45
3.12 Crop production Component of SWAT .....	46
3.12.1 Growth Cycle .....	46
3.12.2. Optimal Growth .....	48
3.12.3 Actual growth .....	49
3.13 Sensitivity Analysis.....	50
3.14 Calibration and Validation .....	51
3.15 Model Setup .....	53
3.16 Arc SWAT Model Inputs .....	54
3.16.1 Weather Data.....	55
3.16.2 Digital Elevation Model (DEM).....	55
3.16.3 Land Use .....	56
3.16.4 Soil Data .....	58
3.16.5 Slope .....	59
3.16.6 Watershed Delineation.....	59
3.16.7 Determination of Hydrologic Response Units (HRUs) .....	60
3.17 Determination of Impacted storage and productivity .....	61
CHAPTER FOUR.....	62
RESULTS AND DISCUSSIONS.....	62
4.1 Climate change scenario results.....	62
4.1.1 Baseline scenarios .....	62
4.1.2. Base line Scenario developed for Anjeni watershed (1986-2001) .....	62
4.1.3 Base line Scenario developed for Debra Markos station (1961-1990)...	65
4.1.4 Downscaling future scenarios .....	67
4.2 SWAT Model Results .....	77
4.2.1 Soil water storage Simulation for Anjeni watershed .....	77
.....	80
4.2.2 Sensitivity Analysis.....	80
4.2.3 Flow Calibration.....	82
4.2.4 Annual Water Balance.....	83
4.2.5 Flow validation .....	85
4.2.6 Seasonal and Monthly Watershed Water Yield.....	87
4.3 Impact of Climate Change on Future Water Availability.....	88
4.3.1 Change in Monthly Soil Water.....	89
4.3.2. Change in Seasonal/Annual Soil Water .....	90
4.4 Impact of Climate Change on Future Crop Productivity .....	93
CHAPTER FIVE .....	100

UNCERTAINTIES AND ADAPTATION OPTION.....	100
5.1 Uncertainties.....	100
5.2 Adaptation option.....	102
CHAPTER SIX .....	105
SUMMERY AND RECOMMENDATIONS.....	105
6.1 Summery.....	105
6.2 Recommendations .....	108
REFERENCES.....	109
APPENDIX A.....	116
APPENDIX B.....	117
APPENDIX C .....	119
APPENDIX D .....	120
APPENDEX E .....	121
APPENDEX F .....	123

## LIST OF FIGURES

Figure3.1: Location of Anjeni watershed.....	16
Figure3.2: Mean monthly rainfall and temperatures of Anjeni station from (1986-2001).....	18
Figure3.3: Average monthly discharge of Minchet River of Anjeni watershed from 1986-1993.....	22
Figure3.4: Photo taken during field visit, shows (Terraced agricultural land), Soil and water conservation practice in Anjeni watershed. ....	23
Figure3.5: SDSM Version 4.2.2 climate scenario generation (Source: (Wilby and Dawson, 2004)).....	28
Figure3.6. the African Continent Window with 2.5° latitude x 3.75° longitude grid size from which the grid box for the study area is selected.....	29
Figure4.1: Average daily precipitation for Anjeni (station) research center for base period.....	63
Figure4.2: Average daily maximum temperature of observed and downscaled at Anjeni Station for the base period.....	64
Figure4.3: Observed and downscaled Average daily minimum temperature of Anjeni Station for the base period.....	64
Figure4.4: Observed and downscaled mean daily precipitation for base line scenarios (1961-1990).....	65
Figure4.5: Observed and downscaled mean daily maximum temperature for base line (1961-1990).....	66
Figure4.6: observed and downscaled mean daily minimum temperature for base period at Debra Markos station (1961-1990) .....	67
Figure4. 7: Downscaled Mean daily precipitation of future period For Debra Markos station, (a) & (b) for A2a& B2a scenarios, respectively.....	69
Figure4.8: Future patterns of annual rainfall at Anjeni station (1984-2099) .....	70
Figure4.9: Downscaled Mean daily precipitation of future period for Anjeni station: (a) & (b) for A2a& B2a scenarios, respectively .....	71

Figure4.10: Change in average monthly maximum temperature (delta values) in the future (1991-2099) from the base period average monthly maximum temperature (a) & (b) for A2a& B2a scenarios respectively .....	73
Figure4.11: Change in average monthly minimum temperature (delta values) in the future (1991-2099) from the base period average monthly precipitation (a) & (b) for A2a& B2a scenarios respectively.....	75
Figure4.13: Delineated watershed of Anjeni Watershed .....	77
Figure4.14: Land Use of Anjeni Watershed .....	78
Figure4.15: Soil Map of Anjeni Watershed.....	79
Figure4.16: Land Slope of Anjeni Watershed .....	80
Figure4.17: Calibration result of average monthly simulated and gauged flows at the outlet of Anjeni watershed.....	84
Figure4.18. Scatter plot of monthly simulated versus measured flow at Anjeni gauged station for calibration period.....	84
Figure 4.19: Validation result of average monthly simulated and gauged flows at the outlet of Anjeni watershed.....	86
Figure4.20: Mean monthly, seasonally and annually observed and SWAT simulation of water yield in the Anjeni watershed for base period (1986-1993) ....	87
Figure4.21: Mean monthly soil moisture variation for both base period and future periods .....	89
Figure 4.22: the percentage change in mean seasonal soil water for the future periods relative to base period.....	91
Figure 4.23: Trends of annual soil water content at Anjeni watershed (1986-2070) .....	92
Figure 4.24: Trends of annual potential Evapotranspiration at Anjeni watershed (1986-2070) .....	93
Figure4.25: Mean annual yields (a) Teff and (b) Wheat observed versus simulated (1986-1993) .....	96
Figure4.26: Trends of mean annual yields(c) Teff and (d) Wheat observed versus simulated (1986-1993).....	96

## LIST OF TABLES

Table 3.1: Major Soil Units, Sub- groups and Area Coverage of Minchet Catchment (Source: Gete, 2000) .....	20
Table 3.2: Types of predictor variables used in SDSM .....	31
Table 3.3: Selected potential predictors for Anjeni and Debra Markos stations ....	35
Table 3.4: Sensitivity Class for SWAT model.....	51
Table 3.5: Transverse Mercator projection parameters for Ethiopia (Dilnesaw, 2006).....	56
Table 3.6: Original land use/land cover types redefined according to the SWAT code and their aerial coverage.....	57
Table 3.7: Soil type of the study area with their aerial coverage .....	58
Table 4.3: Result of the sensitivity analysis of flow in Anjeni watershed .....	81
Table 4.4: Initial and finally adjusted parameter values of the flow calibration at the outlet of Anjeni watershed.....	82
Table 4.5 observed and simulated water yield during calibration period.....	82
Table 4.6: Mean Annual Simulated water balance values (mm) .....	83
Table 4.7: Calibration statistics of average monthly simulated and gauged flows at the outlet of Anjeni watershed.....	85
Table 4.8: Validation statistics of the average monthly simulated and gauged flows at the outlet of Anjeni watershed.....	86
Table 4.9: percentage change in seasonal and annual hydrological parameters or the periods of 2020s and 2050s with respect to base period .....	90
Table 4.10: percentage change of crop production in future periods relative to period.....	97
Table A.1 Summary of average monthly climatic data values of Anjeni station in the study area .....	116
Table A.2 Summary of average monthly climatic data values of Debra Markos station in the study area.....	116
Table B.1 Precipitation calibration parameters for Anjeni station.....	117
Table B.2 Maximum temperature calibration parameters for Anjeni station.....	117

Table B.3 Minimum Temperature calibration parameter for Anjeni station ..... 118

Table D.1 GCMs Selected by IPCC for impact studies ..... 120

Table E.1 Average monthly soil water content out put in (mm)for base period and future climate periods..... 121

Table E.2 Average monthly basin values (hydrological variables) for base period and future climate periods..... 121

Table E.3 Average monthly basin values (hydrological variables) for 2020's climate periods ..... 122

Table E.4 Average monthly basin values (hydrological variables) for 2050's climate periods ..... 122

# CHAPTER ONE

## INTRODUCTION

### 1.1 Back ground

Water is the most important natural resource required for the survival of all living species. Since the available amount of water is limited, scarce, and not spatially distributed in relation to the population needs, proper management of water resources is essential to satisfy the current demands as well as to maintain sustainability. Water resources planning and management in the 21<sup>st</sup> century is becoming difficult due to the conflicting demands from various stakeholder groups, increasing population, rapid urbanization, climate change producing shifts in hydrologic cycles, the use of high-yielding but toxic chemicals in various land use activities, and the increasing incidences of natural disasters. Among these difficulties, climate change impacts of recent global warming due to increasing greenhouse gases on water resources are emerging concerns to decision-makers.

Human activities, primarily the burning of fossil fuels and changes in land cover and use, are nowadays believed to be increasing the atmospheric concentrations of greenhouse gases. This alters energy balances and tends to warm the atmosphere which will result in climate change. Some reports indicate that mean annual global surface temperature has increased by about 0.3 - 0.6°C since the late 19<sup>th</sup> century and it is anticipated to further increase by 1–3.5°C over the next 100 years ([IPCC AR4, 2007](#)). Even though, these changes in global climate appear to most severely affect the mid and high latitudes of the Northern Hemisphere, where temperatures have been noticeably getting warmer since 1970s (IPCC, 2001), the vulnerability is more in low latitudes of the Northern Hemisphere due to low adaptive capacity. Such changes in climate will have significant impact on local and regional hydrological regimes, which will in turn affect ecological, social and economical systems.

Therefore, the study of the various impacts of climate change on hydrological regimes over the coming century has become a priority, for process research and water and watershed management and development strategies.

In recent years, public concern about the consequences of global climate change to natural and socio-economic systems has increased. The assessment of the impact of future climate change on climate affected systems (water resources, agricultural yields, and energy and transport systems) requires climate scenarios in a high spatial resolution. Most of the climate impact models operate on a spatial scale of 1–100 km, the meteorological mesoscale. Thus, the information about possible future climate change has to be provided on the same resolution to be suitable as input for the impact models ([IPCC AR4, 2007](#)).

Being one of the very sensitive parameters, climate change can cause significant impacts on water resources by resulting changes in the hydrological cycle. The change on temperature and precipitation components of the cycle can have a direct consequence on the quantity of Evapotranspiration component, and on both quality and quantity of the runoff component. Consequently, the spatial and temporal water resource availability, or in general the water balance, can be significantly affected, which clearly amplifies its impact on sectors like agriculture, industry and urban development ([Hailemariam, 1999](#)).

Soil moisture contents are directly simulated by global climate models, albeit over a very coarse spatial resolution, and outputs from these models give an indication of possible directions of change. ([Gregory et al., 1997](#)), for example, show with the HadCM2 climate model that a rise in greenhouse gas (GHG) concentrations is associated with reduced soil moisture in Northern Hemisphere mid-latitude summers. This was the result of higher winter and spring evaporation, caused by higher temperatures and reduced snow cover, and lower rainfall inputs during

summer. The local effects of climate change on soil moisture, however, will vary not only with the degree of climate change but also with soil characteristics. The water-holding capacity of soil will affect possible changes in soil moisture deficits; the lower the capacity, the greater the sensitivity to climate changes. Climate change may also affect soil characteristics, perhaps through changes in water logging or cracking, which in turn may affect soil moisture storage properties ([IPCC TAR-WGII, 2001](#)). Infiltration capacity and water-holding capacity of many soils are influenced by the frequency and intensity of freezing. (Boix-Fayos et al., 1998), for example, show that infiltration and water-holding capacity of soils on limestone are greater with increased frost activity and infer that increased temperatures could lead to increased surface or shallow runoff.

There is a growing need for an integrated analysis that can quantify the impacts of climate change on various aspects of water resources such as precipitation, hydrologic regimes, drought, dam operations, etc. Despite the fact that the impact of different climate change scenarios is forecasted at a global scale, the exact type and magnitude of the impact at a small watershed scale remains untouched in most parts of the world. Hence, identifying local impact of climate change at a watershed level is quite important. This gives an opportunity to define the degree of vulnerability of local water resources and plan appropriate adaptation measures that must be taken ahead of time. Moreover this will give enough room to consider possible future risks in all phases of water resource development projects. Therefore, the overall goal of this study is to assess changes in water availability and crop production in the Anjeni watershed (northern Ethiopia) under climate change scenarios.

## 1.2 Problem Statement

Water availability is an essential component of welfare and productivity. Currently, over billions of people do not have access to adequate supplies of safe water. Although these people are dispersed throughout the world, reflecting sub-national variations in water availability (primarily developing countries like Ethiopia, where agriculture serves as a backbone of the economy as well as ensures the well being of the people) face such short severe shortfalls that they are classified as either water-scarce or water-stress; this in large because of increases in demand resulting from economic and population growth. However, climate change will further exacerbate the periodic and chronic shortfall of water, and also result in frequency and magnitude of droughts in some places. One of the most significant potential consequences of changes in climate may be alterations in regional hydrological cycles and subsequent changes in river flow regimes .Such hydrological changes will affect nearly ever aspect of human well-being from agricultural productivity and energy use to other sectors.

However, water storage improves the ability of rural poor to cope with climate shocks by increasing agricultural productivity (and hence income) and by decreasing fluctuations (and hence risks). The Anjeni soil and water conservation is one of the *in-situ* soil storage which improves the agricultural activities in the area. The watershed is one of the Soil and Water conservation research Centre found in northern Ethiopia. Besides controlling soil erosion, conservation in the watershed is used as key water storage for agricultural activities. As the soil storage is fundamentally important for agriculture and has an influence on the rate of actual evaporation, groundwater recharge, and generation of runoff, the impact of climate change on this storage is directly or indirectly affects the agriculture and different hydrological cycles.

Because of uncertainties in Climate Change predictions, this storage option needs to be able to function under a range of climate change scenarios. Strategies to improve livelihoods and enhance the resilience of rural poor vulnerable to climate change should thus include the increased capacity to store water, and diversity of storage types, considering the full range of storage alternatives, and the processes in which they are created. Therefore, the proposed study evaluates the responses of soil water availability and agricultural production to a range of climate change scenarios based on statistical down scaling methods. It provides valuable information that assists all stakeholders and policy makers to build up an innovative thinking on storages and productivities as response to climate change risks and make appropriate decisions.

### **1.3 Hypothesis**

The soil moisture storage in Anjeni watershed might be reduced during the next 2050s period due to climate change mainly due to increases in temperature (High soil evaporation), and decrease in precipitation, which might cause decreases the crop production in the watershed.

### **1.4 Research Questions**

1. What is the climate change scenario for the Anjeni watershed?
2. What is the impact of climate change on water availability and crop production?
3. What are the adaptation options to be taken to mitigate the adverse impacts of climate change on water availability and crop production?

## **1.5 Objective of the study**

The primary objective of this study is to determine quantitatively the expected changes of water availability and crop production in the Anjeni watershed under changing climate scenarios.

In order to meet the main objective of the study, the following specific objectives are adopted:

- ▶ To develop climate change scenario for the Anjeni watershed using SDSM –statistical Downscaling Model.
- ▶ To assess the impact of climate change on water availability and crop yields
- ▶ Develop adaptation strategies that will help to overcome the adverse impacts due to climate change on crop production in the watershed

## **1.6 Scope of the study**

Since it is not possible to cover the whole aspects of the study area like conservation practice with the available time, it is advisable to limit the scope of the problem to a manageable objective. Hence, the study focused on the impact of climate change on water availability and crop production using Statistical downscaling model (SDSM) for downscaling purpose and then the water balance model, SWAT for impact simulation in the Anjeni watershed. It also tried to see how crop productions will response to global climate change with the aid of SWAT model. Finally, the adaptation option to climate shocks will be settle.

## **CHAPTER TWO**

### **LITERATURE REVIEW**

#### **2.1 General**

The environment has been influenced by human beings for centuries. However, it is only since the beginning of the industrial revolution that the impact of human activities has begun to extend to a global scale (Baede et al., 2001). Today, environmental issue becomes the biggest concern of mankind as a consequence of scientific evidence about the increasing concentration of greenhouse gases in the atmosphere and the changing climate of the Earth. Globally, temperature is increasing and the amount and distribution of rainfall is being altered (Cubasch et al., 2001).

Climate change impacts a basin's inflow supply in various ways. It may alter seasonal temperature and precipitation, shift the timing of stream flow runoff, and reduce the ability of existing supplies to meet water needs. The only means available to quantify the non-linear climate response is by using numerical models of the climate system based on well-established physical, chemical and biological principles, possibly combined with empirical and statistical methods. These are designed mainly for studying climate processes and natural climate variability, and for projecting the response of the climate to human-induced forcing (Baede et al., 2001).

The first models used to evaluate climate change are General Circulation Models (GCMs), which examine the impacts of increased greenhouse gases on long-term weather patterns. General Circulation Models (GCMs) describe the global climate system, representing the complex dynamics of the atmosphere, oceans, and land with mathematical equations that balance mass and energy. By simulating interactions among sea ice, land surface, atmospheric chemistry, vegetation, and the oceans, they predict future climates characterized by temperature, air pressure, and wind speed. Because these models are so computationally

intensive, they can only be run on supercomputers at large research institutes. However, the results are made available to the general scientific community and have so far been used for studies of climate change and its impacts on natural, social, and economic systems ([IPCC AR4, 2007](#)).

GCMs results vary due to model attributes, including their components, resolution, flux-adjustment, and emission scenario forcing. Components refer to the individual processes modeled by smaller models with in a given GCM. Current GCMs are referred to as “coupled models” because they are comprised of linked components which model physical processes such as the atmosphere, oceans, land surfaces and sea ice. Atmospheric and ocean components are represented as grid cells in all GCMs while the representation of land surfaces and sea ice vary more. “Couplers” integrate these domains into one unified model by routing the flow of data between components.

A fundamental characteristic of any model is the scale at which it accurately depicts reality. Increasing model resolution often increases its computational demand exponentially. The level of detail for a general circulation model is defined by the number of layers it uses to model the atmosphere and the ocean and its spatial resolution, meaning the size of the cells in its discretization of those layers.

Like other models of complex natural systems, GCMs must be validated. Early GCMs did not accurately replicate the current climate and required correction factors called “flux adjustments” ([IPCC, 1996](#)). However, these adjustments were viewed as poor solutions in the validation process because they introduced model uncertainties and violated the conservation of mass and energy. The newest generation of GCMs has eliminated the need for flux adjustment ([IPCC, 2001](#)). After a model is developed and validated, it can be used to evaluate alternative scenarios.

Also baseline period is needed to define the observed climate with which climate change information is usually combined to create a climate scenario. When using climate model results for scenario construction, the baseline also serves as the reference period from which the modelled future change in climate is calculated.

Climate scenario refers to a plausible future climate that has been constructed for explicit use in investigating the potential consequence of anthropogenic climate change. It is important to emphasize that, unlike weather forecast, climate scenarios are not predictions. Weather forecasts make use of enormous quantities of information on the observed state of the atmosphere and calculate (using the laws of physics) how this state will evolve during the next few days, producing a prediction of the future – a forecast. In contrast, a climate scenario is a plausible indication of what the future could be like over the decades or centuries, given a specific set of assumptions. These assumptions include future trends in energy demand, emissions of greenhouse gases, land use change as well as assumptions about the behavior of the climate system over long time scales. It is largely the uncertainty surrounding these assumptions which determine the range of possible scenarios (Carter, 2007).

Moreover, GCMs were not designed for climate change impact studies and do not provide a direct estimation of the hydrological responses to climate change. For example, assessment of future river flows may require (sub-) daily precipitation scenarios at catchment, or even station scales. Therefore, there is a need to convert GCM outputs into at least a reliable daily rainfall series at the scale of the watershed to which the hydrological impact is going to be investigated. The methods used to convert GCM outputs into local meteorological variables required for reliable hydrological modelling are usually referred to as “downscaling” techniques.

Hydrological models are mathematical formulations which determine the runoff signal which leaves a watershed basin from the rainfall signal received by this basin. They provide a means of quantitative prediction of catchment runoff that may be required for efficient management of water resources. Such hydrological models are also used as means of extrapolating from those available measurements in both space and time into the future to assess the likely impact of future hydrological change. Hydrological modelling is a great method of understanding hydrologic systems for the planning and development of integrated water resources management. The purpose of using a model is to establish baseline characteristics whenever data is not available and to simulate long term impacts that are difficult to calculate, especially in ecological modelling ([Lenhart et al., 2002](#)).

Changes in global climate are believed to have significant impacts on local hydrological regimes, such as in stream flows which support aquatic ecosystem, navigation, hydropower, irrigation system, etc. In addition to the possible changes in total volume of flow, there may also be significant changes in frequency and severity of floods and droughts. Hence hydrological models provide a framework to conceptualize and investigate the relationship between climate and water resource.

[\(Xu, 1999\)](#) summarized the advantages of hydrological models in climate change impact studies as follows:

Models tested for different climatic/physiographic conditions, as well as models structured for use at various spatial scales and dominant process representations, are readily available.

GCM-derived climate perturbations (at different level of downscaling) can be used as model input.

A variety of response to climate change scenarios can be modelled.

The models can convert climate change output to relevant water resource variables related, for example, to reservoir operation, irrigation demand, drinking and water supply.

## **2.2 Pervious Work on related Topic**

Although climate change is expected to have adverse impacts on socio economic development globally, the degree of the impact will vary across nations. The IPCC findings indicate that developing countries, such as Ethiopia, will be more vulnerable to climate change. It may have far reaching implications to Ethiopia for various reasons, mainly as its economy largely depends on agriculture. A large part of the country is arid and semiarid, and is highly prone to desertification and drought. Climate change and its impacts are, therefore, a case for concern to Ethiopia. Hence, assessing vulnerability to climate change and preparing adaptation options as part of the entire program is very crucial for the country (NMSA, 2001).

Climate Change Impact on Lake Zeway Watershed Water Availability, Ethiopia was done using the A2 and B2 scenarios, where A2 is referred as the medium-high emissions scenario and B2 as the medium-low emissions scenario of HadCM3 output. The temporal and spatial resolution disparity between the outputs of the GCM models and the data needed for such impact studies was adjusted using the most common approach called is the statistical downscaling method. This method is advantageous as it is easy to implement, and generation of the downscaled values involves observed historic daily data. The latter advantage ensures the maintenance of local spatial and temporal variability in generating realistic time series data. However, the method forces the future weather patterns to only those roughly similar to historic, which is its demerit.

The study confirmed that the Statistical Downscaling Model (SDSM) is able to simulate all except the extreme climatic events. The model underestimates the farthest values in both extremes and keeps more or less an average event. Nevertheless, the simulated climatic variables generally follow the same trend with the observed one. The model simulated maximum temperature more accurately than minimum temperature and precipitation. The less performance of precipitation simulation is attributed to its nature of being a conditional process. SDSM more accurately reproduced monthly and seasonal climatic variables averaged over years than individual monthly and seasonal values in a single year.

SWAT hydrological model which is physically based, spatially distributed, and it belongs to the public domain was selected for the study. SWAT simulates hydrological outputs based on a changed climate if the changes in the climate parameters are given as an input to the model. Calibration was done using the sensitive parameters identified and the potential evapotranspiration was calculated by using the Priestley-Taylor method. According to the hydrological analysis carried out, more than two-third of the total stream flow in Zeway Watershed is supplied by flow from the shallow aquifer. The largest portion of the precipitation falling in the watershed is lost through evaporation. The evaporation loss was estimated to reach about seven times the total flow. Therefore, it can be deduced that evapotranspiration is the most sensitive parameter that can be more affected by the changing climate than any other hydrological component.

An attempt was also made based on downscaling large scale atmospheric variables from the HadCM3 General Circulation Model (GCM) to meteorological variables at local scale in order to investigate the hydrological impact of possible future climate change in Gilgel Abbay catchment, Ethiopia. Station based meteorological data were processed to obtain aerial averages necessary for the simulation. Statistical DownScaling Model (SDSM) was employed to transform the GCM output in daily meteorological variables appropriate for hydrological impact

studies. Downscaled meteorological variables are minimum temperature, maximum temperature and precipitation and were used as input to the HBV hydrological model to simulate the catchment runoff regime.

The study used HBV-96. HBV-96 is a water balance based mathematical model of the hydrological processes in a catchment used to simulate the runoff properties. It can be described as a semi-distributed conceptual model that allows dividing the catchment into subbasins where the subbasins can be further divided into elevation and vegetation zones. The model consists of subroutines for snow accumulation and melt, a soil accounting procedure, routines for runoff generation and a simple routing procedure. It is possible to run the model separately for several subbasins and then add the contributions to simulate runoff from the entire subbasin. Calibration as well as runoff forecasts can be for each subbasin.

The result of downscaled precipitation reveals that precipitation does not manifest a systematic increase or decrease in all future time horizons for both A2 and B2 scenarios unlike that of minimum and maximum temperature. However, in the main rainy season which accounts 75-90% of annual rainfall of the area, the mean monthly rainfall indicates a decreasing trend in the beginning of the rainy season (May & June) and an increasing trend towards the end of the rainy season (September & October) for both A2 and B2 scenarios in all future time horizons.

The result of hydrological model calibration and validation indicates that the HBV model simulates the runoff considerably good for the study area. The hydrological impact of future change scenarios indicates that there will be high seasonal and monthly variation of runoff compared to the annual variation. In the main rainy season (June-September) the runoff volume will reduce by 11.6% and 10.1% for A2 and B2 scenarios respectively in 2080s.

Therefore, the Abbay river basin would be significantly affected by the changed climate; that is, a considerable seasonal variation is projected. The model suggested that global warming would result in a general increase in dryness, which would decrease water availability. According to this impact assessment study, it can be concluded that the general warming simulated by all GCMs under CO<sub>2</sub> doubling would result in a substantial decrease in annual runoff over the Abbay River Basin. Results of climate change assessment are highly dependent on the input data and uncertainty of the models. Thus, further study in the area with updated data and a variety of models is required.

## **CHAPTER THREE**

### **METHODOLOGY**

This study concerns the impacts of climate change scenarios with the application of a physically based watershed model SWAT2005 in the Anjeni watershed. Statistical downscaling model (SDSM) is used for future climate generation. Both SDSM and SWAT2005 models involves calibration and validation analysis.

#### **3.1 Location of Anjeni Watershed**

Anjeni gauged watershed is situated at about longitude of 37°31'E and latitude of 10°40'N, in the Northern part of Ethiopia which is shown in the figure 3.1. It is bordered by the Debre Markos- Bahir Dar road, 15 km north of Dembecha town on the rural road to Feres Bet and 65 km north-west of Debre Markos (Kefeni, 1995; SCRP, 2000; Ludi, 2004). In administrative terms, Anjeni lies within Dembecha Wereda of West Gojam Administrative Zone, Amhara National Regional State.

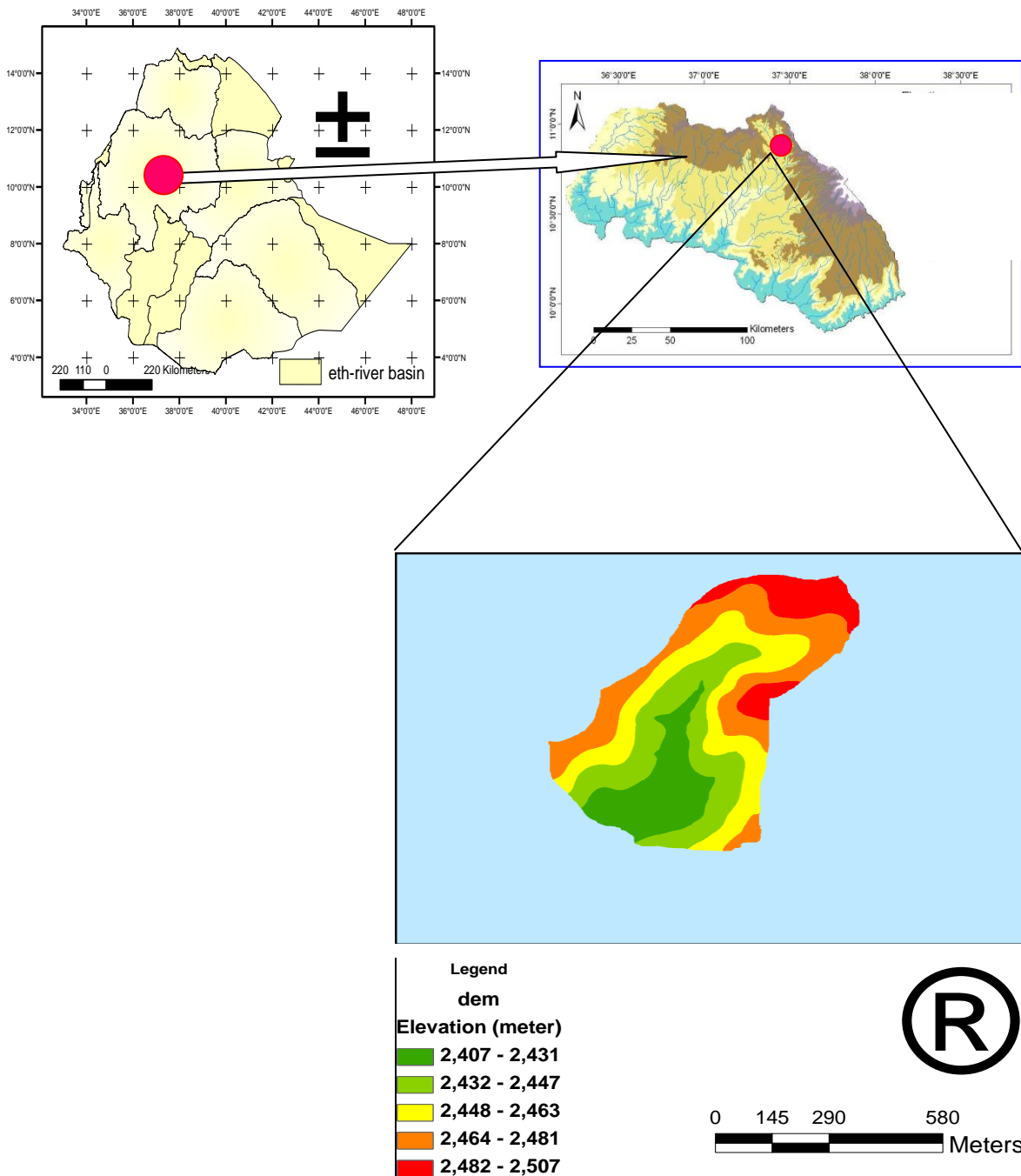


Figure3.1: Location of Anjeni watershed.

Anjeni Peasant Association (PA) covers an area of 575 ha and comprises of a SWC Research Unit with the exception of a small area that belongs to the Jenhala PA. The research site in Minchet catchment, which was established in March 1984 by SCRCP, covers an area of 108.2 ha, but the size of the hydrological catchment is about 113.4 ha (SCRCP, 2000).

### **3.2 Topography**

Although the mean altitude of Anjeni area is about 2,285 m.a.s.l, it actually varies between 2,100 and 2,500 m. The research catchment lies with in an altitudinal range between 2,407-2,507 m.a.s.l. This includes the greatest part of the plateau remnants, almost all of the plateau foot slopes, and all of the alluvial plain. Anjeni is located at the foot of an isolated mountain massif, the Choke Mountains while the topography in the research catchment is dominated by undulating slopes. Besides, the topography of Anjeni is typical of Tertiary volcanic landscapes; it has also been deeply incised by streams, resulting in the current diversity of land forms (Kefeni, 1995; SCRCP, 2000; Ludi, 2004).

### **3.3 Climate**

The Indian and Atlantic Oceans are the sources of moisture for almost all rains in Ethiopia (Degefu, 1987). Two main seasons characterize the study area. The first one is the long rainy season in summer, which lasts from May to September and locally known as '*kiremt*'. The '*kiremt*' season is primarily controlled by the seasonal migration of the Inter Tropical Convergence Zone (ITCZ), which lies to the north of Ethiopia at that time. The second is the dry period, which extends between October to April and locally known as '*Bega*'. In '*Bega*' the ITCZ lies to the south of Ethiopia when the north easterly trade winds traverse Arabia dominates the region. The '*Bega*' season is known as the main harvest season in the area.

Agro-climatically, Anjeni micro-watershed is grouped under Wet Weyna Dega. It is characterized by a mono modal rainfall. It receives rainfall only from May to

September (SCRIP, 2000). According to monthly rainfall distributions, Anjeni area is commonly known as having relatively longer growing period from June to September. The rainfall distribution during this period varies between 240.18 and 398.20 mm with a peak rainfall in July. This period is contributing about 77% of the annual rainfall where as about 12% of the annual rainfall is coming from May and October.

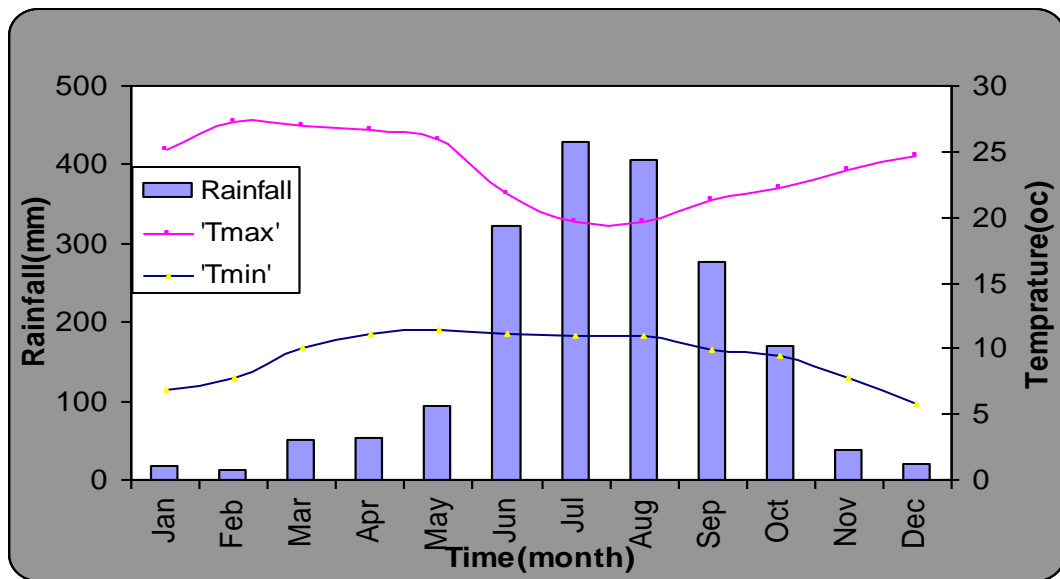


Figure 3.2: Mean monthly rainfall and temperatures of Anjeni station from (1986-2001)

The temperature data from Anjeni SWC Research Unit, shown in figure 3.2, indicates that the lowest daily air temperature is 0°C while the highest is 33°C. As shown in figure 3.2, February is the warmest month with mean monthly minimum and maximum air temperature of 7.8°C and 27.2°C. The highest absolute mean monthly air temperature is in April and May. August as the coldest month has a mean monthly minimum and maximum air temperature of 10.4°C and 19.4°C. The all year averages of mean annual minimum and maximum air temperatures are 9.03°C and 23.3°C. The highest absolute mean annual air temperature was recorded in 1986.

### 3.4 Soils

The upper Blue Nile basin is mainly formed from clay and clay-loam soil type, but the riverbed has loam and sandy-loam type of soil. As part of upper Blue Nile basin, the Anjeni watershed soil is also more of clay and clay-loam type which is mainly belongs to the basaltic trap series of Tertiary volcanic eruptions. The topography of Anjeni is typical of Tertiary volcanic landscapes; it has been deeply incised by streams, resulting in the current diversity of landforms. The soils have developed from a volcanic basement and reworked materials of Tertiary volcanic eruptions, and rarely from sedimentation processes. The infiltration capacity of the soil depends, among others, on the porosity of the soil, which determines its storage capacity and affects the resistance of the water to flow into deep layers. Since the soil infiltration capacity depends on the soil texture, the highest infiltration rates are observed in sandy soil. This shows that, surface runoff is higher in heavy clay and loamy which have low infiltration rate.

The soil classification of Anjeni watershed and its detailed survey was conducted by (Gete, 2000). It consisted of 18 profile pits and 219 auger hole observations in a 50 by 100 m grid. Soils were classified according to FAO-UNESCO, revised legend of the soil map of the world standards (1988/1990). The soils of Anjeni vary within short distances. About eight major soil units and ten sub-groups were identified. Table 3.1 shows the chemical and physical properties of the soils in Anjeni.

According to (Gete, 2000), the valley floor and depressions of the foothills in the catchment are predominantly covered with deep, well-weathered Alisols (41 % of the area). Moderately deep red Nitosols (23.8 %) cover transitional, gently sloping (convex to linear) zones of the catchment. The high, steepest elevations, with mainly convex shapes, are covered with very shallow Regosols and Leptosols (12.4 %). They are probably derived from Nitosols in the truncation process of soil erosion. The hilltop of the catchment and partially the medium steep area of the

slope are covered with moderately deep young Dystric Cambisols (19 %). These soils are transitional soils with a less developed B-horizon, and again probably truncated by soil erosion in the recent past. Small pockets of Luvisols, Lixisols and Acrisols can also be found in the catchment.

The soils of Anjeni are generally acidic and low in organic carbon content, have low to medium total nitrogen and plant available phosphorus contents. This indicates overexploitation of soils and leaching processes. In contrast to these chemical properties, cation exchange capacity of most soils is high. This is probably related to the high clay content of all soils but does not indicate high soil fertility. Both the relatively broad extension of Cambisols and other shallow to very shallow soils (Regosols and Leptosols), as well as the poor chemical properties of all soils are clear signals of accelerated land degradation in the area.

*Table 3.1: Major Soil Units, Sub- groups and Area Coverage of Minchet Catchment (Source: Gete, 2000)*

Major Soil Units	Soil Sub-groups	Area ( ha )	Soil depth range (cm)
Alisols	Humic Alisols	20.9	65-200
	Haplic Alisols	20.6	50-110
Nitosols	Haplic Nitosols	17.2	50-150
	Humic Nitosols	6.6	100-200
Cambisols	Dystric Cambisols	18.9	70-100
Regosols	Eutric Regosols	10	<25-50
Lixisols	Haplic Lixisols	4.8	100-150
Luvisols	Vertic Luvisols	4.2	120-150
Acrisols	Haplic Acrisols	2.6	100- 150
Leptosols	Lithic Leptosols	2.4	<25 -50

### **3.5 Land Use**

The land use map of Anjeni area indicated that 36 % of the land is cultivated for field crops, legumes and vegetables, 36 % of the watershed is pasture land and 28 % of the watershed is forest land. Natural vegetation has almost disappeared in Anjeni area, although some bushes and woody trees can still be observed. These include *Hagenia abyssinica* ( Koso in Amharic ), *Acacia S.P* ( Grar ) , Bamboo ( Kerka), *Rubus aretalus* ( Enjor ), *Schefflera abyssinica* ( Getem ) , *Augaria salicifolia* ( Koba), *Polystacha* ( Anfar), *Erythrina tomentosola* ( Homa), *Embelia Schimperia* (Enkok), *Bersama abyssinica* ( Azamer ) and *Rosa abyssinica* ( kega) (Kefeni, 1995).

Farmers of Anjeni area are leading their life with subsistence farming. They make use of both traditional and introduced conservation measures to enhance the fertility of their farm plots. The land around the research unit which is part of the Blue Nile river basin is almost exclusively used for traditional agricultural purposes, primarily crop production and cattle raising (Kefeni, 1995). In Anjeni, major crops grown are barley, Teff, wheat and maize as grains, lupine (gibbto) and beans as pulses, plus linseed. In addition, minor parts of the cropped area are covered with oil seeds (Nug).

### **3.6 Hydrology**

Minchet is a stream passing through Anjeni watershed where gauging station was found. This small river discharge is highly dependent on seasonal rainfall variability. Hence highest river discharge is measured during main rainy season of the year, which is starting from July to end of September.

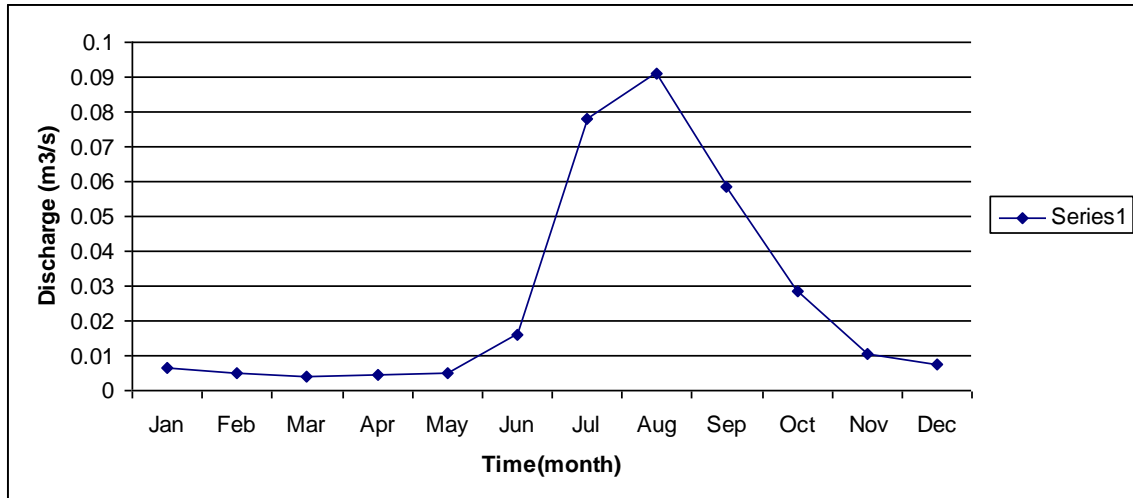


*Figure 3.3: Average monthly discharge of Minchet River of Anjeni watershed from 1986-1993*

### **3.7 Soil and Water Conservation practice in the watershed**

Anjeni watershed is known by its soil and water conservation practices, established by Soil Conservation Research program (SCRIP). The Soil Conservation Research Program was funded by the Swiss Agency for Development and Cooperation (SDC) and the Government of Ethiopia. The implementing agency was the Ethiopian Ministry of Agriculture. The executing agency was the Centre for Development and Environment, Institute of Geography, University of Berne, Switzerland.

Anjeni Research Station was established in March 1984 as the fifth SCRIP research site. Situated in the Gojam Highlands in North-Central Ethiopia, the catchment lies at a favourable altitude and has optimum climatic conditions. Consequently, it is intensively cultivated; there are practically no fallow periods, and present soil and sediment loss rates are extremely high. Ethiopia's "bread basket" – as the region is called – is threatened by loss of potential within very few years. The population pressure is high in the area, and population density is already considerable. A new soil conservation technology and approach was

introduced in Anjeni, first in a small area outside the catchment in 1985, then in the whole catchment from February to April 1986 (Soil Erosion and Conservation Database, 2000).

In Anjeni watershed, the mechanical based type of terrace is used as the soil and water conservation practices. It is a combination of an embankment and a channel constructed across a slope at regular vertical intervals down the slope to reduce slope length and gradient. It is designed for control of surface runoff due to high-rainfall in the areas and for conservation of water in the watershed.

Generally, this conservation type of terrace is constructed for the following benefits, to improve water availability due to water conservation leading to higher actual Evapotranspiration resulting in increasing yields, less soil nutrient losses due to reduced soil erosion, and thus higher nutrient availability resulting in increasing yields, increased lifetime of land for cultivation particularly in the case of shallow areas.



*Figure3.4: Photo taken during field visit, shows (Terraced agricultural land), Soil and water conservation practice in Anjeni watershed.*

There are different types of soil and water conservation technologies (terraces) employed in the Anjeni watershed of Gojam, Ethiopia. Some are well recognized and have formed the basis of much of the research on soil conservation whilst others are less well known and are adapted by farmers to their local environmental conditions. Each conservation technology is suitable for certain characteristics of land (slope, soil type, availability of stone), climate and farming system. Among these, graded *Fanya Juu*, graded bunds, and grass strips are the common ones.

### **3.8 Data used**

#### **1. Meteorological data**

Required daily precipitation data were collected from two stations, one found within the watershed and second near the watershed, Anjeni and Debra Markos respectively. Daily maximum and minimum temperature data were collected from Anjeni watershed found in the watershed and Debra Markos station near the watershed. Daily solar radiation and wind speed data were also obtained from the two stations. Daily potential evapotranspiration rates were calculated in the SWAT model using the Hargreaves method. Meteorological stations were geo-referenced (latitude, longitude and elevation) and the variables adjusted in SWAT using lapse rates in the watershed.

Along with observed meteorological data, the general circulation model (GCM) output of precipitation and temperatures for future time periods were downloaded from global website for future impact assessment.

## **2. Spatial data**

Required landscape data includes tabular and spatial soil data, tabular and spatial land use information, and elevation data. All soil data were taken from soil conservation research program (SCRP), University of Bern, Switzerland. The soil of the area have reclassified based on the available topographic map (1:50,000), Arial photography and satellite images. Since SWAT require many soil proprieties for both the hydrologic and biophysical sub-routines, all of these properties were collected from the watershed along with spatial soil data. These values were then integrated into look up tables and linked to the map in the ArcSWAT interface. Land use is one of the most important factors that affect runoff, evapotranspiration, and land use characteristics in the watershed.

The land use map of the study area was obtained from soil conservation research program (SCRP). The land use of the area have reclassified based on the available topographic map (1:50,000), Arial photography and satellite images. The reclassification of land use map was done to represent the land use according to the specific land cover types such as type of crop, pasture, and forest. Topography is defined by a DEM that describes the elevation of any point in a given area at specific spatial resolution. A high resolution DEM (2 m by 2 m) was obtained from soil conservation research programme (SCRP), University of Bern, Switzerland. The DEM was used to delineate the watershed and to analyze the drainage patterns of the land surface terrain. Subbasin parameters such as slope gradient, slope length of the terrain, and the stream network characteristics such as channel slope, length, and width were derived from the DEM.

## **3.9 Climate Change Scenarios**

The climate change scenarios produced for this study were based on the outputs of GCM results that is established on the SRES emission scenarios. As the objective in this study to get indicative future climate ensembles, the scenarios

developed were only for maximum temperature, minimum temperature, and precipitation values. The outputs of HadCM3 GCM model for the A2 and B2 emission scenarios were used to produce the future scenarios. The SDSM downscaling model was adopted to downscale the global scale outputs of the HadCM3 model outputs into the local watershed scale.

The future time scales from the year 2011 until 2070 were divided into two climate periods of 30 years and their respective changes were determined as deltas (for temperature) and as percentages (for precipitation) from the base period values. The details of all the methodologies used are explained in the following sections.

### **Selection of General Circulation Model**

Use of average outputs of different GCMs can minimize the uncertainties associated with each GCMs and can result in plausible future climates for impact studies. However, as this study was carried out within a very short period of time, only the HadCM3 model was selected for the impact study. Besides, HadCM3 was selected due to the availability of a downscaling model called SDSM that is used to downscale the result of HadCM3 and CGCM1 models. However, the CGCM1 GCM currently does not have predictor files representing the study area window but only the North American Window. Consequently, all the data files used in this study were only for the HadCM3 GCM. The model results are available for the A2 and B2 scenarios, where A2 is referred as the medium-high emissions scenario and B2 as the medium-low emissions scenario. For two of these emission scenarios three ensemble members (a, b, and c) are available where each refer to a different initial point of climate perturbation along the control run. During this study data were available only for the “a” ensembles and hence only the A2a and B2a scenarios were considered.

HadCM3 is a coupled atmosphere-ocean GCM developed at the Hadley Centre of the United Kingdom’s National Meteorological Service that studies climate

variability and change. It includes a complex model of land surface processes, including 23 land cover classifications; four layers of soil where temperature, freezing, and melting are tracked; and a detailed evapotranspiration function that depends on temperature, vapour pressure, vegetation type, and ambient carbon dioxide concentrations (Palmer *et al.*, 2004).

The atmospheric component of the model has 19 levels with a horizontal resolution of 2.5° latitude by 3.75° longitude, which produces a global grid of 96 x 73 cells. This is equivalent to a surface resolution of about 417 km x 278 km at the equator, reducing to 295 km x 278 km at 45° latitude. The oceanic component of the model has 20 levels with a horizontal resolution of 1.25° latitude by 1.25° longitude. HadCM3 has been run for over a thousand years, showing little drift in its surface climate. Its predictions for temperature change are average; and for precipitation increase are below average (IPCC, 2001).

### **3.10 Statistical Downscaling Model (SDSM)**

Among the different approaches used for downscaling, the most common approach is the statistical downscaling method. As described by (Palmer *et al.*, 2004), this method is advantageous as it is easy to implement, and generation of the downscaled values involves observed historic daily data. The latter advantage ensures the maintenance of local spatial and temporal variability in generating realistic time series data.

However, the method forces the future weather patterns to only those roughly similar to historic, which is its demerit. For this study, a model developed based on this statistical approach called SDSM was implemented. The model and its methodology of downscaling are discussed in the following sections.

The Statistical Downscaling Model 4.2.2 was supplied on behalf of the Environment Agency of England and Wales. It is a decision support tool used to

asses local climate change impacts using a statistical downscaling technique. The tool facilitates the rapid development of multiple, low-cost, single-site scenarios of daily surface weather variables under current and future climate forcing (Wilby and Dawson, 2004).

The software manages additional tasks of data quality control and transformation, predictor variable pre-screening, automatic model calibration, basic diagnostic testing, statistical analysis and graphing of climate data. The downscaling process is shown in figure 3.5. The bold boxes represent the main discrete processes of the model.

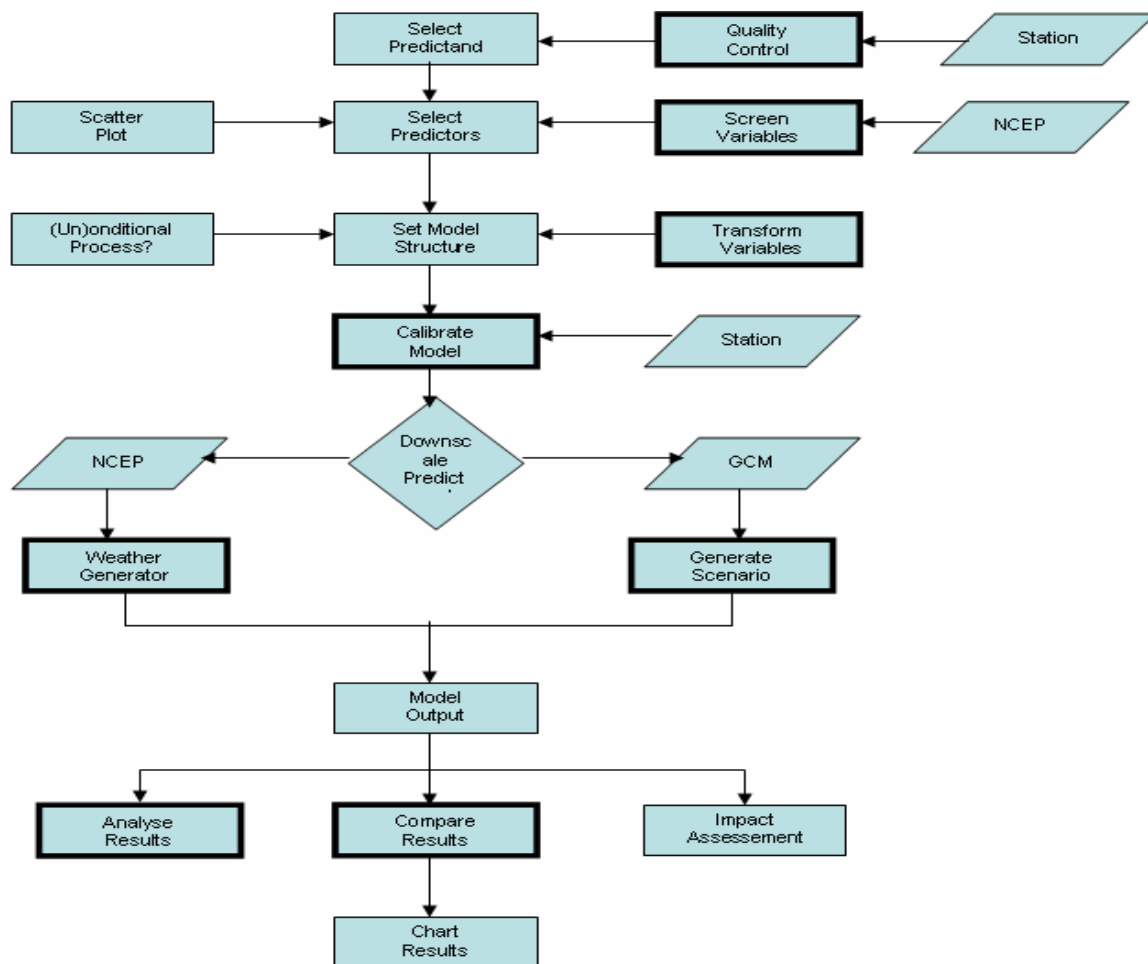


Figure 3.5: SDSM Version 4.2.2 climate scenario generation (Source: (Wilby and Dawson, 2004))

### 3.10.1 SDSM Model Inputs

#### I. SDSM Predictors (HadCM3) Data Files

The SDSM predictor data files are downloaded from the Canadian Institute for Climate Studies (CICS) website <http://www.cics.uvic.ca/scenarios/sdsm/select.cgi>. Even though there was a possibility of selecting predictors from different available GCMs like (HadCM3 and CGCM1), only the HadCM3 GCM has grid boxes representing the study area. CGCM1 model currently has predictor files only for the North American Window. Hence, the data files downloaded were only for the HadCM3 model. The predictor variables of HadCM3 are provided on a grid box by grid box basis of size 2.5° latitude x 3.75° longitude.

As shown in figure 3.6, the study area is completely falls in between 9°25'N to 11°75'N (average 10.5°N) latitude and 38°E to 39°30'E (average 37.5°E) longitude. Hence the nearest grid box for the HadCM3 model (figure 12), which represents the study area, is the one at 10.5°N latitude and 37.5°E longitude (Y=32 & X=11).

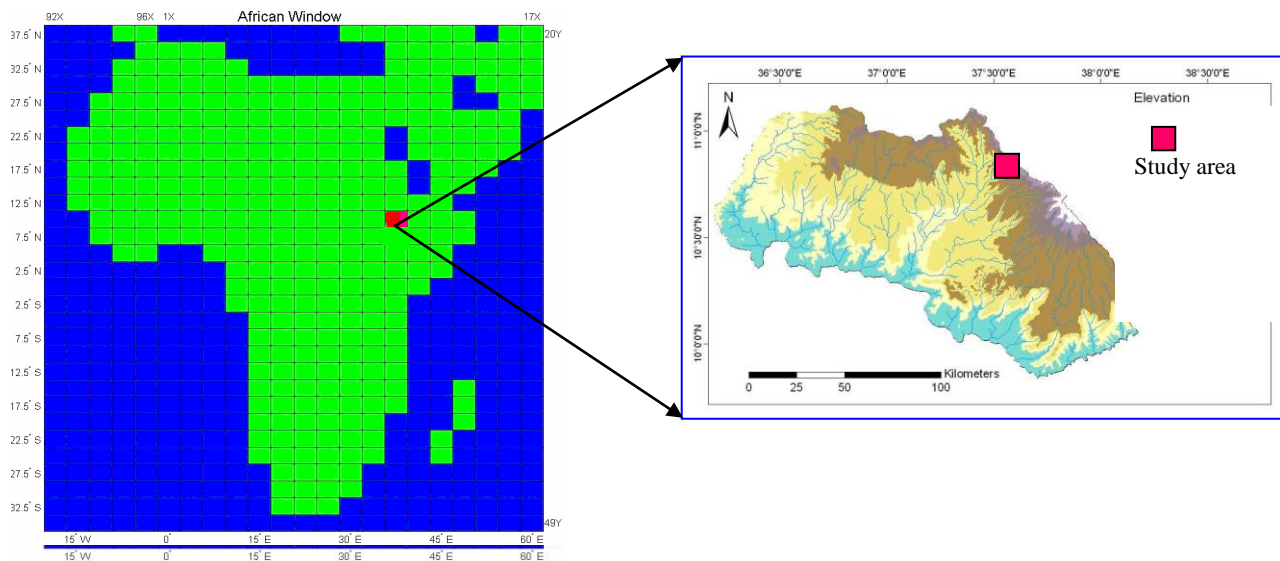


*Figure 3.6. the African Continent Window with 2.5° latitude x 3.75° longitude grid size from which the grid box for the study area is selected*

When the downloaded zip file is unpacked, the grid box consists of three directories:

- NCEP\_1961-2001: This contains 41 years of 26 daily observed predictor data, derived from the NCEP reanalysis, normalized over the complete 1961-1990 period.
- H3A2a\_1961-2099: This contains 139 years of 26 daily GCM predictor data, derived from the HadCM3 A2 experiment, normalized over the 1961-1990 period.
- H3B2a\_1961-2099: This contains 139 years of 26 daily GCM predictor data, derived from the HadCM3 B2 experiment, normalized over the 1961-1990 period.

NCEP data are re-analysis data sets from the National Centre for Environmental Prediction, which were re-gridded to conform to the grid system of HadCM3. These were the data used in the model calibration. Both the NCEP and HadCM3 data have daily predictor values (table 3.2), which were used in the determination of the Predictands. According to (Wilby and Dawson, 2004), the predictors selected with regard to each predictand should be physically and conceptually sensible, strongly and consistently correlated with it, and accurately modelled by GCMs. Further it is recommended that for precipitation downscaling, the predictors should include variables describing atmospheric circulation, thickness, stability and moisture content.

Table 3.2: Types of predictor variables used in SDSM

No	Predictor variable	Predictor description	No	Predictor variables	Predictor description
1	Mslpaf	Mean sea level pressure	14	P5zhaf	5000 hpa divergence
2	P_faf	Surface air flow strength	15	P8_faf	850 hpa airflow strength
3	P_uaf	Surface zonal velocity	16	P8-uaf	850 hpa zonal velocity
4	P_vaf	Surface meridional velocity	17	P8_vaf	850 hpa meridional velocity
5	P_zaf	Surface vorticity	18	P8_zaf	850 hpa vorticity
6	P_thaf	Surface wind direction	19	P850af	850 hpa geopotential height
7	P_zhaf	Surface divergence	20	P8thaf	850 hpa wind direction
8	P5_faf	500 hpa airflow strength	21	P8zhaf	850 hpa divergence
9	P5_uaf	500 hpa zonal velocity	22	P500af	Relative humidity at 500 hpa
10	P5_vaf	500 hpa meridional velocity	23	P850af	Relative humidity at 850 hpa
11	P5_zaf	500 hpa vorticity	24	Rhumaf	Near surface relative humidity
12	P500af	500 hpa geopotential height	25	Shumaf	Surface specific humidity
13	P5thaf	500 hpa wind direction	26	tempaf	Mean temperature at 2 m

## II. Setting of model parameter

For the observed and the NCEP data the year length was set to be the default (366 days), which allows 29 days in February in leap years. However, as HadCM3 have modelled years that do only consist of 360 days, the default value was changed to 360 days. The base period used for the model was from 1/1/1961 to 31/12/1990. The event threshold value is important to treat trace values during the calibration period. For the parameter temperature, this value was set to be 0 while for daily precipitation calibration purpose this parameter was fixed to be 0.1 mm/day so that trace rain days below this threshold value will be considered as a dry day. Missing data were replaced by -999.

Model transformation is the other important part of the model, which specifies the method of transformation applied to the predictand in conditional models. For the daily temperature values no transformation was used as it is normally distributed and its model is unconditional. However, for the daily precipitation, the fourth root transformation was used as its data are skewed and as its model is conditional. The range of variation of the downscaled daily weather parameters can be controlled by fixing the variance inflation. This parameter changes the variance by adding/reducing the amount of “white noise” applied to regression model estimates of the local process. The default value, which is 12 produces approximately normal variance inflation (prior to any transformation), and this was used for the daily temperature values; where as for daily precipitation this value is set to be 18, in order to magnify the variation.

### **3.10.2 SDSM Model Approach**

The processes that were under taken to come up with the downscaled climate Parameters are the following:

#### **I. Selection of Observed climate station data**

There are two stations that are used for downscaling global climate change to local impact assessment, Anjeni and Debra Markos stations. Even though, center of this study is Anjeni research center, there are two reasons to add Debra Markos station. Firstly, climate data used for downscaling (Rainfall and Temperature) from Anjeni research center is from 1986 to 2001, which is not fully sufficient for climate change study. Secondly, both stations are found in one grid cell of GCM HadCM3, 2.5 lat \* 3.75 long and to overcome the problem with precipitation downscaling, which is more of conditional type effected by local climate rather than global predictors, future climate variables of the two stations are compared.

## **II. Quality Control and Data Transformation**

The result of any model depends on the quality of the input data. Input data should, therefore, be checked for missing and unrealistic values in order to come up with good results. Besides, this function of SDSM provides the minimum, maximum, and mean of the input data. All the input data are checked for missing data codes and data errors before the calibration process.

## **III. Screening the downscaling predictor variables**

The central concept behind any statistical downscaling method is the recognition of empirical relationships between the gridded predictors and single site Predictands. This is the most challenging part of the work due to the temporal and spatial variation of the explanatory power of each predictor ([Wilby and Dawson, 2004](#)). The selection was done at most care as the behaviour of the climate scenario completely depends on the type of the predictors selected. Annual analysis period was used which provides the predictor-predictand relationship all along the months of the year. The parameter which tests the significance of the predictor predictand relationship, significance level, was set to be equal to the default value ( $p < 0.05$ ). Moreover, the process type that identifies the presence of an intermediate process in the predictor-predictand relationship was defined.

For daily temperature, which is not regulated by an intermediate process, the unconditional process is selected. However, for daily precipitation, because of its dependence on other intermediate process like on the occurrences of humidity, cloud cover, and/or wet-days; the conditional process was selected. Several analyses were made by selecting 8 out of 26 predictor variables at a time till best predictor-predictand correlations were found. Out of the group, those predictors which have high explained variance are selected. The partial correlation analysis is done for the selected predictors to see the level of correlation with each other. There could be a predictor with a high explained variance but it might be very highly correlated with another predictor. This means that it is difficult to tell that this

predictor will add information to the process and therefore, it will be dropped from the list. Finally scatter plot indicates whether this result is a potentially useful downscaling relationship.

#### **IV. Selection of Potential Predictor Variable**

The first step in the downscaling procedure using SDSM was to establish the empirical relationships between the predictand variables (minimum temperature, maximum temperature, and precipitation) collected from stations and the predictor variables obtained from the NCEP re-analysis data for the current climate. That involved the identification of appropriate predictor variables that have strong correlation with the predictand variable. The next step was the application of these empirical predictor-predictand relationships of the observed climate to downscale ensembles of the same local variables for the future climate. Data supplied by the HadCM3 for the A2 and B2 emission scenarios for the period of 1961–2099 for Debra Markos station and 1986-2001 for Anjeni research center were used. This is based on the assumption that the predictor-predictand relationships under the current condition remain valid under future climate conditions too. Therefore, according to the above procedure the potential predictors selected for maximum temperature, minimum temperature and precipitation for the study area were listed in table 3.3.

Table 3.3: Selected potential predictors for Anjeni and Debra Markos stations

	Predictand	Predictor	symbol
Anjeni station	Maximum temperature	Mean sea level pressure, Surface vorticity, 850 hpa meridional velocity, Mean temperature at 2 m	Ncepmslpaf, ncepp_zaf, Ncepp8_vaf, nceptempaf
	Minimum temperature	Surface meridional velocity, 500 hpa geopotential height , 850 hpa zonal velocity, Surface specific humidity, Mean temperature at 2 m	Ncep_vaf,ncepp500af, ncepp8_uaf, ncepshumaf, and nceptempaf
	Precipitation	Mean sea level pressure, Surface meridional velocity, 500 hpa zonal velocity,850 hpa zonal velocity,850 hpa meridional velocity, Near surface relative humidity	ncepp_uaf, ncepp5_uaf, ncepp8_uaf, ncepr500af Ncepp8_vaf,nceprhumaf,ncepshumaf
Debra Markos station	Maximum Temperature	Surface divergence, 500 hpa geopotential height , 5000 hpa divergence, 850 hpa zonal velocity, 850 hpa vorticity, 850 hpa geopotential height, Mean temperature at 2 m	ncepp5zhaf,ncepp500af, vcepp5zhaf, ncepp8-uaf, ncepp8_zaf, P850af, nceptempaf
	Minimum temperature	Surface vorticity, Surface divergence, 500 hpa geopotential height ,Relative humidity at 500 hpa, Relative humidity at 850 hpa, Surface specific humidity, Mean temperature at 2 m	ncepp_zaf,ncepp_zhaf, ncepp500af,ncepp500af, ncepp850af,ncepshumaf, nceptempaf
	precipitation	Surface vorticity, Surface divergence 500 hpa zonal velocity, Near surface relative humidity, Surface specific humidity	ncepp_zaf, ncepp_zhaf, ncepp5_uaf,nceprhumaf, ncepshumaf

## **V. Model calibration**

This operation is normally carried out based on the outputs of the second step – selection of the predictor variables that uses the NCEP data base of the selected grid box. The mathematical relation between a specific predictand and the selected predictor variables is estimated and the parameters of a multiple linear regression equation are determined.

The temporal resolution of the downscaling model was selected by choosing the model type (monthly, seasonal, or yearly). In Monthly models, model parameters are estimated for each month of the year. Hence, for this study, the calibration was done for the period of 11 years (1986-1996) and (1961-1980) for Anjeni and Debra Markos stations respectively at a monthly model type in order to see the monthly temporal variations. Still the processes selected as explained before are conditional for daily precipitation and non-conditional for daily temperature values.

## **VI. Weather Generator and Validation**

SDSM's Weather Generator enables to produce synthetic current daily weather data based on inputs of the observed time series data and the multiple linear regression parameters produced during the calibration step. Each time-series-data of the observed climate variable is linked to the regression model weights to generate the synthetic time series data into a series of ensembles (runs). The results among the ensembles differ based on the relative significance of the deterministic and stochastic components of the regression models and mainly due to the stochastic component of the downscaling. As indicated in the SDSM manual, variables like local temperatures are largely determined by regional forcing whereas precipitation series display more “noise” arising from local factors. Hence, larger differences can be observed in precipitation ensemble members than that of temperature.

The result of the weather generator was used to validate the calibrated model using independent observed data not used during the calibration procedure and the synthesized artificial weather time series data representing the present condition. Five years of simulation from 1997-2001 was selected for the validation for Anjeni stations and ten years of simulation from 1981-1990 was selected for Debra Markos stations.

## **VII. Scenario Generation - Determination of the Impacted Climate Variables**

SDSM has HadCM3 model output with the A2 and B2 SRES emission scenarios with grid boxes containing the study area. Hence for this study, the HadCM3A2a and HadCM3B2a were the two GCM output files used for the scenario generation. The regression weights produced during the calibration process were applied to the time series outputs of the GCM model.

This is based on the assumption that the predictor-predictand relationships under the current condition remain valid under future climate conditions too. Twenty ensembles of synthetic daily time series data were produced for each of the two SRES scenarios for a period of 139 years (1961 to 2099). The final product of the SDSM downscaling method was then found by averaging the twenty independent stochastic GCM ensembles. The developers ([Wilby and Downson, 2004](#)) suggested that, as the target here is only to see the general trend of the climate change in the future; it is adequate to consider the average of the ensembles. They also added that to preserve inter-variable relationships, the ensemble mean should be used.

### **3.11 Hydrological Modeling with SWAT**

For this case study three different models were tested for climate change impact assessment, which should be responsible for simulation of soil water availability and crop production. These are: The Soil and Water assessment Tool (SWAT),

cropping system Simulation model (CropSyst) and Aqua Crop. Depending on the criterion given for hydrological model discussed in section 3.3.1 and taking into account the objective of the research, even though the two models are available and easy to use, they are failed to fulfil the purpose of study. Overall the semi-distributed physically based model SWAT is selected for this study.

SWAT2005 is a public domain model actively supported by the USDA (United States Department of Agriculture) – ARS (Agricultural Research Service) at the Grass-land, Soil and Water Research Laboratory in Temple, Texas, USA. SWAT is a river basin scale, a continuous time, a spatially distributed model developed to predict the impact of land management practices on water, sediment and agricultural chemical yields in large complex watersheds with varying soils, land use and management conditions over long periods of time ([Neitsch et al., 2005](#)).

SWAT can analyze both small and large watersheds by subdividing the area into homogenous parts. As a physically-based model, SWAT uses hydrologic response units (HRUs) to describe spatial heterogeneity in terms of land cover, soil type and slope within a watershed. The SWAT system embedded within geographic information system (GIS) that can integrate various spatial environmental data including soil, land cover, climate and topographic features.

Currently SWAT is imbedded in Arc GIS interface called Arc SWAT. It is computationally efficient, uses readily available inputs and enables users to study long-term impacts. SWAT is a physically based, continuous time ([Lenhart et al., 2002](#)) and computationally efficient hydrological model, which uses readily available inputs.

### **3.11.1 Arc SWAT Model Approach**

Watersheds can be subdivided into sub watersheds and further into hydrologic response units (HRUs) to account for differences in soils, land use, crops,

topography, weather, etc. The model has a weather generator that generates daily values of precipitation, air temperature, solar radiation, wind speed, and relative humidity from statistical parameters derived from average monthly values. The model computes surface runoff volume either by using modified SCS curve number method or the Green & Ampt infiltration method. Flow is routed through the channel using a variable storage coefficient method or the Muskingum routing method. SWAT has three options for estimating potential evapotranspiration: Hargreaves, Priestley-Taylor, and Penman-Monteith. The model also includes controlled reservoir operation and groundwater flow model. The important equations used by the model are discussed below. The detailed and complete descriptions are given in the SWAT theoretical documentation. SWAT splits hydrological simulations of a watershed into two major phases: the land phase and the routing phase. The difference between the two lies on the fact that water storage and its influence on flow rates is considered in channelized flow ([Neitsch et al., 2002](#)).

### **3.11.2 Weather Generator**

Lack of full and realistic long period climatic data is the problem of developing countries. Weather generators solve this problem by generating data having the same statistical properties as the observed ones ([Danuso, 2002](#)). SWAT requires daily values of precipitation, maximum and minimum temperature, solar radiation, relative humidity and wind speed. The climatic data collected from the ten meteorological stations in the study area however, have too many missing data. As SWAT has a built in weather generator called WGEN that is used to fill the gaps, all the missing values were filled with a missing data identifier, -99. The weather generator first independently generates precipitation for the day. Maximum temperature, minimum temperature, solar radiation and relative humidity are then generated based on the presence or absence of rain for the day. Finally, wind speed is generated independently.

For the sake of data generation, weather parameters were developed by using the weather parameter calculator WXPARM (Williams, 1991) and dew point temperature calculator DEW02 (Liersch, 2003), which were downloaded from the SWAT website ([http://www.brc.tamus.edu/swat/soft\\_links.html](http://www.brc.tamus.edu/swat/soft_links.html)). The WXPARM program reads daily values of solar radiation (calculated from daily sunshine hours), maximum and minimum temperatures, precipitation, relative humidity, and wind speed data. It then calculates monthly daily averages and standard deviations of all variables as well as probability of wet and dry days, skew coefficient, and average number of precipitation days in the month. The DEW02 programs reads daily values of relative humidity, and maximum and minimum temperature values and calculates monthly average dew point temperatures.

### 3.11.3 Hydrological Component of SWAT

The simulation of the hydrology of a watershed is done in two separate divisions. One is the land phase of the hydrological cycle that controls the amount of water, sediment, nutrient and pesticide loadings to the main channel in each sub-basin. Hydrological components simulated in land phase of the hydrological cycle are canopy storage, infiltration, redistribution, evapotranspiration, lateral subsurface flow, surface runoff, ponds, tributary channels and return flow. The second division is routing phase of the hydrologic cycle that can be defined as the movement of water, sediments, nutrients and organic chemicals through the channel network of the watershed to the outlet. In the land phase of hydrological cycle, SWAT simulates the hydrological cycle based on the water balance equation.

$$SW_t = SW_o + \sum_{i=1}^t (R_{day} - Q_{surf} - E_a - W_{seep} - Q_{gw}) \quad \text{-----4.1}$$

In which  $SW_t$  is the final soil water content (mm),  $SW_o$  is the initial soil water content on day  $i$  (mm),  $t$  is the time (days),  $R_{day}$  is the amount of precipitation on day  $i$  (mm),  $Q_{surf}$  is the amount of surface runoff on day  $i$  (mm),  $E_a$  is the amount of evapotranspiration on day  $i$  (mm),  $W_{seep}$  is the amount of water entering the vadose

zone from the soil profile on day  $i$  (mm), and  $Q_{gw}$  is the amount of return flow on day  $i$  (mm).

Using the above equation the soil moisture content for the given area is simulated. Since the soil moisture storage is the main concern of this study, the brief description of some of the key model components are provided in this thesis. More detailed descriptions of the different model components are listed in (Neitsch et al., 2005). Soil water may follow different paths of movement: vertically upward (plant uptake), vertically downward (percolation), or laterally-contributing to stream flow. The vertical movement as plant uptake removes the largest portion of water that enters the soil profile.

The amount of soil water is usually measured in terms of water content as percentage by volume or mass, or as soil water potential, this soil water content is highly depends on the water balance values given in equation 4.1. Mostly, taking the precipitation as source of soil water content and reduction of run off, actual evapotranspiration, and ground water from precipitation is result in availability of water in the soil. Therefore, SWAT model revealed quantitatively the value of soil water content (SW) depends on the above water balance values.

However, water content does not necessarily describe the availability of the water to the plants, nor indicates how the water moves within the soil profile. The only information provided by water content is the relative amount of water in the soil.

Soil water dynamics can be thought of as comparable to a sponge. When a sponge is saturated by soaking it in water when it is lifted out of the water, any excess water will drip off it. This is equivalent to drainage from the macro pores in the soil. Once the sponge has stopped dripping it is at field capacity.

When the sponge is squeezed it is easy to get the first half of the water out. This first squeeze is equivalent to draining the sponge to the stress point and the water is removed like the RAWC (readily available water-holding capacity). Squeezing the second half of the sponge out is much harder. This is like draining the sponge to permanent wilting point. The total water squeezed out of the sponge from when it stopped dripping is the TAWC (Total Available Water-Holding Capacity). But no matter how hard the sponge is squeezed there is no way to get all the water out of it. The water left is the equivalent to the hygroscopic water found in soil.

This sponge analogy is similar to how plant roots find getting moisture from the soil. From field capacity to the stress point it is easy to get the water. From the stress point to the permanent wilting point plants find it much harder to draw water from the soil and their growth is stunted. Below the permanent wilting point no further water can be removed and the plant dies.

**Percolation** is the downward movement of water in the soil. SWAT calculates percolation for each soil layer in the profile. Water is allowed to percolate if only the water content exceeds the field capacity of that layer ([Neitsch et al., 2002](#)).

**Surface runoff** occurs whenever the rate of precipitation exceeds the rate of infiltration. SWAT offers two methods for estimating surface runoff: the SCS curve number procedure and the Green & Ampt infiltration method ([Green and Ampt, 1911](#)). Using daily or sub daily rain-fall, SWAT simulates surface runoff volumes and peak runoff rates for each HRU. In this study, the SCS curve number method was used to estimate surface runoff because of the unavailability of sub daily data for Green & Ampt method.

**Lateral flow** is common in areas with high hydraulic conductivities in surface layers and an impermeable or semi-permeable layer at a shallow depth. Rainfall will percolate vertically up to the impermeable layer and develops a saturated zone

stored above this layer. This is called a perched water table, which is the source of water for lateral subsurface flow. SWAT incorporates a kinematic storage model for subsurface flow (Neitsch *et al.*, 2002).

**The peak discharge** or the peak surface runoff rate is the maximum volume flow rate passing a particular location during a storm event. SWAT calculates the peak runoff rate with a modified rational method. In rational method it assumed that a rainfall of intensity  $I$  begins at time  $t = 0$  and continues indefinitely, the rate of runoff will increase until the time of concentration,  $t = t_{conc}$ . The modified rational method is mathematically expressed as:

$$q_{peak} = \frac{\alpha_{tc} * Q_{surf} * f * Area}{3.6 * t_{conc}} \text{-----} 4.2$$

Where:  $q_{peak}$  is the peak runoff rate (m<sup>3</sup>/s),  $\alpha_{tc}$  is the fraction of daily rainfall that occurs during the time of concentration,  $Q_{surf}$  is the surface runoff (mm), Area is the sub-basin area (km<sup>2</sup>),  $t_{conc}$  is the time of concentration (hr), and 3.6 is a conversion factor.

**Potential evapotranspiration** there are many methods that are developed to estimate potential evapotranspiration (PET). Three methods are incorporated into SWAT: the Penman-Monteith method (Monteith, 1965), the Priestley-Taylor method (Priestley and Taylor, 1972) and the Hargreaves method (Hargreaves *et al.*, 1985). For this study we have used Hargreaves method due to limitation of weather data such as wind speed, and sunshine hours to be used for other two methods. Therefore, such weather data of wind speed, and radiation will derived from imputed weather data of temperatures, precipitation and relative humidity during model run using weather generator.

**Groundwater** the simulation of groundwater is partitioned into two aquifer systems i.e. an unconfined aquifer (shallow) and a deep-confined aquifer in each sub basin.

The unconfined aquifer contributes to flow in the main channel or reach of the sub basin. Water that enters the deep aquifer is assumed to contribute to stream flow outside the watershed (Arnold et al., 1993). In SWAT2005 the water balance for a shallow aquifer is calculated with equation 4.3.

$$aq_{sh,i} = aq_{sh,i-1} + W_{rchrg} - Q_{gw} - W_{revap} - W_{deep} - W_{pump,sh} \text{-----4.3}$$

Where:  $aq_{sh,i}$  is the amount of water stored in the shallow aquifer on day i (mm),  $aq_{sh,i-1}$  is the amount of water stored in the shallow aquifer on day i-1 (mm),  $w_{rchrg}$  is the amount of recharge entering the aquifer on day i (mm),  $Q_{gw}$  is the groundwater flow, or base flow, into the main channel on day i (mm),  $w_{Revap}$  is the amount of water moving into the soil zone in response to water deficiencies on day i (mm),  $w_{deep}$  is the amount of water percolating from the shallow aquifer into the deep aquifer on day i (mm), and  $w_{pump,sh}$  is the amount of water removed from the shallow aquifer by pumping on day i (mm).

### 3.11.3 Sediment Component

SWAT calculates the soil erosion and sediment yield with the Modified Universal Soil Loss Equation (MUSLE) given by (Williams and Berndt, 1977).

$$sed = 11.8 * (Q_{surf} * q_{peak} * area_{hru})^{0.56} * K_{USLE} * C_{USLE} * P_{USLE} * LS_{USLE} * CFRG \text{-----4.4}$$

Where:  $sed$  is the sediment yield on a given day (metric tons),  $Q_{surf}$  is the surface runoff volume (mm /ha),  $q_{peak}$  is the peak runoff rate ( $m^3/s$ ),  $area_{hru}$  is the area of the HRU (ha),  $K_{USLE}$  is the soil erodibility factor (0.013 metric ton  $m^2$  hr/( $m^3$ -metric ton cm)),  $C_{USLE}$  is the cover and management factor,  $P_{USLE}$  is the support practice factor,  $LS_{USLE}$  is the topographic factor and  $CFRG$  is the coarse fragment factor

### 3.11.4 Routing phase of the hydrological cycle

The second phase of the SWAT hydrologic simulation, the routing phase, consists of the movement of water, sediment and other constituents (e.g. nutrients, pesticides) in the stream network. As an optional process, the change in channel dimensions with time due to down cutting and widening is also included.

Similar to the case for the overland flow (discussed in *section 3.11.3*), the rate and velocity of flow is calculated by using the Manning's equation. The main channels or reaches are assumed to have a trapezoidal shape by the model. Two options are available to route the flow in the channel networks: the variable storage and Muskingum methods. Both are variations of the kinematic wave model. While calculating the water balance in the channel flow, the transmission and evaporation are also well considered by the model.

The variable storage method uses a simple continuity equation in routing the storage volume, whereas the Muskingum routing method models the storage volume in a channel length as a combination of wedge and prism storages. In the latter method, when a flood wave advances into a reach segment, inflow exceeds outflow and a wedge of storage is produced. As the flood wave recedes, outflow exceeds inflow in the reach segment and a negative wedge is produced. In addition to the wedge storage, the reach segment contains a prism of storage formed by a volume of constant cross-section along the reach length.

For this study, the variable storage method was adopted. The method was developed by (Williams, 1969) and used in the ROTO (Arnold *et al.*, 1995) model. Storage routing is based on the continuity equation:

$$\nabla V_{stored} = V_{in} - V_{out} \text{-----} 4.5$$

Where:  $V_{IN}$  is the volume of inflow during the time step (m<sup>3</sup> water),  $V_{out}$  is the volume of outflow during the time step (m<sup>3</sup> water), and  $V_{stored}$  is the change in

volume of storage during the time step (m<sup>3</sup> water). Detail of the equation was given in SWAT manual.

### **3.12 Crop production Component of SWAT**

The plant growth component of SWAT is a simplified version of the EPIC plant growth model. As in EPIC, phenological plant development is based on daily accumulated heat units, potential biomass is based on a method developed by Monteith, a harvest index is used to calculate yield, and plant growth can be inhibited by temperature, water, nitrogen or phosphorus stress. The crop part of SWAT consists of three different components. These are plant actual growth part, optimal growth and growth cycle.

#### **3. 12.1 Growth Cycle**

##### **Heat Unit**

The growth cycle of a plant is controlled by plant attributes summarized in the plant growth database and by the timing of operations listed in the management file. As part of this attributes SWAT uses the heat unit theory to regulate the growth cycle of plants.

The heat index used by SWAT is a direct summation index. Each degree of the daily mean temperature above the base temperature is one heat unit. This method assumes that the rate of growth is directly proportional to the increase in temperature. It is important to keep in mind that the heat unit theory without a high temperature cut off does not account for the impact of harmful high temperatures.

SWAT assumes that all heat above the base temperature accelerates crop growth and development. The heat unit accumulation for a given day is calculated with equation 4.6.

$$HU = T_{av} - T_{base} \text{ -----4.6}$$

When  $T_{av} > T_{base}$

Where: HU is the number of heat units accumulated on a given day (heat units),  $T_{av}$  is the mean daily temperature ( $^{\circ}\text{C}$ ), and  $T_{base}$  is the plant's base or minimum temperature for growth ( $^{\circ}\text{C}$ ). The total number of heat units required for a plant to reach maturity is calculated:

$$PHU = \sum_{d=1}^m HU \text{ -----4.7}$$

Where: PHU is the total heat units required for plant maturity (heat units), HU is the number of heat units accumulated on day d where d = 1 on the day of planting and m is the number of days required for a plant to reach maturity. PHU is also and referred to as potential heat units.

## II. Heat Unit Scheduling

SWAT allows management operations to be scheduled by day or by fraction of potential heat units. For each operation the model checks to see if a month and day has been specified for timing of the operation. If this information is provided, SWAT will perform the operation on that month and day. If the month and day are not specified, the model requires a fraction of potential heat units to be specified. It's recommended that, if exact dates are available for scheduling operations, these dates should be used. In this study also since there are no exact dates available for scheduling operation, I used a fraction of potential heat units to be specified by the model.

## III. Plant Types

SWAT categorizes plants into seven different types: warm season annual legume, cold season annual legume, perennial legume, warm season annual, cold season annual, perennial and trees. For this study the watershed's crop to be simulated are considered as warm annual season for Teff and cold annual season for wheat.

### 3.12.2. Optimal Growth

Plant growth is modelled by simulating leaf area development, light interception and conversion of intercepted light into biomass assuming plant species-specific radiation-use efficiency. For each day of simulation, potential plant growth, i.e. plant growth under ideal growing conditions, is calculated. Ideal growing conditions consist of adequate water and nutrient supply and a favourable climate. Differences in growth between plant species are defined by the parameters contained in the plant growth database. The optimal growing conditions of adequate water and nutrient supply and also part of climate were deeply discussed in SWAT 2005 manual.

#### Biomass Production

The total biomass on a given day,  $d$ , is calculated as:

$$bio = \sum_{i=1}^d \Delta bio_i \text{-----4.8}$$

Where  $bio$  is the total plant biomass on a given day (kg /ha), and  $\Delta bio_i$  is the increase in total plant biomass on day  $i$  (kg/ha).

#### Crop yield

The fraction of the above-ground plant dry biomass removed as dry economic yield is called the harvest index. For the majority of crops, the harvest index will be between 0.0 and 1.0. However, plants whose roots are harvested, such as sweet potatoes, may have a harvest index greater than 1.0.

SWAT calculates harvest index each day of the plant's growing season using the relationship:

$$HI = HI_{opt} \cdot \frac{100 \cdot fr_{PHU}}{(100 \cdot fr_{PHU} + \exp[11.1 - 10 \cdot fr_{PHU}])} \text{-----4.9}$$

Where: HI is the potential harvest index for a given day,  $HI_{opt}$  is the potential harvest index for the plant at maturity given ideal growing conditions, and  $fr_{PHU}$  the fraction of potential heat units accumulated for the plant on a given day in the growing season.

The crop yield is calculated as:

$$Yld = bio_{ag} * HI \quad \text{when } HI \leq 1.00 \text{-----4.10}$$

$$yld = bio * \left(1 - \frac{1}{(1 + HI)}\right) \quad \text{When } HI > 1.00 \text{-----4.11}$$

Where: Yld is the crop yield (kg/ha),  $bio_{ag}$  is the aboveground biomass on the day of harvest (kg/ha) HI is the harvest index on the day of harvest, and bio is the total plant biomass on the day of harvest (kg/ha). The aboveground biomass is calculated:

$$Bio_{ag} = (1 - fr_{root}) * bio \text{-----4.12}$$

Where  $fr_{root}$  is the fraction of total biomass in the roots the day of harvest, and bio is the total plant biomass on the day of harvest (kg /ha).

### 3.12.3 Actual growth

Actual growth varies from potential growth due to extreme temperatures, water deficiencies and nutrient deficiencies, which are all considered as growth constraints. In SWAT model, the plant growth factor such as water stress, temperature stress, nitrogen stress, and phosphorus stress are also calculated, which quantifies the fraction of potential growth achieved on a given day the detail of these descriptions also given in SWAT manual.

### 3.13 Sensitivity Analysis

Sensitivity analysis is a technique of identifying the responsiveness of different parameters involving in the simulation of a hydrological process. For big hydrological models like SWAT, which involves a wide range of data and parameters in the simulation process, calibration is quite a cumbersome task. Even though, it is quite clear that the flow is largely affected by curve number, for example in the case of SCS curve number method, this is not sufficient enough to make calibration as little change in other parameters could also change the volumetric, spatial, and temporal trend of the simulated flow. Hence, sensitivity analysis is a method of minimizing the number of parameters to be used in the calibration step by making use of the most sensitive parameters largely controlling the behaviour of the simulated process. This appreciably eases the overall calibration and validation process as well as reduces the time required for it. Besides, as (Lenhart et al., 2002) indicated, it increases the accuracy of calibration by reducing uncertainty.

The sensitivity analysis was undertaken by using a built-in tool in SWAT2003 that uses the Latin Hypercube One-factor-At-a-Time (LH-OAT). Details of this method are explained in (Huisman et al., 2004). After the analysis, the mean relative sensitivity (MRS) of the parameters was used to rank the parameters, and their category of (Lenhart et al., 2002) classification. He divided sensitivity was also defined based on the sensitivity into four classes as shown in *table 3.4*. (Van Griensven, 2006) indicated that there can high (0.20) be a significant variation of hydrological processes between individual watersheds. This, therefore, justified the need for the sensitivity analysis made in the study area. The analysis involved a total of 28 parameters. For the study area the sensitivity analysis should be carried out for a period of five years, which included both calibration period (from January 1, 1987 to December 31, 1990) and the warm-up period (From January 1 to December 31, 1986).

Table 3.4: Sensitivity Class for SWAT model

Class	Index	Sensitivity
I	$0.00 \leq I / < 0.05$	Small to Negotiable
II	$0.05 \leq I / < 0.2$	Medium
III	$0.02 \leq I / < 1$	High
IV	$I / \geq 1$	Very high

Source: (Lenhart et. al 2002)

### 3.14 Calibration and Validation

Calibration is tuning of model parameters based on checking results against observations to ensure the same response over time. This involves comparing the model results, generated with the use of historic meteorological data, to recorded stream flows. In this process, model parameters varied until recorded flow patterns are accurately simulated. Model calibration of SWAT run can be divided in to several steps. Among these Water balance and stream flow generation are the most important part is also considered.

(Refsgaard and Storm, 1996) distinguished three types of calibration methods: the manual trial-and-error method, automatic or numerical parameter optimization method; and a combination of both methods. According to the authors, the manual calibration is the most common and especially recommended in cases where a good graphical representation is strongly demanded for the application of more complicated models. However, it is very cumbersome, time consuming, and requires experience. Automatic calibration makes use of a numerical algorithm in the optimization of numerical objective functions. The method undertakes a large number of iterations until it find the best parameters. The third method makes use of combination of the above two techniques regardless of which comes first. For this study, the first and the third approach was considered.

The manual calibration of this study was done based on the procedures recommended in SWAT2005 user manual. Water balance calibration normally takes care of the overall flow volume and its distribution among the different hydrologic components, whereas temporal flow calibration is concerned about the flow time lag and the hydrograph shape. For this case study also, as the soil moisture data is not available at the station, one of the water balance component with observed data, (stream flow) is used for calibration and validation purpose.

The automatic calibration and uncertainty analysis was done using Parameter Solution (ParaSol) ([Van Griensven et al., 2006](#)). This method was chosen for its applicability to both simple and complex hydrological models.

Calibration for water balance and stream flow is first done for average annual conditions. Once the model is calibrated for average annual conditions, it can be repeated to monthly or daily records to fine-tune the calibration. Accordingly the annual and monthly calibration was taken for the study area. Flow calibration was performed for a period of four years from January 1, 1987 to December 31, 1990 using the sensitive parameters identified. However, flow was simulated for five years from January 1, 1986 to December 31, 1990, within which the first year was considered as a warm up period.

The watershed's total water yield was firstly separated in to base flow and surface flow. In fact water yield is the summation of base flow and surface flow in which the surface flow contributes the major portions of the water yield.

The flow was calibrated manually using the observed flow gauged at the outlet of the watershed. First of all, the surface runoff flow components of gauged flow were balanced with that of the simulated flow.

Afterwards the adjusted flow was further calibrated temporally by making delicate adjustments to ensure best fitting of the simulated flow curves with the gauged flow

curves. Manipulation of the parameter values were carried out within the allowable ranges recommended by SWAT developers.

The factor of goodness fit can be quantified by the coefficient of determination ( $R^2$ ) and Nash-Sutcliffe efficiency (NSE) between the observations and the final best simulations.

Coefficient of determination ( $R^2$ ) and Nash-Sutcliffe coefficient (NSE) are

Calculated by:

$$R^2 = \frac{[\sum_i (Q_{m,i} - \bar{Q}_m)(Q_{s,j} - \bar{Q}_s)]^2}{\sum_i (Q_{m,i} - \bar{Q}_m)^2 \sum_i (Q_{s,i} - \bar{Q}_s)^2} \text{-----4.14}$$

$$NSE = 1 - \frac{\sum_i (Q_m - Q_s)^2}{\sum_i (Q_{m,i} - \bar{Q}_m)^2} \text{-----4.15}$$

In which  $Q_m$  is the measured discharge,  $Q_s$  is the simulated discharge,  $\bar{Q}_m$  is the average measured discharge and  $\bar{Q}_s$  is the average simulated discharge.

### 3.15 Model Setup

The model setup involved five steps: (1) data preparation, (2) sub basin discretization, (3) HRU definition, (4) parameter sensitivity analysis, (5) calibration and uncertainty analysis.

The required spatial data sets were projected to the same projection called Adindan UTM Zone 37 N, which is the transverse Mercator projection parameters for Ethiopia, using ArcGIS 9.2. The DEM was used to delineate the watershed and to analyze the drainage patterns of the land surface terrain. We have used DEM mask that was superimposed on the DEM since the model uses only the masked

area for stream delineation. A predefined digital stream network layer was imported and superimposed onto the DEM to accurately delineate the location of the streams. The Land use/Land cover spatial data were reclassified into SWAT land cover/plant types. A user look up table was created that identifies the SWAT code for the different categories of land cover/land use on the map as per the required format. The soil map was linked with the soil data-base which is a soil database designed to hold data for soils not included in the U.S.

The watershed and sub watershed delineation was done using DEM data. The watershed delineation process include five major steps, DEM setup, stream definition, outlet and inlet definition, watershed outlets selection and definition and calculation of subbasin parameters. For the stream definition the threshold based stream definition option was used to define the minimum size of the sub basin. The Arc SWAT interface allows he user to fix the number of sub basins by deciding the initial threshold area.

The threshold area defines the minimum drainage area required to form the origin of a DEM setup, stream definition, outlet and inlet definition, watershed outlets selection and definition and calculation of sub basin parameters. For the stream definition the threshold based stream definition option was used to define the minimum size of the sub basin. The Arc SWAT interface allows the user to fix the number of sub basins by deciding the initial threshold area. The threshold area defines the minimum drainage area required to form the origin of a stream.

### **3.16 Arc SWAT Model Inputs**

The spatially distributed data (GIS input) needed for the Arc SWAT interface include the Digital Elevation Model (DEM), soil data, land use, and stream network layers. Data on weather is used for prediction of soil moisture and calibration purposes.

### **3.16.1 Weather Data**

SWAT requires daily meteorological data that could either be read from a measured data set or be generated by a weather generator model. In this study, the weather variables used for driving the hydrological balance are daily precipitation, minimum and maximum air temperature, Relative humidity, wind speed and solar radiation for the period 1986 – 2005 base line. These data were obtained from Amhara Region Agricultural Research Institute (ARARI), Ethiopia for Anjeni watershed and Ethiopian National Meteorological Agency (NMA) for stations located around the watershed. Finally, we used Statistical downscaling model (SDSM) for the generation of future climate scenarios for daily precipitation, minimum and maximum air temperature from 2002 to 2070.

### **3.16.2 Digital Elevation Model (DEM)**

Topography is defined by a DEM that de-scribes the elevation of any point in a given area at a specific spatial resolution. A high resolution DEM (2 m by 2 m) was obtained from Soil Conservation Research Program (SCRIP), University of Bern, Switzerland. The DEM was used to delineate the watershed and to analyze the drainage patterns of the land surface terrain. Sub-basin parameters such as slope gradient, slope length of the terrain, and the stream network characteristics such as channel slope, length, and width were derived from the DEM.

Table 3.5: Transverse Mercator projection parameters for Ethiopia (Dilnesaw, 2006)

Projection	Transverse_Mercator
Projected coordinate system	Adindan_UTM_Zone_37N
Geographic Coordinate System GCS_Adindan	GCS_Adindan
Datum	D_Adindan Prime Meridian: 0
False Easting	500000.000
False Northing	0.000
Central Meridian	39.000
Scale Factor	0.9996
Latitude_Of_Origin	0.000
Linear Unit	Meter (1.000)

The DEM was then projected according to table 3.5. The appropriate coordinate system and converted into a GRID format using spatial analysis tool of ArcGIS 9.2 software.

### 3.16.3 Land Use

Land use category was obtained from soil conservation research program (SCRIP), Biniam, 2009. The land uses from him are relatively not simplistic, because it contains all categories of land uses like Agricultural Land-Genetic, Low density Rural Settlement, and others. SWAT has predefined land uses identified by four-letter codes and it uses these codes to link land use maps to SWAT land use databases in the GIS interfaces. Hence, while preparing the lookup-table, the land use types were made compatible with the input needs of the model.

*Table 3.6: Original land use/land cover types redefined according to the SWAT code and their aerial coverage.*

Original land use	Redefined land use according to SWAT database	SWAT code	Area (Ha)	% watershed
No data	No data	SWCH	6.32	7.25
Nug	Alfa alfa	ALFA	4.23	4.40
Grass land	Range Grass	RNGE	10.23	10.82
Wheat	Spring Wheat	SWHT	9.33	9.41
Barely	Spring Barely	BARL	9.72	9.83
Horse bean	Soya Bean	SOYB	1.80	1.81
Maize	Corn	CORN	17.69	18.47
Sinar	Pine	PINE	2.10	2.12
Bush Land	Range brush	RNGB	2.63	2.82
Teff	TEFF	TEFF	13.33	13.43
Fallow	Pasture low density	PAST	1.21	1.30
Bare Land	Bermuda Grass	BERM	6.02	6.16
Pea	Field pea	FPEA	0.45	0.45
Forest	Mixed Forest	FRST	7.66	7.90
linseed	Perl Millet	PMIL	0.52	0.53
Settlement	Urban Low density r residential	URLD	2.88	3.07
New plantation	Tall Fescue	FESC	0.24	0.24

### 3.16.4 Soil Data

SWAT model requires different soil textural and physico-chemical properties such as soil texture, available water content, hydraulic conductivity, bulk density and organic carbon content for different layers (up to 4 layers) of each soil type. These data were obtained mainly from the following sources: Amhara Region Agricultural Research Institute (ARARI), Ethiopia, Abbay River basin Integrated Development Master Plan Project - Semi detailed Soil Survey and Africa CD-ROM (Food and Agriculture Organization of the United Nations (FAO, 1998)), Major Soils of the world CD-ROM (FAO, 2002), Digital Soil Map of the World and Derived Soil Properties CD-ROM (FAO, 1995), Properties and Management of Soils of the Tropics CD-ROM (Van Wambeke, 2003) Major soil types in the basin are Chromic Luvisols, Eutric Cambisols, Eutric Fluvisols, Eutric Leptosols, Eutric Regosols, Eutric Vertisols, Haplic Alisols, Haplic Luvisols, Haplic Nitisols and Lithic Leptosols.

*Table 3.7: Soil type of the study area with their aerial coverage*

<b>Soil type</b>	<b>symbol</b>	<b>Area(ha)</b>	<b>% in the watershed</b>
Lithic Leptosols	LPq	2.3987	3.877
Vertic Luvisols	LVv	1.1257	18.797
Haplic Alisols	Alh	1.1325	17.067
Dystric Cambisols	CMd	1.0358	9.029
Eutric Regosols	Rge	1.8199	6.47
Humic Nitisols	Ntu	6.6090	2.507
Haplic Acrisols	Ach	1.2664	20.04
Humic Alisols	Alu	2.4010	15.117
Haplic Nitisols	NTh	0.95802	4.724
Haplic Lixisols	LXh	4.80494	2.373

The management operations were defaulted by the SWAT2000 ARCGIS interface (Arc SWAT), consisted simply of planting, harvesting, and automatic fertilizer applications for the agricultural lands. Since objective of the study was concerned on the impact of climate change on water availability and crop production by assuming that other SWAT input parameters held constant, the default management activities rather than climate variables (precipitation and temperatures) were taken for simulation purpose.

### **3.16.5 Slope**

Slope is derived from inputted DEM, so that the model uses this slope for the development of Hydrological Response Unit (HRU) in addition to Land use and soil input parameters. Arc SWAT allows the integration of land slope classes (up to five classes) when defining hydrologic response units. There are possibilities to choose simply a single slope class, or choose multiple classes. From the given DEM, slope of watershed varies from minimum 0 to maximum 84% and 16.5%, 19.8% for mean and median respectively. Depending on this variation, this study considers all five classes, by dividing land slope classes as: class1: 0 to 5%, class2: 5-10, class3:10-15%, class4: 15-20%, class5:20-9999%.

### **3.16.6 Watershed Delineation**

The ArcGIS tool in Arc SWAT partitions watersheds into a number of hierologically connected sub basins based on flow directions and accumulations. The watershed and sub basins delineation was carried out based on an automatic delineation procedure using a Digital Elevation Model (DEM) and digitized stream networks. The model fills all of the non-draining zones (sinks) to create a flow vector, and superimposes the digitized stream networks into the DEM to define the location of the stream network.

The Arc SWAT interface proposes the minimum, maximum, and suggested size of the sub basin area (in hectare) to define the minimum drainage area required to form the origin of a stream. Generally, the smaller the threshold area, the more detailed are the drainage networks, and the larger are the number of sub basins and HRUs. However, this needs more processing time and space. As a result, an optimum size of a watershed that compromises both was selected. (Dilnesaw, 2006) did a sensitivity analysis of the threshold area on SWAT model performance and found that the optimum threshold area that can be used for the delineation procedure is  $\pm 1/3$  of the suggested threshold area. Therefore, a threshold area of  $+1/3$  of that suggested by the model was used. With respect to the given area of watershed, only one outlet is defined, which is later taken as a point of calibration and validation of the simulated flows. As a result actual Anjeni watershed outlet is delineated.

### **3.16.7 Determination of Hydrologic Response Units (HRUs)**

The sub basin delineation was followed by the determination of HRUs, which are unique soil, land use and slope combinations within a sub basin modelled regardless of their spatial positioning. This describes better the hydrologic water balance and increases the accuracy of load predictions. SWAT predicts the land phases of the hydrologic cycle separately for each HRU and routes to obtain the total loadings of the sub watershed.

The HRUs can be determined either by assigning only one HRU for each sub watershed considering the dominant soil/land use/slope combinations, or by assigning multiple HRUs for each sub watershed considering the sensitivity of the hydrologic process based on a certain threshold values of soil/land use/slope combinations. For this study, the latter method was adopted as it better describes the heterogeneity within the watershed and as it accurately simulates the hydrologic processes.

### **3.17 Determination of Impacted storage and productivity**

The impacts climate change and management change scenarios are two different scenarios assessed using Arc SWAT model. The future climate variable that is daily precipitation and maximum and minimum temperature found as an output from the GCM model and downscaled by the SDSM model were given as an input to the SWAT model. The remaining climatic and all other land use and soil hydrologic parameters used in model development under current climate conditions were assumed to be constant and remain valid under conditions of climate change. The future two periods, 2020s and 2050s are used as an input in SWAT model. The two periods are prepared as individual stations in the SWAT data base.

SWAT was applied to simulate the impacts of climate change on crop production by assuming that change in precipitation and temperature from base line period affect time of planting dates and sometimes failure in crop due to extreme events. Assuming all other parameters held constant for future time periods, downscaled climate variables of precipitation and temperatures used as input for SWAT model and then change in crop productivity due to changed climate variables will be simulate.

## **CHAPTER FOUR**

### **RESULTS AND DISCUSSIONS**

#### **4.1 Climate change scenario results**

##### **4.1.1 Baseline scenarios**

The base line scenarios downscaled for base period for the two stations; 30-year period from 1961-1990 and 16-year period from 1986-2001 was selected for Debra Markos and Anjeni station respectively, to represent baseline for this study. Thus the HadCM3 GCM was downscaled for the base period for two emission scenarios (A2a and B2a) and some of the statistical properties of the downscaled data were compared with observed data. In both stations the downscaled base line temperatures shows good agreement with observed data. In the case of precipitation, also even though there were little variations in individual months which are due to local effects, the downscaled values have good concurrence with observed data. In general, in both stations the downscaled climate variables (precipitations, maximum and minimum temperatures) have good fit with observed data as shown in the figure from 4.1 to 4.6, which is very important for future climate generations.

##### **4.1.2. Base line Scenario developed for Anjeni watershed (1986-2001)**

To downscale future climate it's necessary to use observed climate data, which is very imperative to calibrate and validate climate model. Thus HadCM3 was downscaled for the base period with two emission scenarios (A2a and B2a) and some of the statistical properties of the downscaled data were compared with observed data. The climatological base line period used for the impact assessment was 1986-2001 for Anjeni research center station. Precipitation, maximum and minimum temperature variables are also downscaled for future climate period (2011-2070).

## I. Precipitation

The downscaled values of precipitation for the base period were averaged into a monthly time step to compare with observed values which are shown in figure 4.1. The SDSM model performs reasonably well in estimating the mean monthly precipitation in many months but there is a relatively large model error in the month of July and August. The result, however, can be taken as satisfactory given that precipitation downscaling is necessarily more problematic than temperature, because daily precipitation amounts at individual sites are relatively poorly resolved by regional scale predictors, rather it depends on local factors like topography.

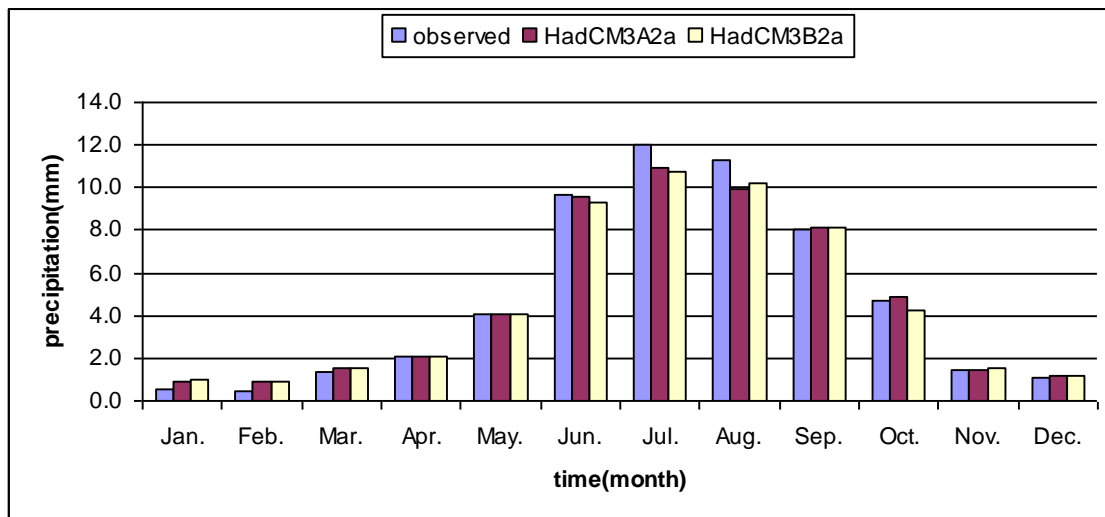


*Figure 4.1: Average daily precipitation for Anjeni (station) research center for base period*

## II. Maximum temperature

The projected maximum temperature for baseline period shows good agreement between observed and downscaled values (Fig. 4.2). It shows maximum temperature on dry seasons as observed data. Except for months of October and February in which the model underestimates, the model showed good agreement with observed rainfall data.

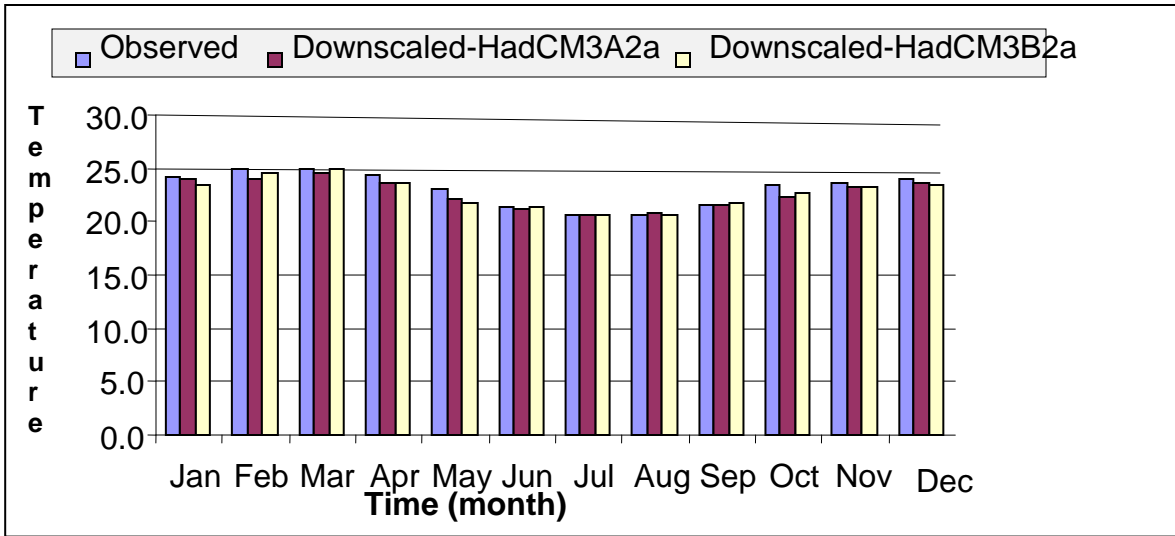


Figure4.2: Average daily maximum temperature of observed and downscaled at Anjeni Station for the base period

### III. Minimum Temperature

Except little variation in months of May, and June, the projected minimum temperature for baseline period showed good agreement with observed data (Fig.4.3). In general the model out put has similar trends with observed data which is satisfactory result for future projection of minimum temperature.

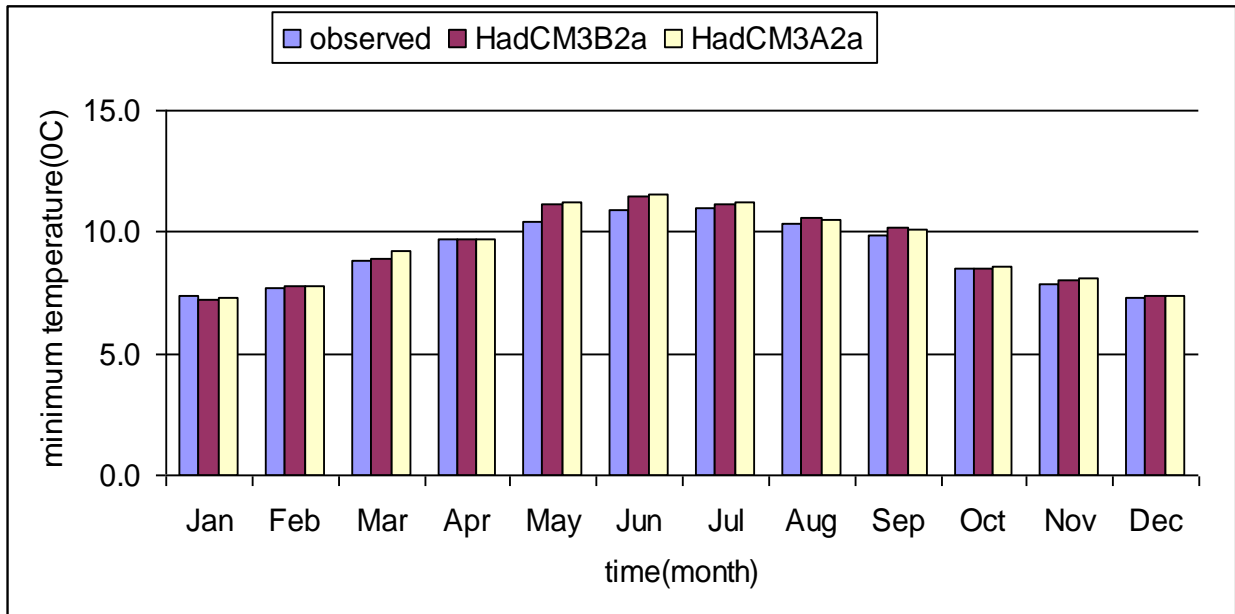


Figure4.3: Observed and downscaled Average daily minimum temperature of Anjeni Station for the base period

### 4.1.3 Base line Scenario developed for Debra Markos station (1961-1990)

#### I. precipitation

For the sake of comparison with the observed values, the generated values of the base period were averaged to a monthly time step. The comparison statistics with the observed values are shown in the figure 4.4.

As has been shown in the Fig.4.4, the SDSM performs reasonably well in estimating mean daily precipitation in many months except months of July and August, in which the model shows underestimation. However the result is taken as satisfactory, given that the precipitation downscaling is less defined by large scale weather parameters and also SDSM is poor in performing extreme events. This lack of replicating the extreme values was also observed by SDSM developer and they described it as “the model is less skilful at replicating the frequency of events”. Out of these two months the downscaled precipitation values follow the same trend as observed values.

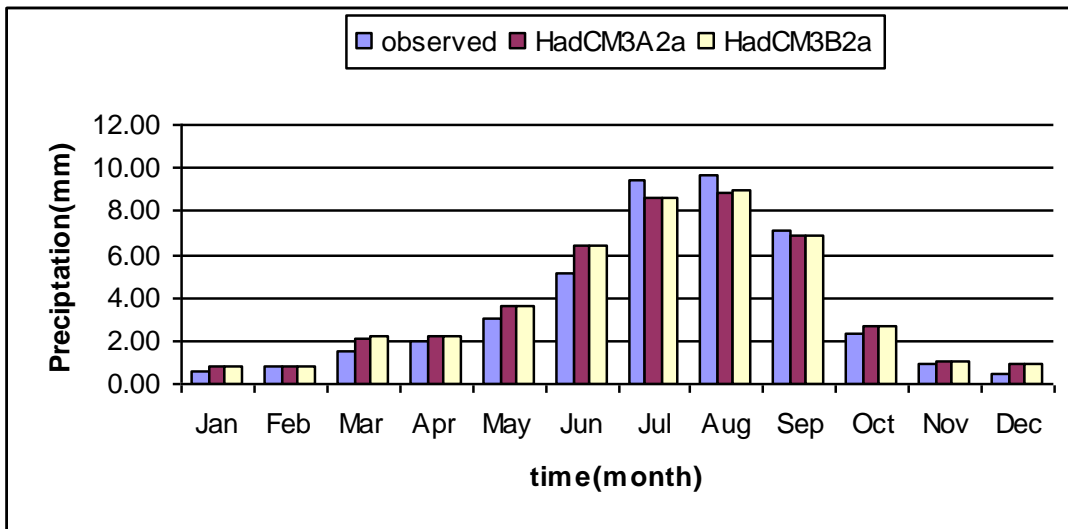


Figure4.4: Observed and downscaled mean daily precipitation for base line scenarios (1961-1990)

## II. Maximum temperature

As compared with observed maximum temperature, the statistical downscaling model slightly shows slight overestimation for the wettest months of June, July and August (Fig.4.5). Otherwise it showed better fit with other months. In other words, the patterns and trend of the downscaled maximum temperature shows good agreement with observed values.

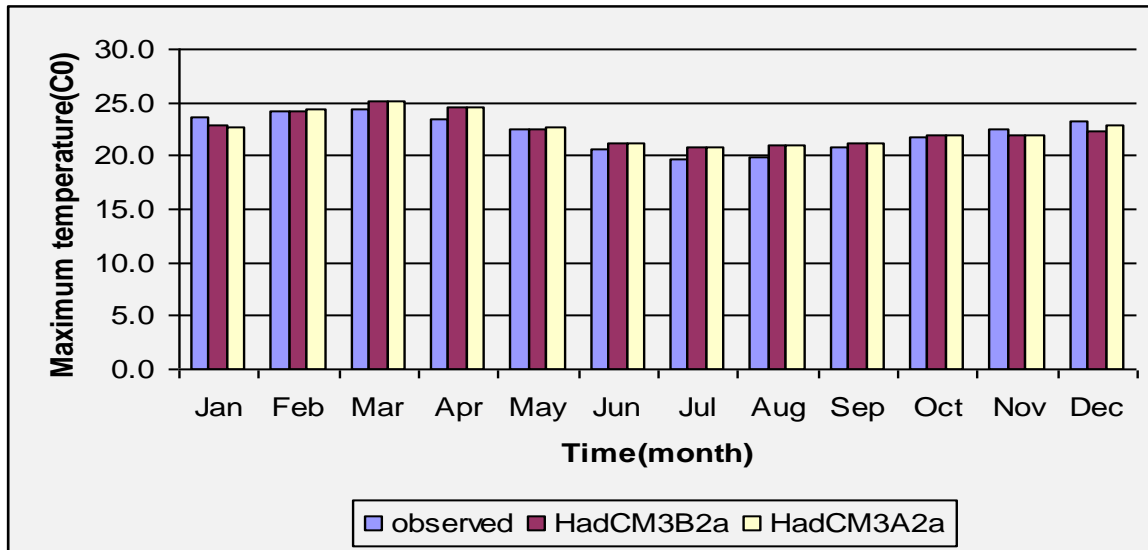


Figure4.5: Observed and downscaled mean daily maximum temperature for base line (1961-1990)

## III. Minimum temperature

The monthly minimum temperature downscaled for HadCM3A2a and HadCM3B2a for Debra Markos station shows (Fig.4.6) slight underestimation for many months. Except for months of December, October, July and slightly for April in which model has best performance, the downscaled minimum temperature for this particular area has slight deviations from the observed values. Where as, in the Anjeni Station for the same HadCM3A2a and HadCM3B2a grid, the Downscaled minimum temperature relatively shows good agreement with observed data.

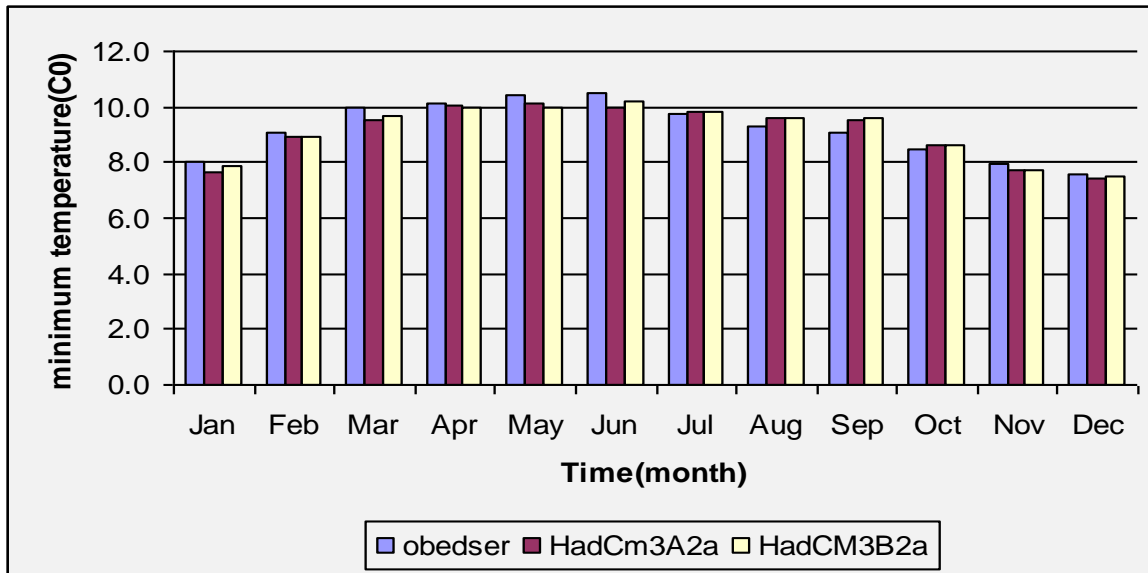


Figure4.6: observed and downscaled mean daily minimum temperature for base period at Debra Markos station (1961-1990)

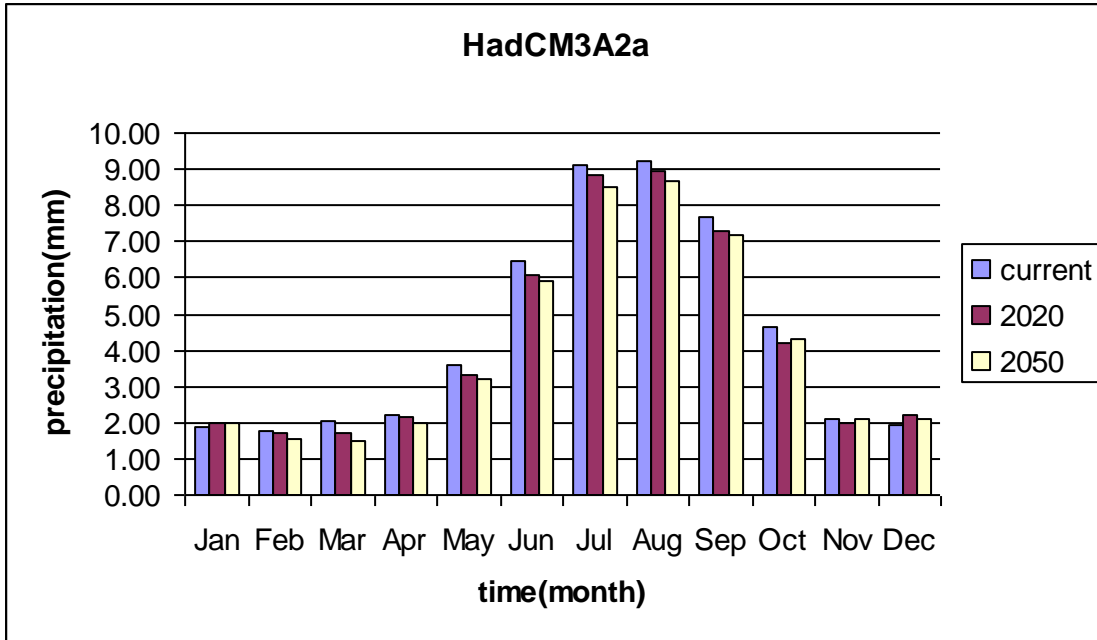
#### 4.1.4 Downscaling future scenarios

Future climate scenarios downscaled for three climate variables (precipitation, maximum and minimum temperature) are shown in the figure 4.7- 4.10. With the aid of statistical downscaling model the GCMs global predictors are used for development of future climate scenarios and the analysis done for 2020s, 2050s and 2080s for both A2 and B2 scenarios.

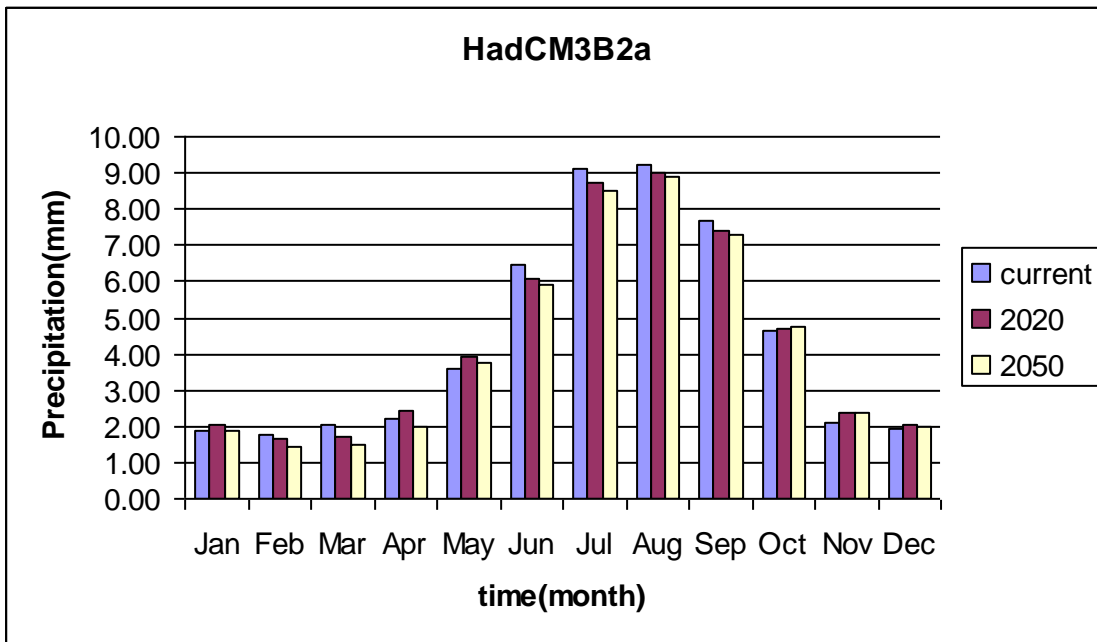
#### I. Precipitation

For Debra Markos station the future rainfall projections show the decreasing trends for all three periods by reproducing the actual patterns of precipitation for both A2 and B2 scenarios (Fig.4.7). As compared to the current situation (1991-2010), the 2020s, 2050s, and 2080s periods shows decreasing trends for all months. Where as when individual months are considered, the 2020s period shows relatively wettest condition during o months of November, December and January. Wettest condition will also occur for other two periods in relatively lower values.

For Kiremt months (June, July and August) rainfall will experience a decrease in amount for both scenarios in all periods. Where as for dry months rainfall will experience increase in total amount for both scenarios in all periods. The projection of precipitation for the periods 2080s and 2050s shows future decrease in rainfall amount in all months. Where as projection of precipitation for 2020s shows relatively small future changes in the beginning of rainy season, and decrease in rainfall for Kiremt season and relatively increase in rainfall amount at the end of rainy season.



(a)



(b)

Figure4. 7: Downscaled Mean daily precipitation of future period For Debra Markos station, (a) & (b) for A2a& B2a scenarios, respectively

Where as, for Anjeni station (Fig.4.9) the projected precipitation does not exhibit similar trends for future periods as compared to current period for both A2 and B2 scenarios. According to projected precipitation at Anjeni station, the average monthly precipitation does not show increasing or decreasing trends for both A2 and B2 scenarios in all time periods. In Fig.4.8 future rainfall shows decreasing trend from mid of 2020s onwards and then shows increasing trend in 2050s. In main rainy season (Jun, July, and August), rainfall will show decreasing in probably less amount and increases towards the months of September and October which initially experience lower rainfall amount for base period. However, for months of March, April, and May the rainfall experience increase in total amount in future periods. In general future projection of precipitation for Anjeni station will show increasing trend in rainfall amount at the beginning of rainy season April and May, and then probably decreasing trend for main rainy season and then relatively continuous wettest conditions for dry months.

As discussed above the projection of precipitation using HadCM3A2a and HadCM3B2a from one grid cells but for different stations resulted in different outcomes. This observation has revealed the fact that the statistical downscaling model projection depends on the statistics of the station observed data and also precipitation is highly affected by local weather system.

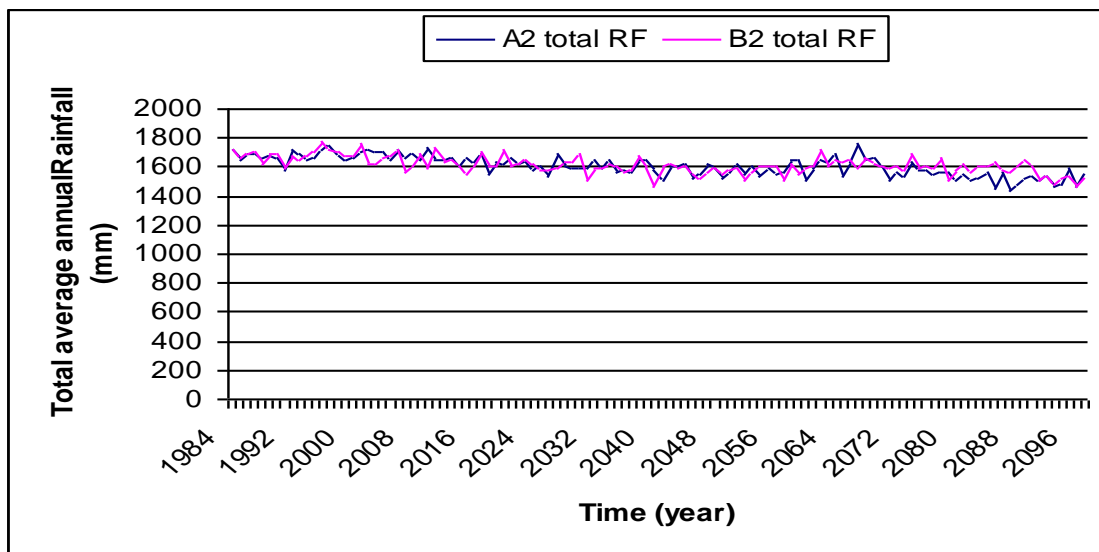
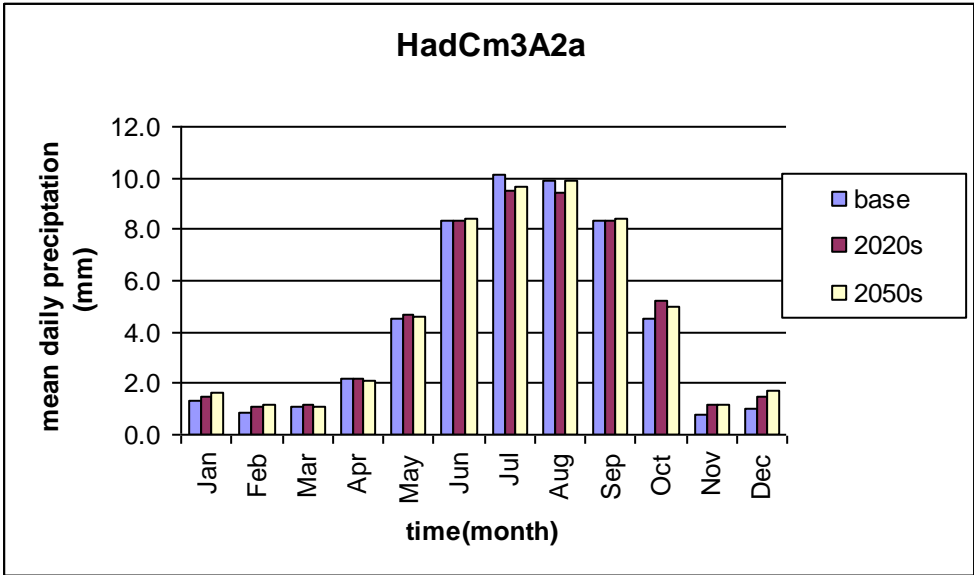
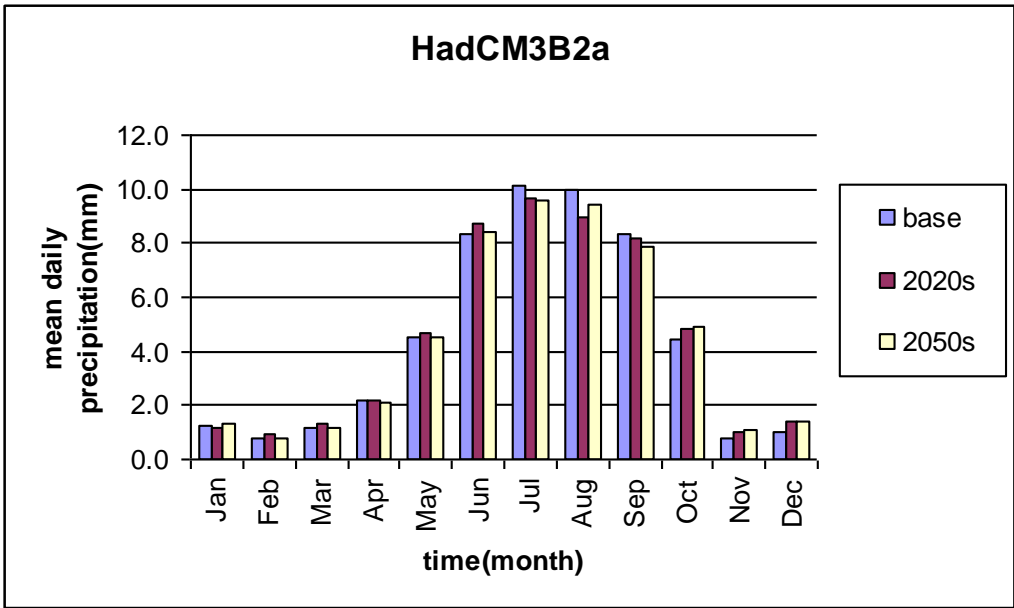


Figure4.8: Future patterns of annual rainfall at Anjeni station (1984-2099)



(a)



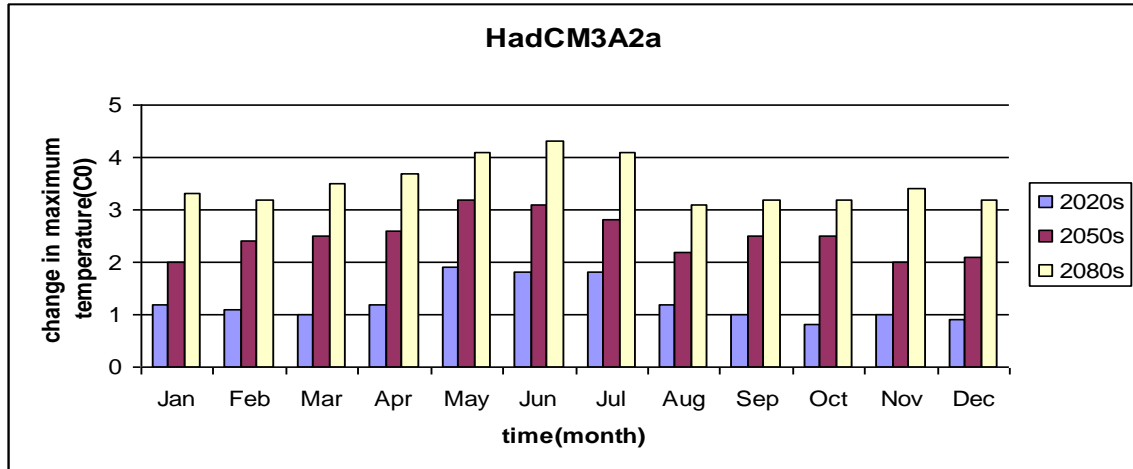
(b)

Figure4.9: Downscaled Mean daily precipitation of future period for Anjeni station: (a) & (b) for A2a& B2a scenarios, respectively

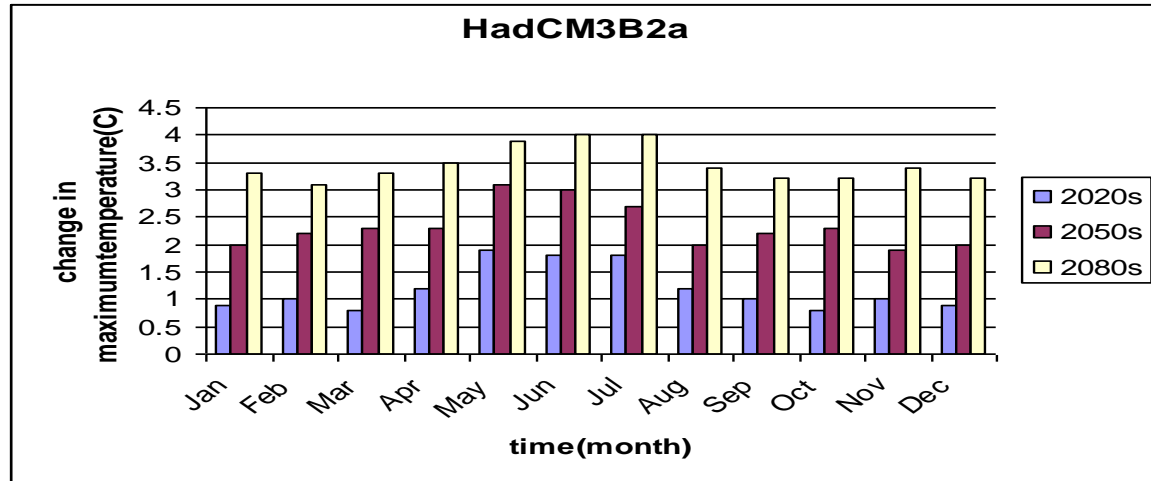
## II. Maximum Temperature

Unlike that of precipitation, the projected maximum temperature shows similar trends and patterns for two stations, which is increasing trend for both A2a and B2a scenarios. This might be due to the fact that local temperature change is highly defined by global variables used by general circulation models. Figure:4.10 (a and b) shows change in maximum temperature at Debra Markos station relative to base period for both A2a and B2a scenarios. It shown that a change in maximum temperature for future periods will vary from month to month, and the highest maximum temperature projected for months of May, June, and relatively for month of July.

The projected maximum temperature in 2020s indicated that maximum temperature will rise by  $1.2^{\circ}C$ . In 2050s the increment will be  $2.4^{\circ}C$  and  $2.0^{\circ}C$  for A2a and B2a scenarios, respectively. Where as, in 2080s the maximum temperature will be increased by  $3.8^{\circ}C$  and  $3.2^{\circ}C$  for A2a and B2a scenarios, respectively. This shows that the future period will experience increasing trend in maximum temperature for both A2a and B2a scenarios. However, the increments will be less for B2a scenario relative to A2a scenario. This is due to the fact that A2a represents medium high scenario which produces more CO<sub>2</sub> as compared to B2a scenario which is medium low scenario.



(a)



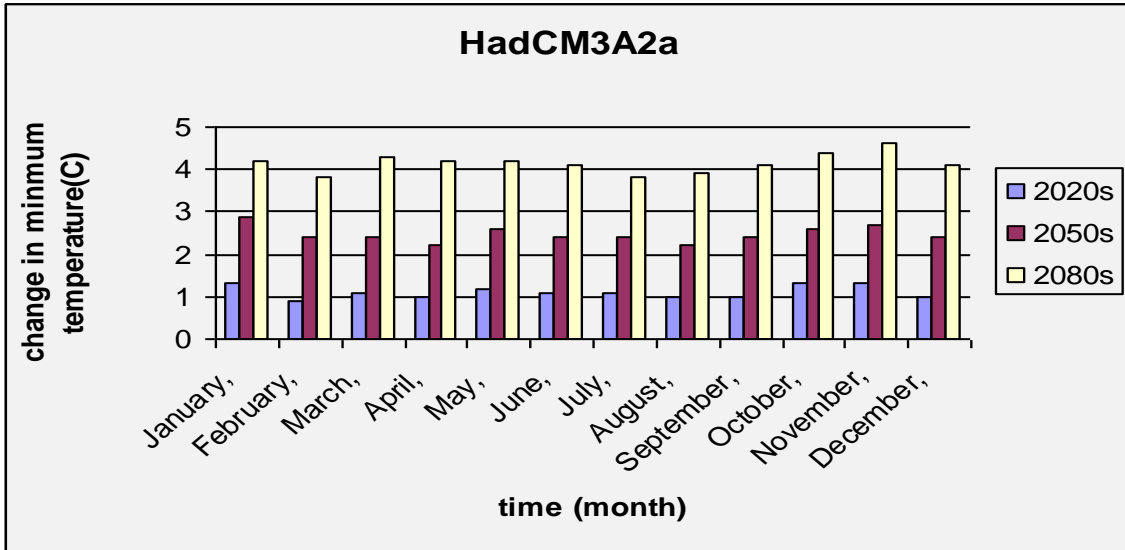
(b)

Figure 4.10: Change in average monthly maximum temperature (delta values) in the future (1991-2099) from the base period average monthly maximum temperature (a) & (b) for A2a & B2a scenarios respectively

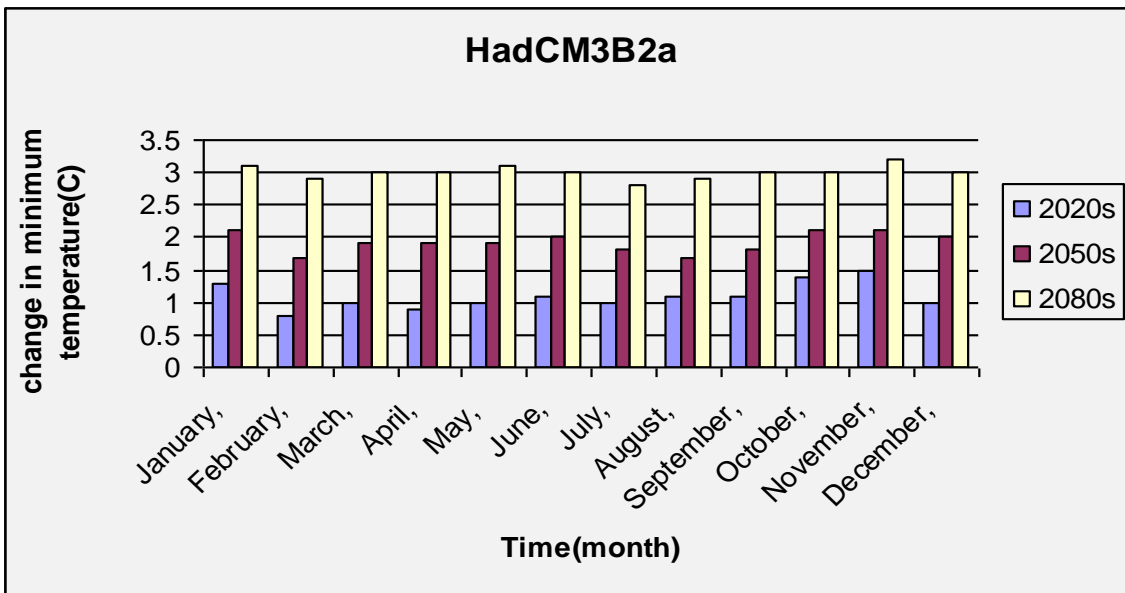
### III. Minimum Temperature

Like case of projected average monthly maximum temperature, minimum temperature also reflects increasing trend in future climate periods. The projected minimum temperature for future periods for A2a and B2a scenarios are shown in Figure 4.11. As change of minimum temperature for both Debra Markos and Anjeni stations shows similar future trends in minimum temperature, only Debra Markos station is discussed here.

Even though all months show similar trends in the future climate periods, the highest maximum projected minimum temperature will occur during months of November, December and January for both A2a and B2a scenarios. The downscaled minimum temperature in 2020s indicated that the minimum temperature will rise by  $1.2^{\circ}C$  for both A2a and B2 scenarios. For 2050s the increment will be  $2.2^{\circ}C$  for A2a and  $1.9^{\circ}C$  for B2a scenarios respectively. The increment will be expected to be high in 2080s, which is  $3.8^{\circ}C$  for A2a and  $2.9^{\circ}C$  for B2a scenarios respectively.



(a)



(b)

Figure 4.11: Change in average monthly minimum temperature (delta values) in the future (1991-2099) from the base period average monthly precipitation (a) & (b) for A2a & B2a scenarios respectively.

Generally, it is important to recall that, the SDSM out put for both stations shows that there is an increasing temperature trends for the future climate periods. This shows that the dependability of local temperature on global predictors. In the case of precipitation, even though the two stations are found in one grid of GCM, SDSM output of precipitation values are different. This might be due to dependence of precipitation on local variables like topography and other local weather parameters. In addition to uncertainties in precipitation downscaling, which is more of conditional type, the statistics of the station data may be the reasons for variability of precipitation output from statistical downscaling model.

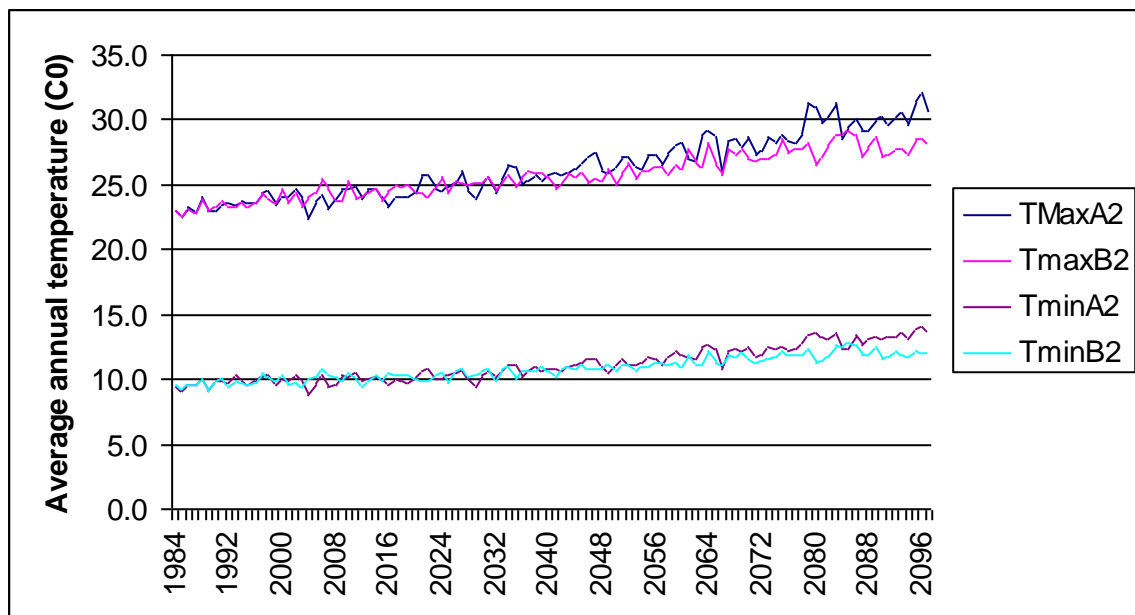


Figure 4.12: Trends of average annual maximum and minimum temperature at Anjeni Station (1984-2099)

## 4.2 SWAT Model Results

### 4.2.1 Soil water storage Simulation for Anjeni watershed

For effective simulation of soil storage the whole watershed is divided into 27 sub basins based on threshold area of 1.5 ha and 188 HRUs. Figure 4.13 shows delineated watershed and subbasins.



*Figure4.13: Delineated watershed of Anjeni Watershed*

Each HRU is composed of land use, soil, and slope parameters. The land used for this analysis consists of 16 land use types which described in table 3.6; with the dominance of Agricultural land use (Wheat 18.46%, Teff 13.42% and Maize and Barley covers the total area of 9.4 and 9.8 respectively).

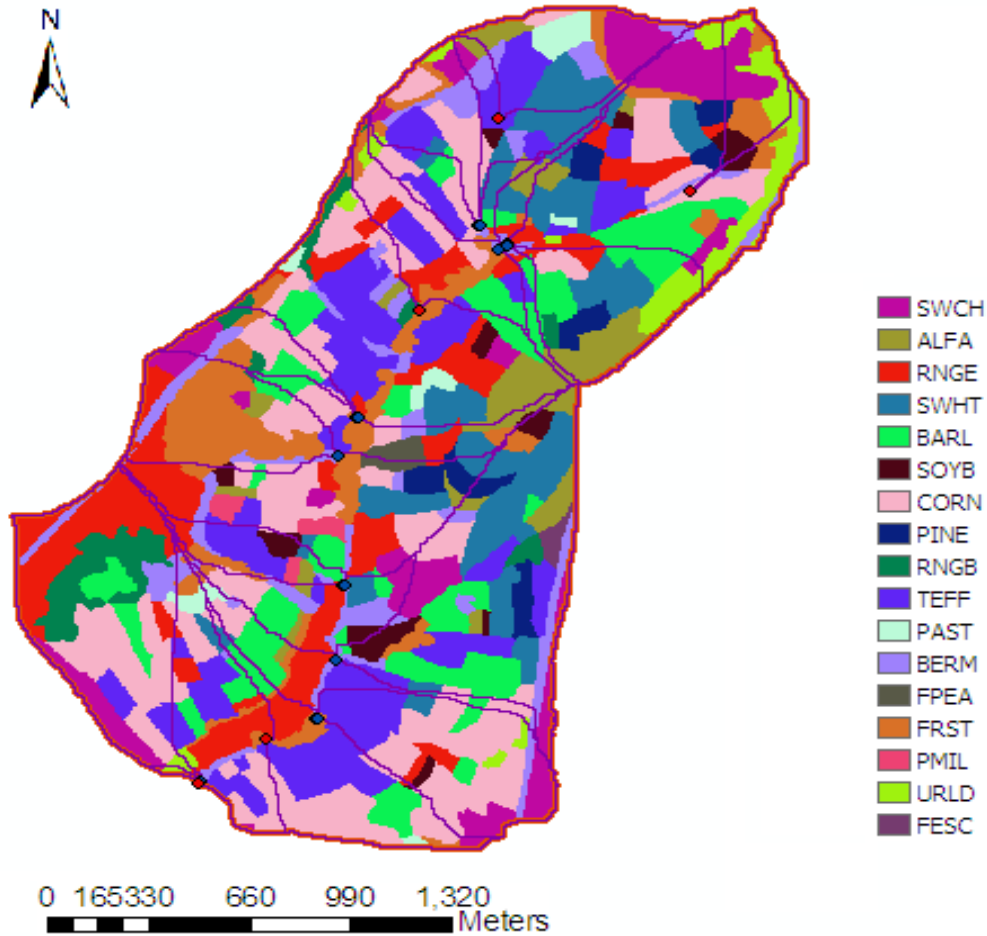


*Figure4.14: Land Use of Anjeni Watershed*

The second components of HRU was soil type, with detailed total area coverage is given in the Table 3.7. The watershed is covered with ten different soil types and the major ones are Haplic Acrisols, Vertic Luvisols, Haplic Alisols and Humic Alisols with their total aerial coverage of 20.04%, 18.797%, 17.067% and 15.117% respectively.

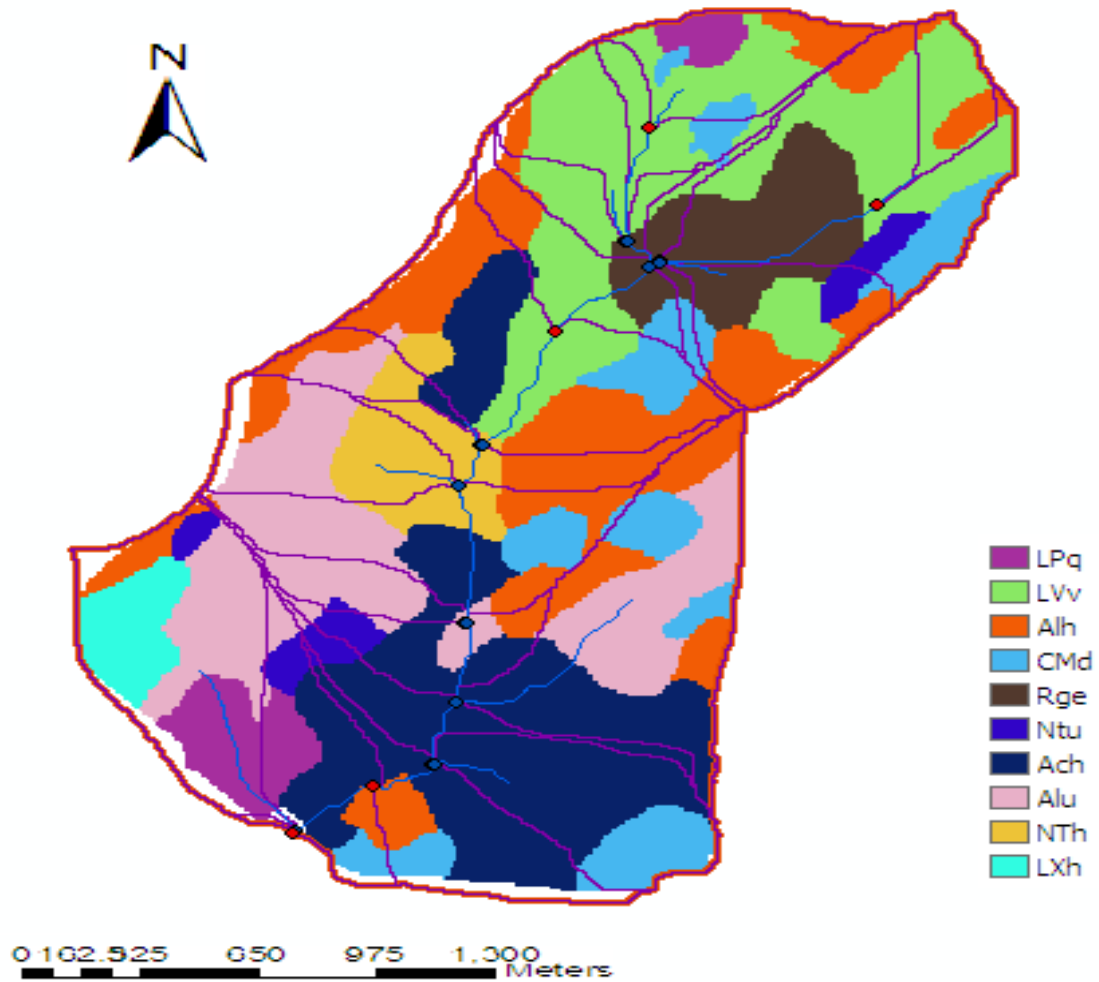


*Figure4.15: Soil Map of Anjeni Watershed*

For best definition of HRUs, slope was divided into five classes for Anjeni watershed as described in the methodology part, which is clearly shown in the figure 4.16.

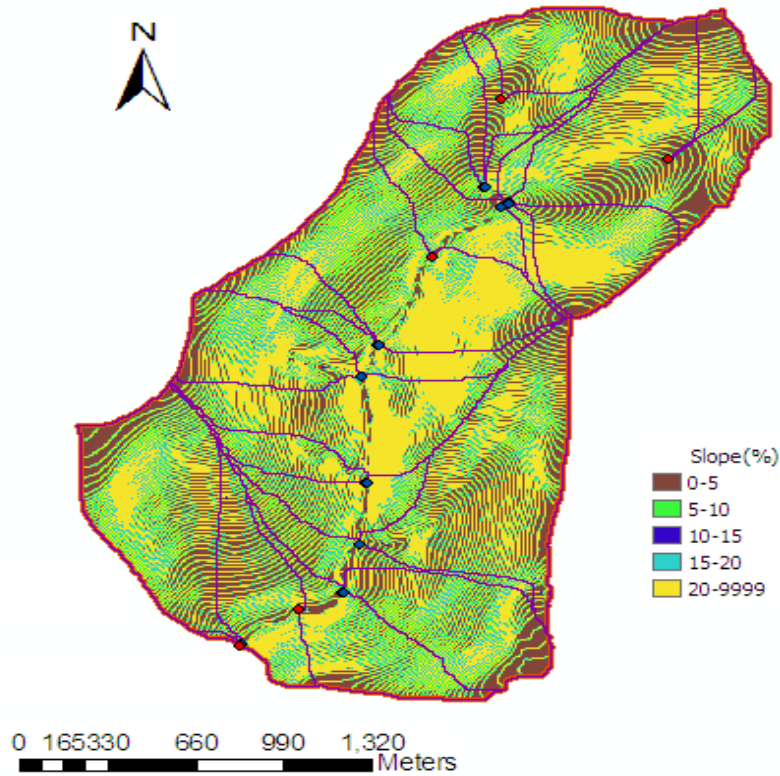


Figure4.16: Land Slope of Anjeni Watershed

#### 4.2.2 Sensitivity Analysis

Even though 28 parameters were considered for the sensitivity analysis, only 13 of them are effective for monthly flow simulation analysis. As shown in Table 4.3, the first eight parameters showed a relatively higher sensitivity, being the Alfa base flow parameter being the most sensitive of all. The four most sensitive parameters controlling the surface runoff in the watershed are the Base flow alpha factor (ALPHA\_BF), the threshold water depth in the shallow aquifer for flow (GWQMN), curve number (CN2), Ground water delay (Gw\_Delay), the soil evaporation compensation factor (ESCO), Plant uptake compensation facto (Epc), and the soil available water capacity (SOL\_AWC)

Table 4.3: Result of the sensitivity analysis of flow in Anjeni watershed

<b>Ran k</b>	<b>Parameters</b>	<b>Description</b>	<b>Lower bound</b>	<b>Upper bound</b>	<b>Relative sensitivity</b>	<b>Category of sensitivity</b>
1	Alpha_Bf	Alpha base flow(days)	0	1	1.14	Very high
2	Gwqmn	Threshold water depth in the shallow aquifer for flow [mm]	0.00	5000.0	0.5	High
3	CN2	Initial SCS CNII value r	-25%	25%	0.39	High
4	Gw_Delay	Ground water delay	-10	10	0.27	High
5	Esco	Soil evaporation compensation factor	0.00	1.0	0.24	High
6	Epc0	Plant uptake compensation facto	-25%	25%	0.18	High
7	Sol_Awc	Soil available water capacity [mm WATER/mm soil]	-25%	25%	0.18	High
8	Sol_Z	Soil depth [mm]	0.00	3000.0	0.13	Medium
9	Slope	Average slope steepness [m/m]	0.00	0.60	0.08	Medium
10	Sol_K	Saturated hydraulic conductivity [mm/hr]	-25%	25%	0.07	Medium
11	Surlag	Surface runoff lag time [days]	0.00	10.00	0.05	Medium
12	Gw Revap	Ground water Revap	-0.036	0.036	0.04	small

### 4.2.3 Flow Calibration

Some of the initial/default and finally adjusted parameter values are shown in table 4.4.

*Table 4.4: Initial and finally adjusted parameter values of the flow calibration at the outlet of Anjeni watershed*

S.NO	Parameters	description	Effects on simulation	range	Initial value	Adjusted value
1	CN2	Initial SCS CNII value	Increase surface runoff	-25% - 25%	default	10%
2	RevapMN (mm)	Threshold depth of water in the shallow aquifer for Revap to occur	Decrease ground water	0 to 500	default	1
3	ESCO	Soil Evaporation compensation factor	Increase surface runoff	0.0 - 1	default	0.95
4	GWmn (mm)	Threshold depth of water in the shallow aquifer required for return flow to occur	Decrease Ground water	0.02 - 0.2	default	100

As shown in the table 4.5, the average annual simulated water yield compared with observed one, which was found to be good start up for further calibration purpose

*Table 4.5 observed and simulated water yield during calibration period*

	Total water yield (mm)	Base Flow (mm)	Surface flow (mm)
Actual	715.7		
Simulated	786.78	328.23	426.84

#### 4.2.4 Annual Water Balance

Average annual water balance in the watershed for both calibration and validation period was given below. The standard land phase hydrologic parameters used in SWAT were considered for annual water balance.

*Table 4.6: Mean Annual Simulated water balance values (mm)*

	<b>Calibration period (1986-1990)</b>	<b>validation period (1991-1993)</b>
Precipitation	1679.4	1611.3
Surface runoff	618.5	384.52
Base flow	328.23	316.19
Revap or shallow aquifer recharges	25.17	23.49
Shallow aquifer recharges	53.03	108.64
Deep AQ Recharge	53.04	108.64
Total AQ recharge	212.14	434.56
Total water yield	734.21	668.62
Percolation out of soil	213.7	437.56
Actual evapotranspiration	793.8	770.7
Potential evapotranspiration	1529.6	1451.2
Transmission losses	51.57	32.01

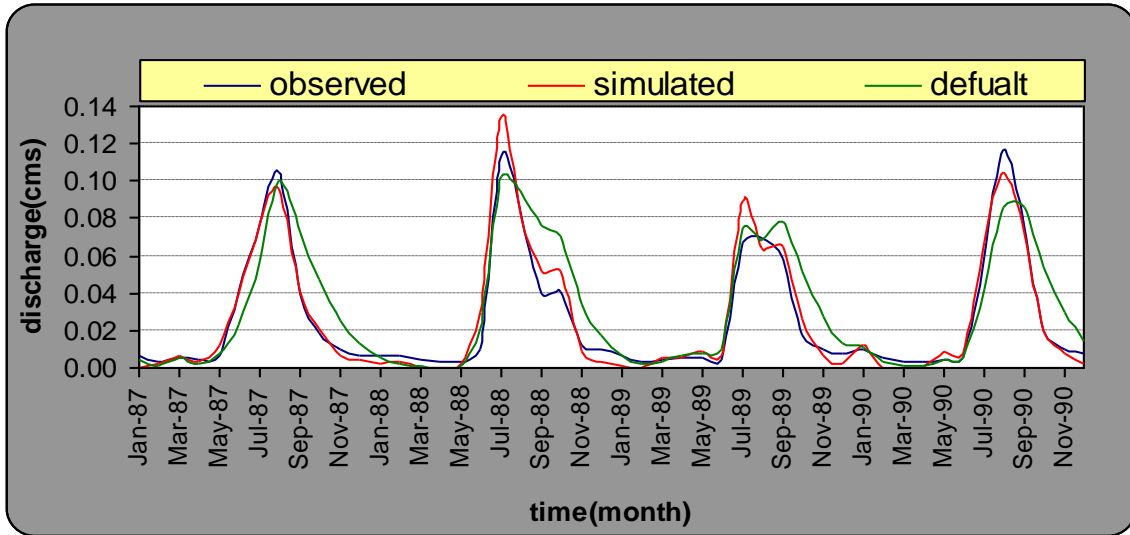


Figure4.17: Calibration result of average monthly simulated and gauged flows at the outlet of Anjeni watershed

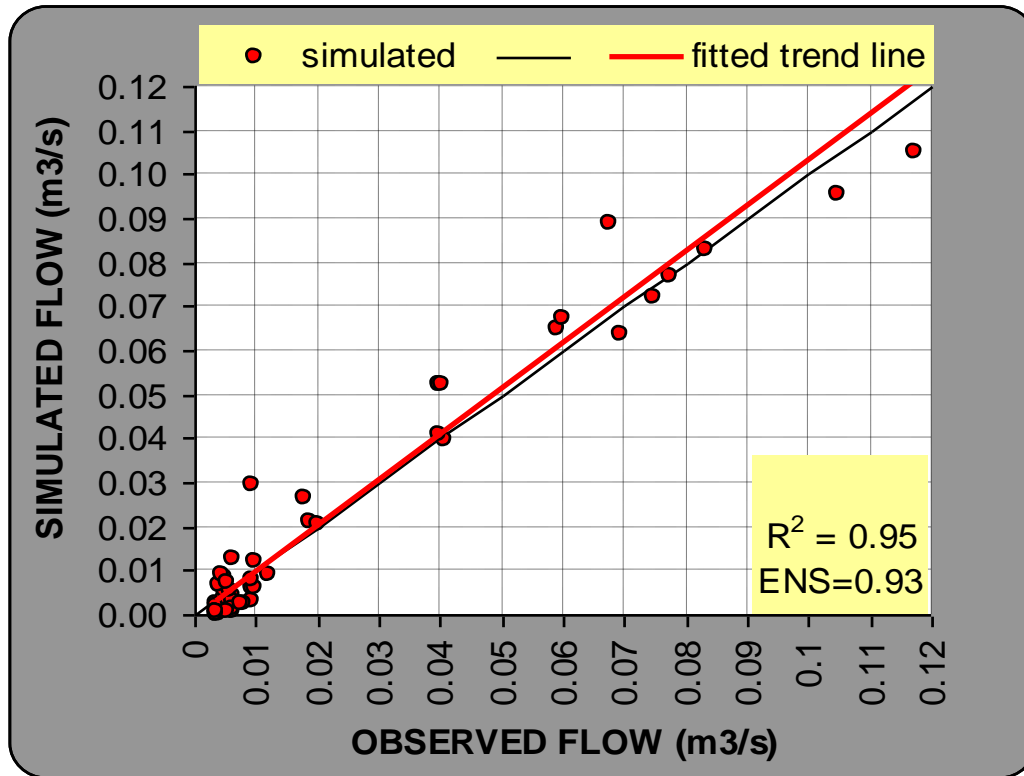


Figure4.18. Scatter plot of monthly simulated versus measured flow at Anjeni gauged station for calibration period

The calibration results in Table 4.7 show that there is a good agreement between the simulated and gauged monthly flows. This is demonstrated by the correlation coefficient ( $R^2=0.95$ ) and the Nash-Suttcliffe simulation efficiency ( $E_{NS} =0.92$ ) values. The NS results fulfilled the requirements suggested by (Santhi et al., 2001) for  $R^2 >0.6$  and  $E_{NS} > 0.5$ .

*Table 4.7: Calibration statistics of average monthly simulated and gauged flows at the outlet of Anjeni watershed*

period	Total flow cumec		Average flow cumec		$R^2$	$E_{NS}$
	observed	simulated	observed	simulated		
1986-1990	1.533634	1.471706	0.025561	0.024528	0.95	0.93

#### **4.2.5 Flow validation**

Validation proves the performance of the model for simulated flows in periods different from the calibration periods, but without any further adjustment in the calibrated parameters. Consequently, validation was performed for three years period from January 1, 1991 to December 31, 1993 from which one year taken as warm-up period. The correlation coefficient ( $R^2=0.89$ ) and the Nash-Suttcliffe simulation efficiency ( $E_{NS} =0.86$ ) shows good agreement between observed and simulated values. Both values fulfilled the requirement of  $R^2 >0.6$  and  $E_{NS} > 0.5$ , which is recommended by (Santhi et al., 2001).

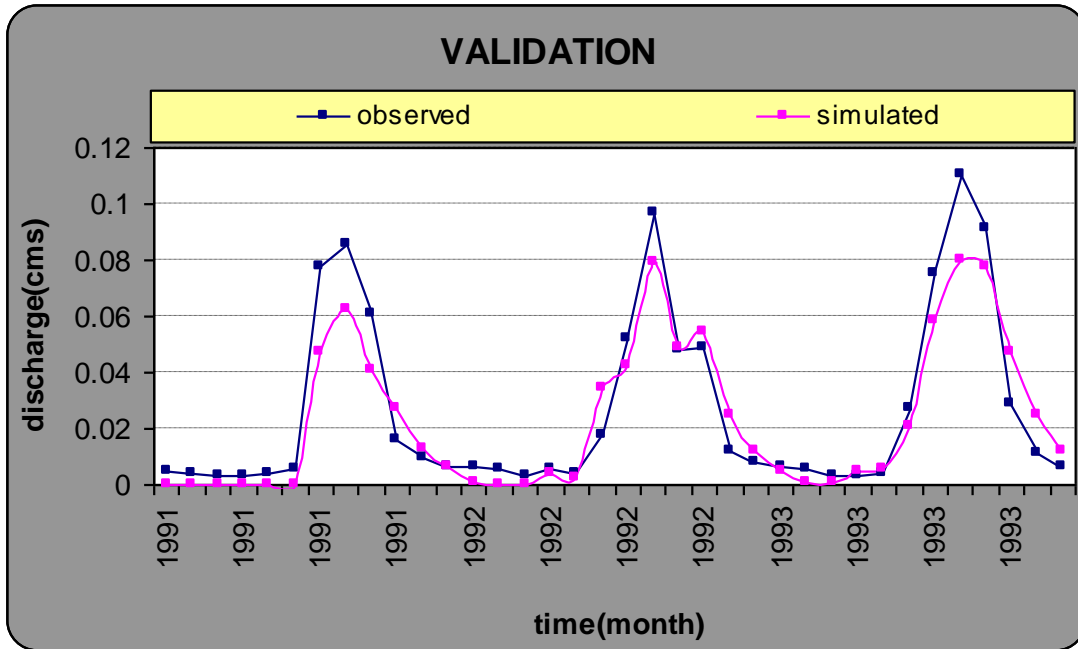


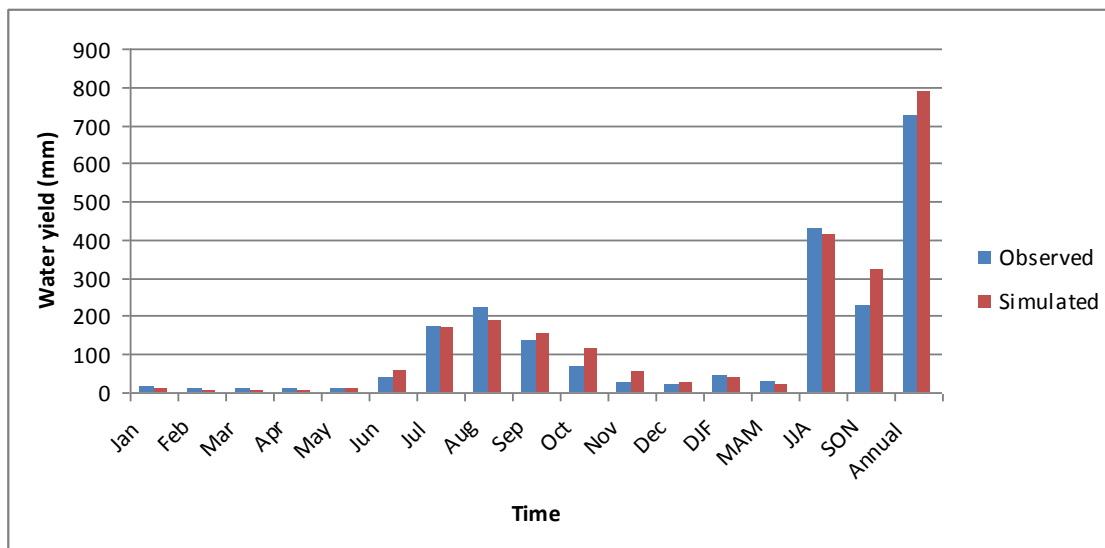
Figure 4.19: Validation result of average monthly simulated and gauged flows at the outlet of Anjeni watershed

Table 4.8: Validation statistics of the average monthly simulated and gauged flows at the outlet of Anjeni watershed

period	Total flow cumec		Average flow cumec		$R^2$	$E_{SN}$
	observed	simulated	observed	simulated		
1991-1993	0.961542	0.838012	0.02671	0.023278	0.89	0.86

#### 4.2.6 Seasonal and Monthly Watershed Water Yield

The mean monthly observed aerial water yield in the watershed was compared with simulated water yield; the result shows good agreement between the two values. As shown in the figure 5.20, the model simulation has good agreement with observed one. Except for extreme events in the main rainy season especially July and August, in which the model underestimates and minor overestimation in the months of September, October and November the observed and estimated values have good agreement with each other. On season basis, the model shows slight underestimation in JJA and some what overestimation in SON otherwise, the simulated flows shows have good resemblance with observed values. On Annual basis also the model shows a slight overestimation with respect to observed values as shown in the Figure 5.20. Apart from these sporadic deviations, the model demonstrated satisfactory performance in capturing the patterns and trend of the observed flow series, which confirmed the appropriateness of the model for future scenario simulation.



*Figure4.20: Mean monthly, seasonally and annually observed and SWAT simulation of water yield in the Anjeni watershed for base period (1986-1993)*

### **4.3 Impact of Climate Change on Future Water Availability**

Soil water availability is largely dependent on the amount of precipitation falling on its watershed area and the actual evapotranspiration amount released into the atmosphere. Hence, there is no doubt that changes in precipitation and temperature can significantly influence annual soil moisture patterns.

Impact of climate change on water availability was assessed based on climate change scenarios downscaled for the watershed by using SDSM model as discussed in previous sections. Even though future projected precipitation and temperatures were downscaled using two different climate change scenarios (A2 and B2) for the three future climate periods (2020s, 2050s and 2080s), only the climate variables downscaled using A2 scenario for two future periods (2020s and 2050s) was considered for future impact assessment.

This is due to the fact that, in the developing countries like Ethiopia, the developed climate scenario of medium-high emission (A2) was proposed. Secondly, the projection of climate variables with both scenarios shows no significant variation for all time periods. The third and last reason for excluding B2 scenario and the last climate period (2080s) for this study was due to the limitation of research period.

The SWAT simulation for the 1986 to 2005 period was used as a baseline period against which the climate impact was assessed. The daily precipitation and minimum and maximum temperature from the regional climate change model for the future two periods of 30 years: 2011-2040 and 2041-2070 were directly used as input for SWAT by preparing the weather generator parameter for both periods. The SWAT model was then re-run for the future periods with the downscaled climate variables. Other climate variables as wind speed, solar radiation, and relative humidity were assumed to be constant through out the future simulation periods. Even though it is definite that in the future land use changes will also take

place, this was also assumed to be constant as the objective of this study is only to get indicative results with respect to the change in the climate variables keeping all other factors constant.

### 4.3.1 Change in Monthly Soil Water

The soil water content in a given time period, calculated from land phase of SWAT water balance equation is used for estimation of future soil water storage variation with respect to the base period. As shown in figure 4.21 below, the average monthly soil moisture of the A2 scenario for both 2020s and 2050s climate periods has portrayed decreasing trends in the months of main rainy season (Jun, July and August). Although there might be a general decreasing pattern of the average monthly soil moisture, the over all decrease in the months of main rainy season (June, July, August and September) seems to be considerable. These months are the main Kiremt season for the study area, in which the soil water storage attains its maximum field capacity. However, the soil moisture has shown increasing trends during the months of dry seasons the seasons.

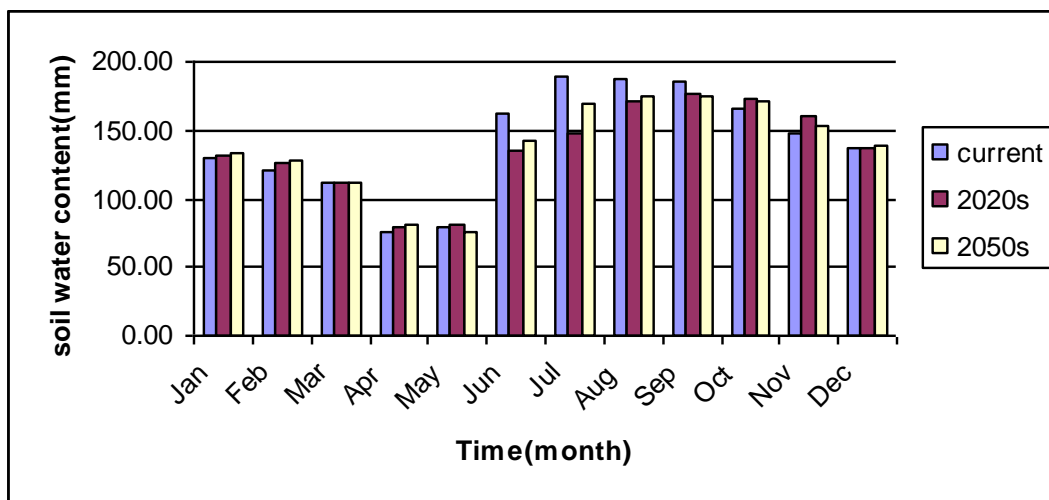


Figure4.21: Mean monthly soil moisture variation for both base period and future periods

### 4.3.2. Change in Seasonal/Annual Soil Water

By considering the soil water balance, the variation in soil water storage is aggregated on seasonal and annual basis, as shown in figure 4.20. Some of the hydrological variables considered for assessing impacts of climate change on the soil water storage are the basic variables that are highly influencing the spatial and temporal variability of soil water. Precipitation is the main source of the soil water storage. Hence, changes in this parameter highly influence the soil water in any time horizon. Therefore, understanding the impact of climate change on the rainfall for the given time period would offer good reasonable implication for estimation of climate change impacts on the soil water storage.

The percentage change in seasonal and annual hydrological variables of future periods with respect to the base period is given in Table 4.9.

*Table 4.9: percentage change in seasonal and annual hydrological parameters or the periods of 2020s and 2050s with respect to base period*

period	season	Surface run off(mm)	Lateral run off(mm)	Water yield(mm)	PET(mm)
2020s	DJF	72.5	97.75	35.9	4.1
	MAM	9.1	94.34	64.1	12.7
	JJA	-78.5	-54.2	-70.4	9.5
	SON	20.0	-5.2	-49.3	2.76
	Annual	-66.7	-27.2	-53.6	8.7
2050s	DJF	94.8	98.9	42.1	7.3
	MAM	-28.3	88.9	45.9	18.5
	JJA	-76.7	-40.9	-64.4	15.3
	SON	-36.7	5.1	-34.6	4.4
	Annual	-19.5	88.9	22.4	10.7

As soil moisture is highly dependent on the above hydrological variables, the change in mean seasonal soil water also following similar patterns of these

variables for the future time periods. Figure 4.22 illustrates the estimation of percentage change in mean seasonal and annual soil water in the future. In both 2020 and 2050 periods, the mean JJA soil moisture per month might decrease by 15.3% and 9.9% respectively. In contrast, 3.6% increase in mean seasonal soil moisture of SON season might occur in the 2020. Where as an increment in mean seasonal soil moisture by 3.14% and 4.4% in DJF and 4.2% and 2.1% in MAM might happen in 2020 and 2050 respectively. This is mainly because of the dominant impact of the average seasonal precipitation increase in DJF and decrease in JJA for both time periods. In general, the mean seasonal and annual change of soil moisture varies with precipitation and evapotranspiration with in that prospective climate periods. Additionally, the future soil moisture will also vary with changing water yields, Surface runoff and Lateral run off which are directly or in directly affected by climate change.

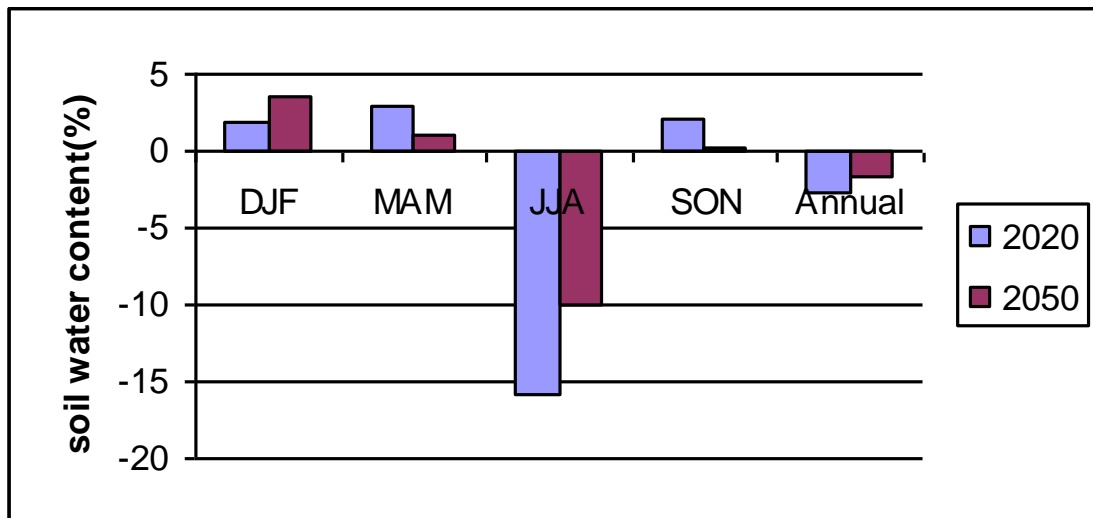


*Figure 4.22: the percentage change in mean seasonal soil water for the future periods relative to base period.*

In general, the watershed's soil water content is primarily influenced by rainfall and then by evaporation due to increased temperature. As given in Fig. 23, below, the soil water content shows decreasing trends in mid of 2020s and recovery time in 2050s climate periods following rainfall trends.

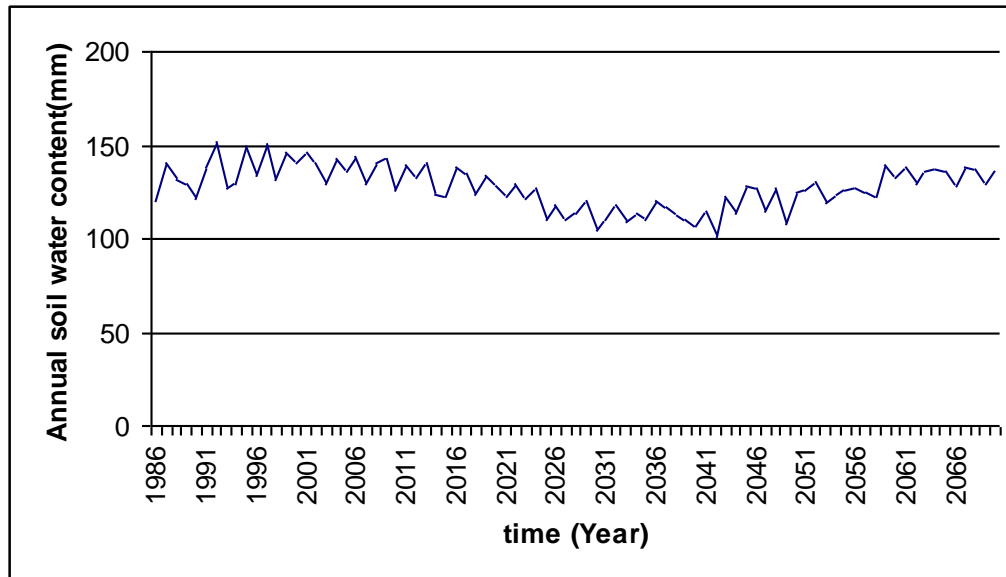


*Figure 4.23: Trends of annual soil water content at Anjeni watershed (1986-2070)*

In addition to precipitation, a watershed's soil water content is determined by the hydrologic variables of water balance. Even though the affects of hydrologic variables such as ground water and runoff on soil water are determined by soil and land use parameters in addition to climate variables, they are no explicitly assessed in this study. However, the effects evaporation on soil water content is checked because it directly influenced by climate variable that is temperature. There fore, it's crucial to account the effect Evaporation on soil water content in such away that due to increased temperature in the future time period, evaporation is also increased, which is result in reduction in soil water content.

The result from SWAT model (Fig. 24) shows that there is an increasing trend in annual Potential evapotranspiration with increasing temperature. The composed changes in precipitation and increase in evapotranspiration result in worthless reduction in soil water content in the watershed.

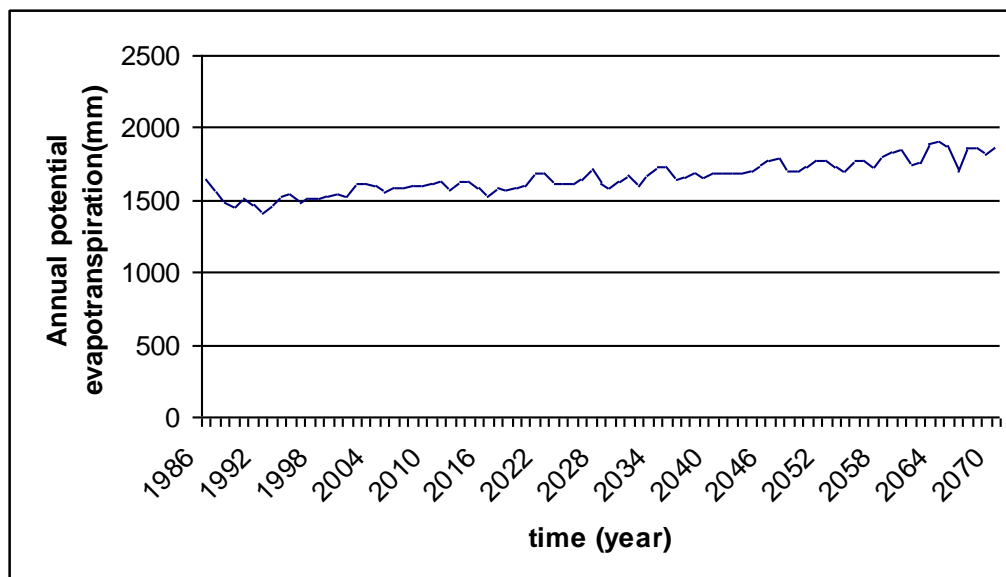


*Figure 4.24: Trends of annual potential Evapotranspiration at Anjeni watershed (1986-2070)*

#### **4.4 Impact of Climate Change on Future Crop Productivity**

Crop productivity is highly dependent on the surrounding climate variables like precipitation and temperatures at each stage of their growth and development. The optimal requirement of this climate variables at each stage of crop growth and development vary from place to place and time to time. Hence there is no doubt that, the spatial and temporal variation of such climate variables as temperature and precipitation considerably influence crop production.

As crop production is highly dependent on precipitation then, soil moisture and temperature and hence on the optimal growth and development, the future variation of precipitation and temperature leads to the variation in moisture and crop production. Hence, assessing the response of crop production to changes in global climate in terms of soil moisture variation due to changes in precipitation is crucial for rain-fed agricultural productivity.

Similar to soil moisture analysis, the SWAT simulation of the 1986 to 2005 period was used as a base period against which the climate impact was assessed for crop production as well.

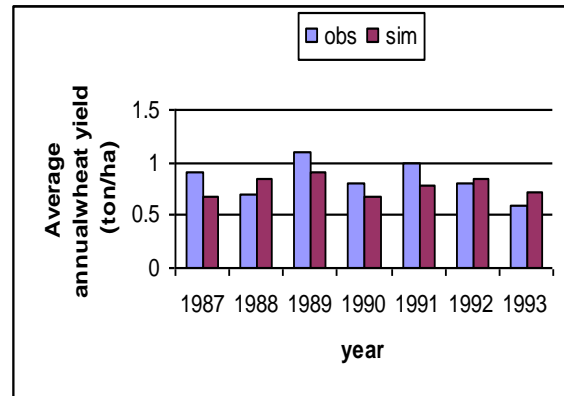
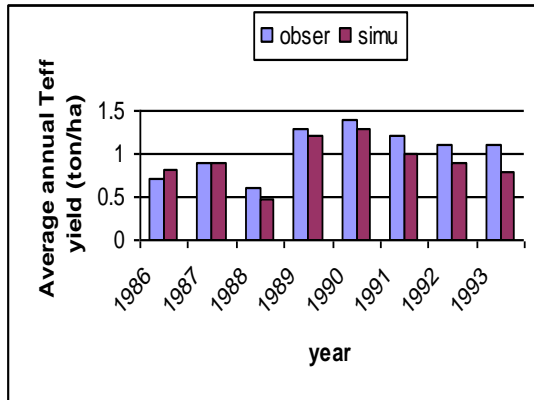
The daily precipitation and minimum and maximum temperatures from the regional climate change models for the future two periods of 30 years: 2011-2040 and 2041-2070 used as input for SWAT. In this case the original downscaled climate variables of precipitation, maximum and minimum temperatures directly used in SWAT by preparing the weather generator parameters for both periods. The model was then re-run for the future periods with the downscaled climate change variables. Other climate variables such as wind speed, solar radiation, and relative humidity were assumed to be constant throughout the future simulation periods. In addition the management activities like fertilizer and phosphorus adjustments for crop production were also assumed considered as constant and the default value given in the SWAT model were used.

Even though it is definite that in the future land use changes will also take place in the future, this was also assumed to be constant as the objective of this study is only to get indicative results with respect to the change in the climate variables keeping all other factors constant. As per the objective of the study only the planting and harvest date and plant total heat unit was supplied for dominant crop (wheat and Teff) in Anjeni watershed by assuming all other parameters constant and taking only the default values suggested in the SWAT model.

The two crops are characterized by cold annual crop (wheat) and warm annual crop (Teff) as it defined in SWAT manual. The length of growing period for wheat is 150 day and that Teff is 120 days. The two crop wheat and Teff are utilized at 0°C and 6°C base temperature and 15°C and 25°C optimum temperature respectively. According to information taken from ARARI, Anjeni watershed wheat crop was

planted at the beginning of June and Harvested around the October. Where as the planting and harvesting date of Teff was at the end of June and/or at the beginning of July and October respectively. The SWAT simulation crop yield production outputted as the product of Harvest index and Biomass as discussed in methodology part. Since the values of harvest index and biomass were not known, after many trials during calibration period the value of 0.5 and 0.85 and 40 ton/ha and 5 ton/ha were taken as a satisfactory values for wheat and Teff respectively. Therefore, using these values the calibrated and validated crop yield for both wheat and Teff were shown in the figure 4.25 and 4.26.

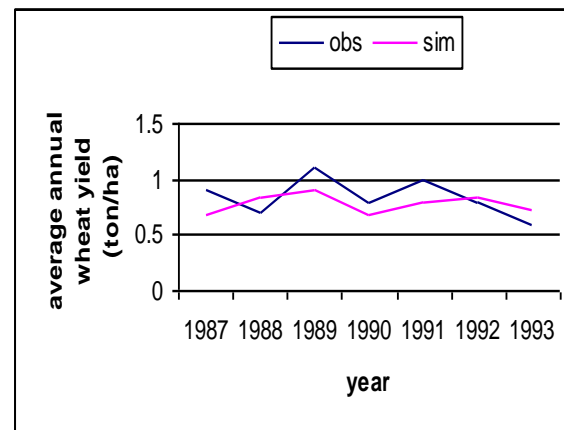
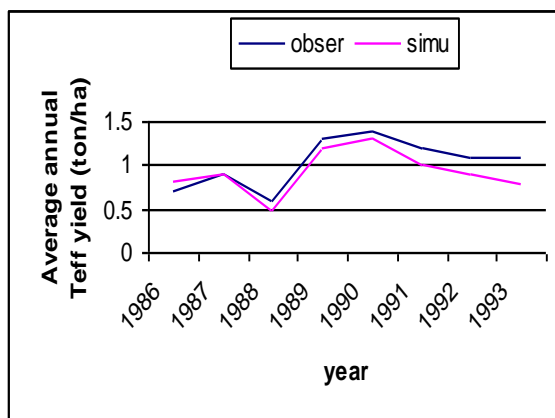
For the sake of comparison observed mean annual crop production for two different crop productions (wheat, and Teff) were compared with SWAT simulated outputs. For both crops the eight year data from 1986-1993 were used for calibration as well as validation. Among different simulation evaluation criteria for crop production in SWAT, (R-square, and histogram), histogram is used in this study for calibration and validation evaluation criterion. As shown in figure 4.25 and 4.26, the simulation result relatively underestimated the respective observed values. For Teff crop the model shows relatively good agreement between observed and simulated values, where as for Wheat crop the model underestimates for simulation years. Since it's difficult to get actual simulation relative to observed values with scarce data and limited time, the output result could be taken as reasonable. As the objective of the study is to consider how productivity respond to changes in precipitation and temperatures, and hence soil moisture, the result is taken as reasonable as both simulated and observed results shows similar trends as shown in Figure 4.25 and 4.26.



(a)

(b)

Figure 4.25: Mean annual yields (a) Teff and (b) Wheat observed versus simulated (1986-1993)



(c)

(d)

Figure 4.26: Trends of mean annual yields (c) Teff and (d) Wheat observed versus simulated (1986-1993)

The above figures show the annual mean observed and simulated wheat and Teff yield. In all cases the ability of the model to simulate the yield is relatively low. This may be due to limited input data used for calibration. As the aim of the study mostly focused on the soil moisture which influences crop production, the crop yield output could be taken as a satisfactory result that can be used for assessing

the response of crop production to changes in soil moisture at different climate periods.

*Table 4.10: percentage change of crop production in future periods relative to period*

<b>Crop type</b>	<b>2020</b>	<b>2050</b>
Wheat	Reduced by 35%	Reduced by 20%
Teff	Reduced by 12%	Reduced by 7%

The crop production is primary influenced by soil moisture content, starting from germination period to harvest time. The amount of soil moisture required for crop at different developmental stage is quite different. The crop moisture uptake is maximum during middle stage between germination and mature periods. Therefore, the spatial and temporal variability of soil moisture highly affect the over all development of the crop. Hence, the analyzing of soil water for the given climate period should give the over all status of crop production in the given watershed.

As shown in Table 4.10, the decrease in wheat crop production in the future period is mainly due to decrease in projected precipitation and increase in temperatures during that periods, which will result in over all decrease in soil moisture. Relatively Teff production sustains the projected climate variables and hence, shows small reduction in both climate periods relative to wheat yield. This is due to the fact that, the two crops are responding differently to the projected climate parameters.

The SWAT model out put of the two crops (wheat and Teff) shows that, the two crop yield response differently to the projected climate change.

Wheat yield: In 2020s, wheat crop yield reduced by 35% following moisture conditions in a watershed, due to reduction of rainfall in Anjeni watershed. However, as compared to 2020s climate period the reduction in wheat yield is minimized to 20% in 2050s climate period.

Teff yield: In the case of Teff yield, in both 2020s and 2050s climate periods the reduction is small, that is about 12% and 7% respectively as compared to that of wheat yield. There are two approaches to reason out why the two crop yields responses differently for projected climate change.

- 1) From projected climate change point of view: As it shown in section 4.1.4, rainfall reduction for future climate period was seasonal wise. That is rainfall shows decreasing trend for Kiremt season and increasing trends in both horizon. This result in yield reduction in two ways. The first one is indirect affect on yield by reducing soil moisture during growth and development periods (rainfall deficit) and the second one is direct affect on yield during harvest period (rainfall excess). Therefore, the reduction of wheat yield in 2050, though rainfall is recovered from its 2020s reduction is due to excess rainfall during harvest period in 2050s climate period. However, in the case of Teff yield the excess rainfall during harvesting period will not expected to reduce the yield because Teff yield harvested earlier due to its short length of growing period. In addition to rainfall, increased temperature in future time period will have negative impact on yield production by increasing evaporation from the soil surface which results in decreasing soil moisture available for crop growth and development.
- 2) From SWAT model out put Point of view: As it explained in section 3.12.1, to simulate crop production using SAWT, the model uses the heat unit theory to regulate the crop growth and development. This heat unit is also used as schedule mechanism in the management operation of the SWAT model. That is if months and days are not specified by user during model simulation, the model requires a fraction of potential heat unit to be specified based on climate data used.

While scheduling by heat units is convenient, there are some negatives to using this type of scheduling that users need to take into consideration. In the real world, applications of fertilizer or pesticide are generally not scheduled on a rainy day. However when applications are scheduled by heat units, the user

has no knowledge of whether or not the heat unit fraction that triggers the application will occur on a day with rainfall or not. If they do coincide, there will be a significant amount of the applied material transported with surface runoff (assuming runoff is generated on that day), much higher than if the application took place even one day prior to the rainfall event.

Therefore, as heat unit scheduling mechanism in management operation is used in this study, the above negative side of using heat unit might reduce crop yield in advance. Other effects like pesticide, plant rotation have also some effects on annual yield production in a watershed. These all result in yield reduction for both crops in both climate periods.

In general, assessing climate change impact on yield production in this study considers only future changes in precipitation and temperature. Hence future land use changes and some crop input variables such as pesticide did not considered at this time. And also SAWT model need more time and genuine data to calibrate. These all factors may result in yield reduction by taking into account the changes in climate variables.

## **CHAPTER FIVE**

### **UNCERTAINTIES AND ADAPTATION OPTION**

#### **5.1 Uncertainties**

Climate change impact assessment on water availability and crop production in the Anjeni watershed consider two model analyses and out puts, which are depends on simplified assumptions. Hence, it is unquestionable that the uncertainties presented in each of the models and model outputs kept on cumulating while progressing towards the final output. These Uncertainties include: Uncertainty Linked to Data quality, General circulation Model (GCMs), Emission scenarios, Downscaling Method, and Hydrological model.

The uncertainty related to data used for Downscaling model and Hydrological model consists of problem with data quality and Missing data. Despite appropriate data checking and filling missing values was done using the weather generator component of the statistical Downscaling Model before the analysis, certain level of error was also introduced during this stage. GCM outputs have also a lot of uncertainties. There are considerable uncertainties in the radiative forcing changes, especially aerosol forcing, associated with changes in atmospheric concentrations (Mearns et al., 2001). Hence, no single GCM model can be considered “best” (McAvaney et al., 2001). Although uncertainties can be minimized by using outputs of different GCMs, this study made use of only the HadCM3 model outputs.

Besides, GCMs use the future forcing scenarios to produce ranges of climate change. These scenarios represent a set of assumptions about population growth, economic and technological development, and socio-political globalization, where all of these variables contain a high degree of uncertainty. The IPCC report on emission scenarios, SRES, (IPCC, 2001) clustered these scenarios into six

groups. Despite their equal probability, model results based on these scenarios may vary noticeably. Hence, choosing among the scenarios adds to the uncertainty.

The coarser resolutions make GCMs not to be used directly for impact studies. Though “downscaling” is a solution towards narrowing the temporal and spatial resolution disparity, the techniques involved are still another source of uncertainty.

The SDSM statistical downscaling technique used in this study needed the screening of weather parameters (predictors). Finding good predictors-Predictand correlation was a core part of the downscaling process. However, even after several trial and errors, the correlation coefficients found were very small especially for the precipitation and minimum temperature Predictand variables. The knowledge gap related to the atmospheric physics of the local climatic process may be one of the obstacles in choosing the best predictor combinations. Beyond that, SDSM downscaling is based on the assumption that the predictor-Predictand relationships under the current condition remain valid for future climate conditions too, which might not be the case and hence another source of uncertainty.

In the case of crop production analysis, SWAT simulate crop production well, but the weather generator part of SWAT need all meteorological variables to be used by Penman –Monteith evapotranspiration calculation method. However, in this study Hargreaves method was used which is other uncertainty. Besides, crop simulation with the aid of SWAT model fully depends on the model’s default values, except climate data of precipitation, maximum and minimum temperature, which is another sort of uncertainties. The assumptions involved in the hydrologic model simulations are also a portion of the Uncertainty.

As described in Methodology part, the determination of the impacted water availability and productivity only based on the precipitation and temperature changes in the future. The other climatic variables as wind speed, solar radiation, and relative humidity were assumed to be constant throughout the future simulation periods. Even though it is definite that in the future land use changes will also take place, this is also assumed to be constant. Hence, these assumptions can definitely lead to a certain level of additional uncertainty.

## 5.2 Adaptation option

The Anjeni watershed is known by its *in-situ* soil water conservation. The conservation practice was initially carried out for controlling soil erosion, which is then also used as soil storage by increasing infiltration and decreasing run off. This conservational management is considered as good beginning and considered as initial adaptive capacity for agricultural activities. Rainfed agriculture is primary farming system in the watershed.

Adaptation to climate change can be the range of actions taken in response to changes in local and regional climatic conditions (Smit et al., 2000). These responses include autonomous adaptation, i.e., actions taken by individual actors such as single farmers or agricultural organizations, as well as planned adaptation, i.e., climate-specific infrastructure development, regulations and incentives put in place by regional, national and international policies in order to complement, enhance and/or facilitate responses by farmers and organizations. As it reported by (Howden et al., 2007), the benefits of adaptation to be greater with moderate warming (<2°C) than with greater warming and under scenarios of increased rainfall than those with decreased rainfall. Accordingly, since the projected future climate for the watershed indicted that incremental of future temperature by about 1-3 °C in temperature and variation of seasonal rainfall and probably reduced by

about 3 to 9 percent, its critical to settle some adaptation options which will be taken by individual farmers and/or decision makers.

The condensed Kiremt seasonal rainfall in the future time period will result in the reduction of season based soil infiltration and longer dry periods in the watershed. Similarly the increased future temperature will result in high evapotranspiration demand from crops and hence depletes moisture more rapidly. This kind of seasonal variation in rainfall and temperature will then reduce over all soil water storage in the watershed. In contrast, future projection of rainfall indicated that increase in rainfall before and after main rainy season, which result in high soil moisture storage and small dry spell length.

There fore, during Kiremt season of that period, it's highly advisable for farmers to use plant with short length of growing period, less water extract plants and use irrigation if possible or shifting planting date to both horizons (other seasons rather than Kiremt season). Depending on these result the possible adaptation options to be implemented are divided into two parts. The first one is action taken by individual farmers/communities independently of police based on set of technology and management options available under current climate and the second one is actions that require concerted action from local, regional and/or international policy.

1. Action taken by individual farmers/communities independently of police based on set of technology and management options available under current climate
  - Crop calendars shifts (planting date, input schedules, harvesting date)
  - Cultivar and crop changes
  - Management changes

- Diversifying income
- Seasonal climate forecasts
- Creating awareness among the people on efficient utilization of water

2. Action that require concerted action from local, regional and/or international policy

- Land use incentives
- Irrigation infrastructures
- Efficient water use technologies
- Transport and storage infrastructure
- Revising land tenure arrangements including attention to property rights
- Accessible, efficient markets for products and inputs (Fertilizer, seed, labor) and for financial services including insurance.
- Creating awareness among the people on efficient utilization of water

Moreover, watershed based management activities (re-thinking towards natural resource conservation and/or to go in for artificial restoration of hydrological system by enhancement of water storage and infiltration of rainfall in the watershed) may be the central part of the whole adaptation options. To ensure sustainability, inter-sectoral collaboration is essential. Get together among different organization Specially creation of linkage between National meteorological Agency (NMA), Research institutes, higher institutes, Agricultural and Water Bureaus under both Governmental non-governmental organizations for transmitting valuable information for all stake holders and decision makers and take responsibilities to create awareness about climate information up to local level is vital to the shocks with climate change.

## CHAPTER SIX

### SUMMERY AND RECOMMENDATIONS

#### 6.1 Summery

This study attempts to quantify the climate change impact on soil water availability and crop production using the statistical downscaling model output and water balance simulation modelling approach of SWAT model. In doing so this study reached to the following summaries.

- ▶ Using a numbers of models for impact assessment confer valuable out puts and at the same time introduce number of uncertainties. For this study also two different models were used which give different model out puts. Each of them possesses a level of uncertainties as discussed in *section5*
- ▶ The study has revealed that the Statistical Downscaling Model (SDSM) is able to simulate all except the extreme climatic events. The model underestimates the farthest values in both extremes and keeps more or less an average event. Nevertheless, the simulated climatic variables generally follow the same trend with the observed one.
- ▶ The model simulated maximum and minimum temperature more accurately than precipitation. This is due to the fact that the maximum and minimum temperatures are highly affected by large scale variables. Accordingly, the major large scale predictors highly affect local maximum temperature
- ▶ The less performance of precipitation simulation is attributed to its nature of being a conditional process and it being highly influenced by local weather system such like topography, rather than global weather system.

- ▶ SDSM reproduced monthly and seasonal climatic variables averaged over years more accurately than individual monthly and seasonal values in a single year. Hence, SDSM result indicates that both maximum and minimum temperature show increasing trend in both 2020s and 2050s periods.
- ▶ The average annual maximum temperature will be increased by about 2.1°C for both A2 and B2 scenarios in 2020s and 3.4 °C for A2 and 3.6 °C in B2scenarios in 2050s. The mean annual minimum temperature will also increase by 1.1 °C for both A2 and B2 in 2020s and 2.5 °C for A2 and 1.9 °C for B2 scenarios in 2050s.
- ▶ The result of projected rainfall indicated that there is a probability of precipitation decreasing in the main rainy season (JJA) and increasing in precipitation at both horizons in future periods. A decrease in average Kiremt precipitation by about 8.78% and 7% in 2020 and 5.6% and 6.3% in 2050 for both A2 and B2 scenarios, respectively.
- ▶ The result of hydrological model calibration and validation indicated that the SWAT model simulates the stream flow appreciably well for the study area. The model performance criterion which is used to evaluate the model result, the regression coefficient and the Nash-Sutcliffe simulation efficiency values obtained proved this fact.
- ▶ According to the hydrological analysis carried out, ground water parameters (Alpha base flow (Alpha\_Bf), soil available water capacity (SOL\_AWC), the threshold water depth in the shallow aquifer for flow (GWQMN), the groundwater Revap coefficient (GW\_REVAP), and the saturated hydraulic conductivity (Sol\_K), curve number (CN2), and Evapotranspiration (soil evapotranspiration factor (ESCO) and sub basin slope are the most sensitive parameters affecting the soil water of the watershed.

- ▶ Hydrological impact of future climate change scenario indicated that there will be high seasonal variation of soil water than in the monthly or annual basis. Relative to base period, the soil water in the main rainy season (JJA) will reduce by 15.9% in 2020 and 9.9% in 2050. In contrast, the soil water in the small rainy season (DJF) will increase by 1.2% in 2020 and 3.8% in 2050.
- ▶ Relative to base period the main rainy season, Jun, July, and August (JJA) of the Anjeni watershed shows a reduction in mean rainfall by 8.7 % in 2020 and 5.6 % in 2050 and an increase in temperature in both periods which resulted in the mean annual soil water content reduction of about 15.8% in 2020 and 9.8 % in 2050s, and a reduction in crop production (wheat).
- ▶ In general taking in account the uncertainties in GCM models explained in section 5, this short study showed that there will be an increasing trend in temperature and seasonal variation of rain fall, which will result in a reduction of both water availability and crop production in the future periods.

## 6.2 Recommendations

- The model simulations considered only future climate change scenarios assuming all other things constant. But change in land use scenarios, soil, management activities and other climate variables will also contribute some impacts on water availability and crop production.
- This study only considered how productivity will respond to the probable variation of seasonal rainfall in terms of soil moisture and increased temperature in future time periods. Hence inclusion of other metrics like metrics for biophysical factors (crop calendar and full information about water status), socio-economic data, and agricultural system characteristics should give a reasonable result.
- SWAT simulation of the model with full data, Genuine and/or experimental data related to own crop might give appreciable outputs.
- The physically based, spatially distributed, and public domain Soil and Water Assessment Tool (SWAT) is found to be a very appropriate tool to simulate both historical as well as impacted hydrological processes in the watershed
- Since all SRES scenarios have equal probability of occurrence, future studies should also consider the entire range of reasonably possible future scenarios.
- Also increased atmospheric carbon dioxide (CO<sub>2</sub>) has both positive and negative impact on crop production. Hence, addition of the future increased CO<sub>2</sub> to present study should offer appreciable results.
- Out put of this study is based on a single GCM and one emission scenario. However, further study should consider the wide range of uncertainties associated with models and try to reduce these uncertainties by using different and a number of GCM outputs, downscaling techniques, and emission scenarios.

## REFERENCES

1. Abdo Kedir, Rientjes, T.H., and Gieske, A.S., 2007. SNNPR Water Resources Development Bureau, Awassa, Ethiopia.
2. Arnold, J.G., Allen, P.M, and Bernhardt, G., 1993. A comprehensive surface-groundwater flow model, *Journal of Hydrology* 142: 47-69pp
3. Arnold, J.G., Allen, P.M., Muttiah, R., and Bernhardt, G., 1995. Automated base flow separation and recession analysis techniques. *Ground Water* vol 33(6): 1010-1018pp
4. Baede, A.P.M., Ahlonsou, E., Ding, Y., and Schimel, D., 2001. The Climate System, an Overview. In: *Climate Change 2001: The Scientific Basis. Contribution of Working Group I to the Third Assessment Report of the Intergovernmental Panel on Climate Change*, [(eds.), Houghton, J.T., Ding, Y., Griggs, D.J., Noguer, M., van der Linden, P.J., Dai, X., Maskell, K., and Johnson, C.A.], Cambridge University Press, Cambridge, United Kingdom and New York, NY, USA, 881pp.
5. Carter, T.R., 2007. General Guidelines on the use of scenario data for Climate Impact and Adaptation Assessment. Finnish Environmental Institute, Helsinki, Finland.
6. Cubasch, U., Meehl, G.A., Boer, G.J., Stoufer, R.J., Dix, M., Noda, A., Senior, C.A., Raper, S., and Yap, K.S., 2001. Projections of future climate change. *Climate Change 2001: The Scientific Basis. Contribution of Working Group I to the Third Assessment Report of the Intergovernmental Panel on Climate Change*, [(Eds.), Houghton, J. T., Ding, Y., Griggs, D. J. Noguer, M., van der Linden, P.J., Dai, X., Maskell, K., and Johnson, C. A.], Cambridge University Press, 525-582.
7. Degefu Wolde, 1987. Some Aspects of Meteorological Drought in Ethiopia. In *Drought and Hunger in Africa: Denying Famine a Future*, (Ed. Glantz, M.H.) Cambridge University Press, New York

8. Danuso, F., 2002. Climak. A Stochastic Model for Weather Data Generation, Italian Journal of Agronomy 6(1):57-71, Italy: 67-68pp.
9. Dilnesaw Alamirew, 2006. Modelling of Hydrology and Soil Erosion of Upper Awash River Basin. PhD Thesis, University of Bonn: 233pp.
10. Di Luzio, M., Srinivasan, R., and Arnold, J. G., 2002. Integration of watershed tools and SWAT model into BASINS. J. American Water Resource. Assoc. 38(4): 1127-1141.
11. FAO (Food and Agricultural Organization). 2002. Major Soils of the World. Land and Water Digital Media Series. FAO Soil Bulletin.No (19), Rome. Italy.
12. FAO, 1995. Digital Soil Map of the World and Derived Soil Properties (CDROM) Food and Agriculture Organization of the United Nations,FAO
13. FAO, 1998. The Soil and Terrain Database for northeastern Africa (CDROM) FAO, Rome.
14. Green, W. H., and Ampt, G. A., 1911. Studies on soil physics: 1. the flow of air and water through soils. J. Agric. Sci. 4: 11-24.
15. Gete Zeleke., 2000. Landscape Dynamics and Soil Erosion Process Modelling in the North-Western Ethiopian Highlands. African Studies Series 16. Berne: Geographica Bernensia.
16. Gregory, A., Nakicenovic, N., Alcamo, J., Davis, G., DeVries, B., Fenhann, J., Gain, S., Gruebler, K., Jung, T. Y., Kram, T., Lebre LaRovere, E., Michaelis, L., Mori, S., Morita, T. ,Pepper, W., Pitcher, L., Price, K., Riahi, A., Roehrl, H.H., Rogner, A., Sankovski, M. ,Schlesinger, P. ,Shukla, S., Smith, R., Swart, S., VanRooijen, N., and Dadi, Z., 1997. Special Report on Emissions Scenarios: A Special Report of Working Group III of the Inter governmental Panel on Climate Change. Cambridge University Press, 600 pp.

17. Hailemariam Kinfe, 1999. Impact of Climate Change on the Water Resources of Awash River Basin, Ethiopia, Climate Research. International and Multidisciplinary Journal, 12: 91-96.
18. Hargreaves, G.L., Hargreaves, G.H., and Riley, J.P., 1985. Agricultural benefits for Senegal River basin. J. irrig. And Drain. Engr; 111(2): 113-124.
19. [http://www.brc.tamus.edu/swat/soft\\_links.html](http://www.brc.tamus.edu/swat/soft_links.html), SWAT(ArcSWAT)website accessed June,10,2009
20. <http://www.cics.uvic.ca/scenarios/sdsm/select.cgi> SDSM predictor data files are downloaded from the Canadian Institute for Climate Studies (CICS) website accessed July,20,2009
21. [http://www.brc.tamus.edu/swat/soft\\_links.html](http://www.brc.tamus.edu/swat/soft_links.html) Weather parameter calculator WXPARM (Williams, 1991) and dew point temperature calculator DEW02 programs accessed July,20,2009
22. Howden, M., Soussana, J. F., Tubiello, F. N., Chhetri, N., Dunlop, M. & Aggarwal, P. K., 2007. 'Adaptation strategies for climate change', Proceedings of the National Academy of Sciences 104, 19691–19698. 167, 170
23. Huisman, S., Ann van Griensven, Raghavan Srinivasan, Lutz Breuer, 2004. European SWAT School, Advanced Course, 112pp. (Intitute for Landscape Ecology and Resouce Management , University of Giessen, Hienrich-Buff-Ring 26, 35392 giessen, Germany)
24. Houghton, J.T., 2001. Climate change 2001: the scientific basis: contribution of working group I to the third assessment report of the intergovernmental panel on climate change, [(Eds.) Houghton, J.T., Ding, Y., Griggs, D.J., Noguer, M., van der Linden, P.J., Dai, X., Maskell, K., and Johnson, C.A.] , Cambridge University Press.
25. IPCC AR4 (Intergovernmental Panel on Climate Change Fourth Assessment Report), 2007. IPCC: Climate change 2007: synthesis report (<http://www.ipcc.ch/pdf>). [Accessed 20 June 2008]

26. IPCC (Intergovernmental Panel on Climate Change). 1996. Climate Change 1995. The Science of Climate Change. Contribution of Working Group I to the Second Assessment Report of the Intergovernmental Panel on Climate Change, [(Eds.) Houghton, J.T., Ding, Y., Griggs, D.J., Noguer, M., van der Linden, P.J., Dai, X., Maskell, K., and Johnson, C.A.] , Cambridge University Press, Cambridge and New York, 572 pp.
27. IPCC TAR-WGII (Intergovernmental Panel on Climate Change Third Assessment Report, Working group two on Impact assessment). 2001. Synthesis report (<http://www.ipcc.ch/pdf>)[ Accessed 11 May 2008]
28. IPCC (Intergovernmental Panel on Climate Change). 2001. The Data Distribution Center, DDC, <http://ipcc-ddc.cru.uea.ac.uk/> [Accessed 15 May 2009]
29. Kefeni Keeled, 1995. Soil Conservation Research Project: The Soils of the Anjeni Area Gojam Research Unit, Ethiopia (with 4 Maps). Research Report 27. Berne: University of Berne, Switzerland and Ministry of Agriculture, Ethiopia.
30. Lenhart, T., Eckhardt, K., Fohrer, N., Frede, H.G., 2002. Comparison of two different approaches of sensitivity analysis. Physics and Chemistry of the Earth 27 (2002), Elsevier Science Ltd., 645–654pp.
31. Lierch, S., 2003. Dew02 Users' Manual, Berlin, 5pp. PDF Manual from [http://www.brc.tamus.edu/swat/soft\\_links.html](http://www.brc.tamus.edu/swat/soft_links.html) accessed July,20,2009
32. Ludi, E., 2004. Economic Analysis of Soil Conservation: Case Studies from the Highlands of Amhara Region, Ethiopia. Africa Studies Series A18. Berne: Geographical Bernensia.
33. Mearns, L.O., Hulme, M., Carter, T.R., Leemans, R., Lal, M., and Whetton, P., 2001. Climate Scenario Development. In: Climate Change 2001: The Scientific Basis. Contribution of Working Group I to the Third Assessment Report of the Intergovernmental Panel on Climate Change, [(Eds.)

- Houghton, J.T., Ding, Y., Griggs, D.J., Noguer, M., van der Linden, P.J., Dai, X., Maskell, K., and Johnson, C.A.], Cambridge University press, Cambridge and New York, pp 739-768. Available for download from: <http://www.ipcc.ch> (chapter 13 of the IPCC WG1 Assessment)
34. McAvaney, B.J., Covey, C., Joussaume, S., Kattsov, V., Kitoh, A., Ogana, W., Pitman, A.J., Weaver, A.J., Wood, R.A., and Zhao, Z.C., 2001. Model Evaluation. In: [(Eds.) Houghton, J.T., Ding, Y., Griggs, D.J., Noguer, M., van der Linden, P.J., Dai, X., Maskell, K., and Johnson, C.A.)], *Climate Change 2001: The Scientific Basis. Contribution of Working Group I to the Third Assessment Report of the Intergovernmental Panel on Climate Change*. Cambridge University Press, Cambridge, p 471-523
  35. Monteith, J.L., 1965. Evaporation and the environment. In *The State and Movement of Water in living Organisms, XIX<sup>th</sup> Symposium*. Soc. For Exp. Biol., Swansea, Cambridge University Press. pp. 205-234
  36. Neitsch, S.L., Arnold, J.G., Kiniry, J.R., and Williams, J.R., 2005. Soil and Water Assessment Tool, Theoretical Documentation: Version 2005. Temple, TX. USDA Agricultural Research Service and Texas A & M Black land Research Centre.
  37. Neitsch, S.L., Arnold, J.G., Kiniry, J.R., Srinivasan, R., and Williams, J. R., 2002. Soil and Water Assessment Tool (SWAT) User's Manual, Version 2000, Grassland Soil and Water Research Laboratory, Blackland Research Center, Texas Agricultural Experiment Station, Texas Water Resources Institute, Texas Water Resources Institute, College Station, Texas, 472pp
  38. NMSA (National Meteorological Service Agency). 2001. Initial National Communication of Ethiopia to the United Nations Framework convention on Climate Change (UNFCCC). National Meteorological Services Agency, Addis Ababa, Ethiopia. Addis Ababa. Ethiopia.
  39. Palmer, Richard N., Erin Clancy, Nathan T. Van Rheenen, and Matthew W. Wiley, 2004. *The Impacts of Climate Change on the Tualatin River Basin*

- Water Supply: An Investigation into Projected Hydrologic and Management Impacts, Draft Report. Department of Civil and Environmental Engineering, University of Washington, 67pp.
40. Setegn Shimelis G., Ragahavan Srinivasan, Bijan Dargahi, 2007. Stream flow Calibration and Validation of SWAT2005/ArcSWAT in Anjeni Gauged Watershed, Northern Highlands of Ethiopia. In the proceedings of the 4th International SWAT Conference, July 02-06, UNESCO-IHE, Delft, The Netherlands. On press
  41. Refsgaard, J. C., and Storm, B., 1996. MIKESHE. In Computer Models in Watershed Hydrology, 809-846. [(ed.) Singh, V. J.], Highland Ranch, Colo.: Water Resources Publications
  42. Santhi, C., Arnold, J.G., Williams, J.R., Dugas, W.A., Srinivasan, R., and Hauck, L.M., 2001. Validation of the SWAT Model on a Large River Basin with Point and Non point Sources, Journal of the American Water Resources Association, Vol. 37, No. 5, 1169-1188pp.
  43. SCRP, 2000. Area of Anjeni, Gojam, Ethiopia: Long-term Monitoring of the Agricultural Environment 1984-1994. SCRP, Centre for Development and Environment. Switzerland.
  44. Smit, B., Burton, I., and Klein, R., 2000. 'An anatomy of adaptation to climate change and variability', Climatic Change 45(1), 223–251. 168
  45. (USDA- SCS) United State Department of Agriculture-Soil Conservation Service. 1972. National Engineering Handbook Section 4 Hydrology, Chapters 4-10.
  46. Van Griensven, A., Meixner, T., Grunwald, S., Bishop, T., Diluzio, M., and Srinivasan, R., 2006. A global sensitivity analysis tool for the parameters of multi-variable catchment models. (Publisher and place of publication)
  47. Van Wambeke, A., 2003. Properties and management of soils of the tropics. FAO Land and Water Digital Media Series No. 24, FAO, Rome.

48. Robert L. Wilby and Christian W. Dawson, August 2004. Using SDSM Version 3.1. A decision support tool for the assessment of regional climate change impacts. User Manual: 67pp.  
<http://www.staff.lboro.ac.uk/~cocwd/SDSM/index.html> [Accessed 11 April 2009]
49. Williams, J.R., 1969. Flood routing with variable travel time or variable storage coefficients. *Trans. ASAE* 12(1):100-103.
50. Williams, J.R., and Berndt, H.D., 1977. Sediment Yield Prediction Based on Watershed Hydrology. *Transactions of American Society of Agricultural Engineers* 20(6):1100-1104.
51. Xu, C.Y., 1999. From GCM to River flow: A review of downscaling methods and hydrologic modelling approaches, *progress in physical Geography*, 23(2), pp. 229-249.
52. Zeray, L., 2007. Climate Change Impact on Lake Ziway Watershed Water Availability, Ethiopia

## APPENDIX A

*Table A.1 Summary of average monthly climatic data values of Anjeni station in the study area*

<b>ANJENI STATION</b>			
LATITUDE(degree)		10.41	
LONGITUDE(degree)		37.31	
ALTITUDE(m)		2405	
MONTH	RAIN(MM)	TMAX(°C)	TMIN(°C)
JAN	17	25.2	6.8
FEB	12.9	27.2	7.8
MAR	51.2	26.9	10
APR	52.2	26.7	11.1
MAY	94.1	25.9	11.4
JUN	321.2	21.8	11.1
JUL	429.9	19.7	10.9
AUG	405.3	19.7	10.9
SEP	277.4	21.3	9.9
OCT	170.4	22.3	9.4
NOV	37.9	23.6	7.7
DEC	21.3	24.6	5.8

*Table A.2 Summary of average monthly climatic data values of Debra Markos station in the study area*

<b>DEBRA MARKOS STATION</b>						
LATITUDE(degree)		10.2				
LONGITUDE(degree)		37.31				
ALTITUDE (m)		2515				
MONTH	RAIN(MM)	TMAX(°C)	TMIN((°C)	SOLAR	WIND(M/S)	RH (%)
JAN	13.13	23.7	8.9	0.67	1.99	45.31
FEB	14.4	25.2	10.3	0.21	2.76	19.50
MAR	56.21	25.1	11.1	0.29	2.27	29.43
APR	81.36	24.9	11.8	0.34	2.64	32.87
MAY	87.33	24.7	11.8	0.56	2.05	55.46
JUN	168.79	21.9	10.8	0.77	2.08	77.26
JUL	273.38	19.6	10.9	0.8	1.45	79.94
AUG	306.68	19.6	10.8	0.82	1.61	82.63
SEP	210.74	21.1	10.1	0.71	2.34	71.53
OCT	84.79	21.8	9.8	0.73	1.69	73.07
NOV	21.26	22.7	8.8	0.53	2.01	53.45
DEC	26.19	23.1	8.7	0.31	2.43	31.05

## APPENDIX B

SDSM calibration parameters

*Table B.1 Precipitation calibration parameters for Anjeni station*

### CORRELATION MATRIX

	1	2	3	4
1 Rainfall(84-2001).dat	1			
2 ncepmslpaf.dat	0.144	1		
3 ncepp__zaf.dat	-0.020	-0.316	1	
4 ncepp8_vaf.dat	-0.246	-0.209	0.137	1

### PARTIAL CORRELATIONS WITH Rainfall(84-2001).dat

	Partial r	P value
ncepmslpaf.dat	0.106	0.0000
ncepp__zaf.dat	0.045	0.0260
ncepp8_vaf.dat	-0.226	0.0000

*Table B.2 Maximum temperature calibration parameters for Anjeni station*

### CORRELATION MATRIX

	1	2	3	4	5
1 Tmax.dat	1				
2 ncepmslpaf.dat	-0.413	1			
3 ncepp__zaf.dat	-0.035	-0.308	1		
4 ncepp8_vaf.dat	0.552	-0.224	0.147	1	
5 nceptempaf.dat	0.347	-0.482	0.213	0.178	1

### PARTIAL CORRELATIONS WITH Tmax.dat

	Partial r	P value
ncepmslpaf.dat	-0.318	0.0000
ncepp__zaf.dat	-0.287	0.0000
ncepp8_vaf.dat	0.542	0.0000
nceptempaf.dat	0.196	0.0000

*Table B.3 Minimum Temperature calibration parameter for Anjeni station*

CORRELATION MATRIX

	1	2	3	4	5	6	7	8
1 AnjTmin.dat.prn	1	-0.512	-0.181	0.273	0.421	0.509	0.058	0.749
2 ncepp__vaf.dat	-0.512	1	0.142	-0.152	-0.592	-0.719	0.169	-0.509
3 ncepp5_uaf.dat	-0.181	0.142	1	-0.380	-0.014	0.039	-0.047	-0.192
4 ncepp500af.dat	0.273	-0.152	-0.380	1	0.050	0.094	0.249	0.276
5 ncepp8_uaf.dat	0.421	-0.592	-0.014	0.050	1	0.514	-0.053	0.413
6 ncepshumaf.dat	0.509	-0.719	0.039	0.094	0.514	1	-0.146	0.505
7 nceptempaf.dat	0.058	0.169	-0.047	0.249	-0.053	-0.146	1	0.056
8 Autoregression	0.749	-0.509	-0.192	0.276	0.413	0.505	0.056	1

PARTIAL CORRELATIONS WITH AnjTmin.dat.prn

	Partial r	P value
ncepp__vaf.dat	-0.074	0.0000
ncepp5_uaf.dat	-0.049	0.0006
ncepp500af.dat	0.079	0.0000
ncepp8_uaf.dat	0.081	0.0000
ncepshumaf.dat	0.123	0.0000
nceptempaf.dat	0.063	0.0000
Autoregression	0.598	0.0000

## APPENDIX C

Symbols and description of Weather Generator Parameters (WGEN) used by the SWAT model

<u>Symbol</u>	<u>Description</u>
A TMPMX	Average or mean daily maximum air temperature for month (°C).
B TMPMN	Average or mean daily minimum air temperature for month (°C).
C TMPSTDMX	Standard deviation for daily maximum air temperature in month (°C).
D TMPSTDMN	Standard deviation for daily minimum air temperature in month (°C).
E PCPMM	Average or mean total monthly precipitation (mm H <sub>2</sub> O).
F PCPSTD	Standard deviation for daily precipitation in month (mm H <sub>2</sub> O/day).
G PCPSKW	Skew coefficient for daily precipitation in month.
H PR_W1	Probability of a wet day following a dry day in the month.
I PR_W2	Probability of a wet day following a wet day in the month.
J PCPD	Average number of days of precipitation in month.
K SOLARAV	Average daily solar radiation for month (MJ/m <sup>2</sup> /day).
L DEWPT	Average daily dew point temperature in month (°C).
M WNDV	Average daily wind speed in month (m/s).

## APPENDIX D

*Table D.1 GCMs Selected by IPCC for impact studies*

Centre	Centre acronym	Country	Global Climate Model	Grid resolution
Australia's Commonwealth Scientific and Industrial Research Organization	CSIRO	Australia	CSIRO-MK3.0	1.9° x 1.9°
Canadian Centre for Climate Modelling and Analysis	CCCma	Canada	CGCM3 (T47)	2.8° x 2.8°
			CGCM3 (T63)	1.9° x 1.9°
Beijing Climate Centre	BCC	China	BCC-CM1	1.9° x 1.9°
Institute of Atmospheric Physics	LASG	China	FGOALS-g1.0	2.8° x 2.8°
Centre National de Recherches Meteorologiques	CNRM	France	CNRM-CM3	1.9° x 1.9°
Institute Pierre Simon Laplace	IPSL	France	IPSL-CM4	2.5° x 3.75°
Max-Planck Institute for Meteorology	MPI-M	Germany	ECHAM5-OM	1.9° x 1.9°
Meteorological Institute, University of Bonn	MIUB	Germany	ECHO-G	3.9° x 3.9°
Model and Data Group at MPI-M	M&D	Germany	ECHO-G	3.9° x 3.9°
National Institute of Geophysics and Volcanology	INGV	Italy	SXG 2005	1.9° x 1.9°
Meteorological Research Institute, Japan	NIES	Japan	MIROC3.2 (hires)	1.1° x 1.1°
			MIROC3.2 (medres)	2.8° x 2.8°
National Institute for Environmental Studies	MRI	Japan	MRI-CGCM2.3.2	2.8° x 2.8°
Meteorological Research Institute of KMA	METRI	Korea	ECHO-G	3.9° x 3.9°
Bjerknes Centre for Climate Research	BCCR	Norway	BCM2.0	1.9° x 1.9°
Institute for Numerical Mathematics	INM	Russia	INM-CM3.0	4° x 5°
UK Met. Office	UKMO	UK	HadCM3	2.5° x 3.75°
			HadGEM1	1.3° x 1.9°
Geophysical Fluid Dynamics Laboratory	GFDL	USA	GFDL-CM2.0,	2.0° x 2.5°
			GFDL-CM2.1	2.0° x 2.5°
Goddard Institute for Space Studies	GISS	USA	GISS-AOM	3° x 4°
			GISS-E-H	4° x 5°
			GISS-E-R	4° x 5°
National Centre for Atmospheric Research	NCAR	USA	PCM CCSM3	2.8° x 2.8° 1.4° x 1.4°

## APPENDIX E

*Table E.1 Average monthly soil water content out put in (mm)for base period and future climate periods*

	Base	2020s	2050s
Jan	129.39	130.92	133.87
Feb	120.66	126.88	127.60
Mar	111.07	112.22	111.98
Apr	75.63	78.88	81.26
May	78.68	81.83	74.95
Jun	162.81	135.26	142.65
Jul	189.78	147.56	168.69
Aug	187.11	171.23	174.73
Sep	184.77	176.47	174.84
Oct	165.69	172.75	171.29
Nov	147.77	159.71	152.70
Dec	136.84	136.54	138.85

*Table E.2 Average monthly basin values (hydrological variables) for base period and future climate periods*

base period					
	SURF Q	LAT Q	WATER YIELD	ET	PET
	(MM)	(MM)	(MM)	(MM)	(MM)
Jan	2.42	0.08	10.09	22.53	132.67
Feb	1	0.04	2.78	21.92	138.92
Mar	4.3	0.08	4.53	51.86	155.58
Apr	4.09	0.13	3.8	85.56	149.58
May	9.69	0.4	9.42	91.8	145.48
Jun	54.72	3.64	56.26	101.64	116.51
Jul	142.38	9.32	166.72	98.82	105.14
Aug	121.86	9.79	189.05	93.63	105.01
Sep	68.97	6.8	153.45	91.22	114.37
Oct	35.28	3.22	114.52	70.72	122.4
Nov	3.7	0.49	52.92	46.32	120.09
Dec	0.98	0.16	25.51	29.38	124.62

*Table E.3 Average monthly basin values (hydrological variables) for 2020's climate periods*

2020s	SURF Q	LAT Q	WATER YIELD	ET	PET
	(MM)	(MM)	(MM)	(MM)	(MM)
Jan	1.81	0.6	14.84	64.18	138.14
Feb	1.09	0.17	6.07	62.85	140.76
Mar	2.06	0.27	6.61	77.56	156.82
Apr	5.08	0.6	6.77	104.92	150.36
May	12.58	1.47	15.75	120.77	146.9
Jun	19.31	2.56	27.82	119.98	126.74
Jul	24.9	3.63	42.49	124.4	120.8
Aug	24.22	4.24	51.79	117	120.48
Sep	23.92	4.18	58.2	106.41	123.74
Oct	18.13	3.39	56.88	98.36	132.26
Nov	11.86	2.39	47.72	84.19	134.82
Dec	4.69	1.36	31.24	71.55	133.72

*Table E.4 Average monthly basin values (hydrological variables) for 2050's climate periods*

2050s	SURF Q	LAT Q	WATER YIELD	ET	PET
	(MM)	(MM)	(MM)	(MM)	(MM)
Jan	4.03	1.07	15.63	74.23	147.11
Feb	0.85	0.4	4.17	59.4	142.43
Mar	0.52	0.2	7.55	56.38	160.57
Apr	2.16	0.55	5.24	62.63	157.69
May	10.28	1.79	13.11	65.1	152.06
Jun	17.12	3.28	27.97	80.01	129.3
Jul	27.55	4.9	50.62	91.21	129.71
Aug	29.53	5.27	68	96.91	128.11
Sep	28.57	4.99	81.05	124.08	136.45
Oct	22.98	3.43	71.4	137.7	138.5
Nov	16.77	2.63	57.47	130.38	136.43
Dec	8.09	1.62	34.75	101.13	135.71

## APPENDIX F

Table F.1: Mean annual yield [t/ha] per crop (1985 - 1993, Minchet catchment, Anjeni)

Year	Season	Barley				Wheat				Tef			
		n	a	b	c	n	a	b	c	n	a	b	c
1985	1	<b>4</b>	0.6	0.5	0.5								
	2					<b>2</b>	0.8	1.2	1.0	<b>2</b>	0.7	1.0	1.1
1986	1												
	2	<b>6</b>	0.6	0.5	0.5	<b>14</b>	1.0	0.9	1.1	<b>4</b>	0.7	0.7	0.6
1987	1	<b>4</b>	0.3	0.3	0.3								
	2	<b>10</b>	0.4	0.4	0.3	<b>11</b>	1.0	0.8	0.8	<b>4</b>	1.0	1.0	0.9
1988	1	<b>8</b>	0.4	0.3	0.3								
	2	<b>6</b>	0.4	0.4	0.4	<b>14</b>	0.7	0.6	0.7	<b>6</b>	0.8	0.6	0.5
1989	1	<b>8</b>	0.8	0.6	0.6								
	2	<b>6</b>	0.9	0.8	0.5	<b>9</b>	1.3	1.1	0.8	<b>5</b>	1.6	1.2	1.2
1990	1	<b>8</b>	0.5	0.4	0.4								
	2	<b>6</b>	0.6	0.5	0.3	<b>9</b>	0.9	0.9	0.6	<b>9</b>	1.8	1.4	1.0
1991	1	<b>10</b>	0.5	0.5	0.4								
	2	<b>9</b>	0.6	0.3	0.3	<b>5</b>	1.1	0.9	0.9	<b>9</b>	1.6	1.1	0.7
1992	1												
	2	<b>1</b>	0.7			<b>5</b>	1.0	0.7	0.7				
1993	1	<b>11</b>	0.7	0.6	0.5								
	2	<b>8</b>	0.7	0.6	0.3	<b>4</b>	0.6	0.7	0.6	<b>12</b>	1.4	1.0	0.9

Notes: The values are calculated as total yield. The yield measured on farmers' fields, test plots, and micro-plots is converted in t/ha without any correction factor for area loss through conservation structures. Bold numbers (n) indicate the number of measurements, normal numbers the average total yield per season (a = above / b =between / c = below conservation structures. Each n equals to an entire set (a, b, c) of yield samples)